Distribution Agreement

In presenting this thesis or dissertation as a partial fulfillment of the requirements for an advanced degree from Emory University, I hereby grant to Emory University and its agents the non-exclusive license to archive, make accessible, and display my thesis or dissertation in whole or in part in all forms of media, now or hereafter known, including display on the world wide web. I understand that I may select some access restrictions as part of the online submission of this thesis or dissertation. I retain all ownership rights to the copyright of the thesis or dissertation. I also retain the right to use in future works (such as articles or books) all or part of this thesis or dissertation.

Signature:

_____ _____

Yixiang Li Date

Role of TGF-β and acetylated KLF5 signaling axis in prostate cancer drug resistance

By

Yixiang Li
Doctor of Philosophy

Graduate Division of Biological and Biomedical Science
Cancer Biology

_____

Jin-Tang Dong, Ph.D.
Advisor

_____

Lawrence H. Boise, Ph.D.
Committee Member

_____

Melissa Gilbert-Ross, Ph.D.
Committee Member

_____

Carlos S Moreno, Ph.D.
Committee Member

_____

Shi-Yong Sun, Ph.D.
Committee Member

Accepted:

_____

Lisa A. Tedesco, Ph.D.
Dean of the James T. Laney School of Graduate Studies

_____

Date

Role of TGF-β and acetylated KLF5 signaling axis in prostate cancer drug resistance

By

Yixiang Li
Bachelor's of Science
Nankai University, 2013
Master's of Science in Public Health
Emory University. 2015

Advisor: Jin-Tang Dong, Ph.D.

An abstract of
A dissertation submitted to the Faculty of the
James T. Laney School of Graduate Studies of Emory University
in partial fulfillment of the requirements for the degree of
Doctor of Philosophy
in
Graduate Division of Biological and Biomedical Science
Cancer Biology
2020

Abstract

Role of TGF-β and acetylated KLF5 signaling axis in prostate cancer drug resistance
By Yixiang Li

Prostate cancer is the second leading cause of cancer-related deaths in the United States. Docetaxel (DTX) is the first line treatment for castration resistant prostate cancer; however, almost all patients that receive DTX eventually develop resistance. Utilizing cytotoxicity assays of DTX, Matrigel colony formation assays, mouse xenograft and tibia injection models, we investigated whether TGF-β and acetylated KLF5 affect DTX resistance in prostate cancer. We found that KLF5 is indispensable in TGF-β–induced DTX resistance. Moreover, KLF5 acetylation at lysine 369 mediates DTX resistance *in vitro* and *in vivo*. Furthermore, we used two approaches in exploring mechanisms mediating the TGF-β and acetylated KLF5 signaling axis in prostate cancer drug resistance. First, a luciferase reporter system was used to evaluate transcriptional activities. Gene expression was analyzed by RT-qPCR and Western blotting. We showed that the TGF-β/acetylated KLF5 signaling axis activates Bcl-2 expression transcriptionally. DTX-induced Bcl-2 degradation depends on a proteasome pathway, and TGF-β inhibits DTX-induced Bcl-2 ubiquitination. Second, RNA-seq and ChIP-seq modalities were used to determine direct downstream targets of acetylated KLF5. We found CXCR4 could be another promising mediator of acetylated KLF5 induced DTX resistance. Our studies demonstrated that the TGF-β-acetylated KLF5-Bcl-2 signaling axis mediates DTX resistance in prostate cancer and blockade of this pathway could provide clinical insights into chemoresistance of prostate cancer.

Role of TGF-β and acetylated KLF5 signaling axis in prostate cancer drug resistance

By

Yixiang Li
B.S., Nankai University, 2013
M.S.P.H., Emory University, 2015

Advisor: Jin-Tang Dong, Ph.D.

A dissertation submitted to the Faculty of the
James T. Laney School of Graduate Studies of Emory University
in partial fulfillment of the requirements for the degree of
Doctor of Philosophy
in
Graduate Division of Biological and Biomedical Science
Cancer Biology
2020

Acknowledgments

Many people helped me along the Ph.D. journey that deserve my gratitude.

I thank my thesis advisor, Dr. Jin-Tang Dong, for allowing me to pursue my research interests and providing me valuable guidance on how to be an independent scientific researcher. I thank my committee members, Drs. Carlos Moreno, Shi-Yong Sun, Paula Vertino, Melissa Gilbert-Ross, and Lawrence Boise for insights and advice about this thesis. I thank Dr. Jianping Ni for her strong support in experiments and delicious home-made snacks. I also thank Dr. Baotong Zhang, for his guidance in the past five years. He instructed me to focus on details and to plan for a long term career goal. Those valuable suggestions and discussions benefit my graduate studies and future career.

I would also like to thank my family for all of the generous support and enormous encouragement they gave me in completing this degree. To my wife, Lingwei Xiang, thank you for being supportive of me throughout this entire process, discussing ideas, and preventing several wrong turns. She also supported the family during much of my graduate studies. My son, Elvin Li, has continually provided the requisite breaks from biology and the motivation to finish my degree with expediency. My parents, Jun Li and Wenling Yang deserve special thanks for their continued support both emotionally and financially. Without such a group of people behind me, I would not be in this place today.

Table of Contents

Chapter 1: Introduction 8

1.1 Cancer 8
1.2 Prostate cancer 9
1.3 Docetaxel 12
1.4 KLF5 14
1.5 Transforming growth factor-β (TGF-β) 16
1.6 Figures 21

Chapter 2: TGF-β/acetylated KLF5 axis mediates docetaxel drug resistance 26

2.1 Introduction 26
2.2 Material and methods 28
2.3 Results 33
2.4 Discussion 39
2.5 Figures 41

Chapter 3: Mechanisms mediating the TGF-β/acetylated KLF5 induced drug resistance in prostate cancer 48

3.1 Introduction 48
3.2 Material and methods 51
3.3 Results 56
3.4 Discussion 65
3.5 Figures 69

Chapter 4: Discussion 85

4.1 Summary and conclusions 85
4.2 Novel role of TGF-β/Acetylated KLF5 signaling in DTX resistance in prostate cancer 86
4.3 Clinical implications 87
4.4 Future directions 89
4.5 Figures 92

References 96

Chapter 1: Introduction

1.1 Cancer

1.1.1 Cancer overview

Cancer is a collection of different types of malignancies that result from uncontrolled cell growth and have the ability to spread to other organs. Advances in cancer research have expanded our understanding of cancer and led to novel screening methods, new treatment and preventive modalities. However, cancer remains a significant public health issue and a devastating health problem.

1.1.2 Cancer statistics

According to the Global Cancer Observatory, more than 18 million people were diagnosed with cancer, and cancer is among the leading cause of death with 9.5 million cancer-related deaths globally in 2018 [1]. In the United States, more than 1.7 million people are estimated to be diagnosed with cancer, and cancer is the second leading cause of death, resulting in more than 600,000 deaths [2]. Prostate cancer is the second leading cause of cancer-related deaths in American males accounting for nearly 1 in 5 new diagnoses of cancers [2]. In the United States, one in every six males will suffer from prostate cancer in their lifetime.

1.1.3 Cancer Hallmarks

Twenty years ago, a set of characteristics defining transformed cell behavior were first introduced by Hanahan and Weinberg and classified as cancer hallmarks including cell death resistance, invasion, and metastasis, replicative immortality, activated angiogenesis, growth arrest evasion, and self-sufficiency in growth signaling [3]. Changes in these six branches ultimately lead to cancer formation and metastasis. In 2011, four new features that support

cancer malignancy were added to the cancer hallmarks (Hallmarks II). These additional features included two hallmarks: deregulated cellular energy metabolism, and avoiding immune destruction, and two traits: tumor-promoting inflammation, genomic instability and mutation [4]. The cancer hallmarks are considered essential properties of cancer development and serve as blueprints for cancer biology research and literature. For example, recognition of immune system response in the tumor microenvironment in the revised hallmarks resulted in breakthroughs in cancer immunotherapy research and therapeutic strategy development [5]. Treatments targeting these properties have been investigated. Various types of drugs have been developed to target specific hallmarks, but many have proven successful only for a limited time or within specific settings. The important principle of drug resistance was derived from the concept of shifting hallmark dependence during therapy [4]. Therefore, it is insufficient to view the hallmarks as independent, isolated, and static targets; the complementarity of the hallmarks, their co-dependence, and the evolutionary dynamics that rule them are important considerations in developing cancer therapy [6].

1.2 Prostate cancer

1.2.1 Prostate cancer epidemiology

Prostate cancer is a type of malignancy that originates within the prostate. As the second leading cause of cancer-related deaths and the most common malignancy among men in the United States, prostate cancer was estimated to cause more than 30,000 deaths and 170,000 new cases in 2019 [2]. The Digital Rectal Exam (DRE) is used to screen for prostate cancer. Also, various diagnostic modalities can be performed to detect prostate cancer in both early and late stages including blood tests for prostate specific antigen (PSA) level, PET scan, MRI scan, and

biopsy. Notably, a combined examination with DRE and PSA blood test has been shown to effectively enhance early detection of prostate cancer[7]. However, the PSA level has been particularly debatable in modern prostate cancer diagnosis. In the 1970s, PSA was found to correlate with prostate cancer grade and used as a crucial marker of prostate cancer incidence and recurrence. Therefore, the PSA test was used to diagnose previously unscreened men in the late 1980 and early 1990s. Large scale PSA testing led to a rapid increase in prostate cancer incidence. However, in 2008, the US Preventive Services Task Force (USPSTF) recommended against widespread usage of the PSA test to screen for asymptomatic prostate cancer (Grade D) in the elderly population (age 75 +) [8, 9]. The USPSTF showed that the PSA level is a marker that shows less specificity, and using PSA level as marker led to overtreatment of prostate cancer and unnecessary prostatectomies. Currently, informed decision making (Grade C) based on a combination of reviewed evidence has been used as a recommendation to screen men ages 55 to 69 [10-12].

1.2.2 Prostate cancer progression

In patients with localized disease and fairly small tumor volume, surgery and radiation are usually used early in cancer development, and this is often enough to "cure" the patients. Around one-third of patients will develop chronic disease, which is defined as increasing PSA but in a hormone-naïve environment [13]. Next, for those patients with increasing PSA, they receive either continuous or intermittent androgen deprivation therapy (ADT). The vast majority of these patients will respond with decreased PSA-levels and tumor burden [7]. However, over time, selective pressure of malignant cells will inevitably result in advanced-stage prostate cancer and most of these cases will eventually progress to castration-resistant disease.

Historically, secondary hormonal treatments, such as anti-androgens or synthesizing androgen suppressants, were used to treat these patients. Finally, chemotherapy may need to be implemented for patients who develop radiographic evidence of elevated tumor burden or other clinical signs of disease progression. Chemotherapy can decrease the tumor burden, often with associated declines in PSA, but ultimately result in partial or transient remission in the vast majority of patients[14]. Patients who progress into this post-chemotherapy state then progress with further clinical deterioration and ultimately death [15] (Figure 1.1).

1.2.3 Castration Resistant Prostate Cancer (CRPC)

As a systemic treatment of metastatic prostate cancer, androgen deprivation therapy inhibits the growth of androgen dependent prostate cancer cells. In androgen dependent prostate cancer, androgen binds with the androgen receptor to activate a series of biological processes including cell proliferation [16], immune response modulation [17], drug resistance [18], and stemness [19]. Effectively targeting the androgen receptor with an antagonist eliminates proliferation of cells that require androgen to survive. However, several studies have shown that most patients who received androgen deprivation therapy eventually develop CRPC [14, 20, 21]. Zong and others proposed two models exploring the incidence of CRPC (Figure 1.2) [13]. (1) In the selection model [22], due to tumor heterogeneity, ADT selectively eliminates cells that depend on androgen and provides nutrition and space for pre-existing androgen independent prostate cancer cells. (2) In the adaptation model, prostate cancer cells acquire a castration resistant phenotype via ADT-induced adaptive changes including intratumoral androgen upregulation, AR gene amplification, mutation, changes in co-regulatory molecules, rewired AR signaling, and activation of pro-survival, anti-apoptotic pathways [23, 24]. Currently,

abiraterone [25] and enzalutamide [26], Sipuleucel-T [27, 28], docetaxel [29, 30], carbazitaxel[31], and Radium 223[32] are approved by the US Food and Drug Administration (FDA) for CRPC treatment.

1.2.4 Treatment of advance stage prostate cancer

In 1941, Charles Huggins first reported the effect of ADT in patients with metastatic PC. Since then, suppression of the AR signaling through ADT has remained the pillar of metastatic PC treatment for 80 years. Currently, ADT involves surgical castration or natural castration by administering luteinizing hormone-releasing hormone (LHRH) agonists or antagonists with or without anti-androgen medications [33]. Although several lines of ADT therapies are generally used and provide almost guaranteed remissions that lasts one to two years, cancer cells become resistant and lead to metastatic castration-resistant prostate cancer (mCRPC) in most patients.

1.3 Docetaxel

Docetaxel is a semisynthetic derivative of 10-deacetylbaccatin-III from the bark of Pacific yew trees (*Taxus brevifolia*). Originally, extract from six 100-years-old yew trees was used to treat one cancer patient [34]. Currently, docetaxel is semi-synthesized from taxoid made by the Taxus species [35]. In 2004, docetaxel, a member of the class of taxane antineoplastic agents, was approved as first-line chemotherapy and became the standard of care of CRPC based on two pivotal phase 3 randomized studies showing significant survival advantage [29, 36]. Docetaxel is a cell cycle-arresting medicine that binds with β-tubulin to inhibit microtubule depolymerization and disrupt microtubule dynamics [37] (Figure 1.3). Microtubules play a critical role in cell metabolite transportation and mitosis. Stabilization of microtubules

effectively disrupts intracellular trafficking, arrests the cell cycle in M phase, and induces cell death [37, 38]. Moreover, docetaxel is reported to promote nuclear accumulation of FOXO1 [39], a regulatory factor that inhibits AR activity by disrupting the transcription of the AR-V7 variant, an essential mediator of abiraterone and enzalutamide resistance [40]. In addition, docetaxel inhibits the nuclear translocation of AR in prostate cancer cells [41].

1.3.1 Drug resistance

Docetaxel induces cytotoxicity in prostate cancer by stabilizing microtubules in actively proliferating cells. It binds to β-tubulin to inhibit the depolymerization of microtubules [42]. Extensive research demonstrated that up-regulation of the drug efflux pump contributes to docetaxel resistance and inhibiting multidrug resistance sensitizes cells to chemotherapy [43-45]. Also, several research groups reported overexpression of β-tubulin and multiple mutations that induce docetaxel resistance by suppressing binding affinity between docetaxel and β-tubulin [46-48]. Moreover, the epithelial-mesenchymal transition (EMT) has emerged as a critical mechanism mediating docetaxel resistance by coordinating various intracellular signaling pathways and biological processes, including phosphatidylinositol-3-kinase (PI3K/Akt) signaling and cancer stem cell properties [49-53]. Also, it has been reported that evasion of apoptosis via p38/p53/p21 signaling induces docetaxel resistance in prostate cancer [54], and alteration of the mitochondrial apoptotic pathway mediates docetaxel resistance in breast cancer cells [55]. Furthermore, fibronectin, a component of the tumor microenvironment that is crucial for growth, differentiation, adhesion, and migration [56], led to docetaxel resistance in the human hepatic cancer stem cell niche [57], in human lung cancer cells through Erk and Rho kinase [58], and in ovarian and breast cancer cells [59].

1.4 KLF5

1.4.1 KLF5 structure

The human *KLF5* gene, also known as *IKLF5* and *BTEB2*, is ~18.5 kb long located at 13q21 with four exons and three introns. The *KLF5* transcript contains a 324-bp 5'-untranslated region (UTR) and a 1,652-bp 3'-UTR whereas the coding region is 1,374-bp encoding a 457 amino acid polypeptide. As a member of the Krüppel-like factor family, KLF5 protein contains three zinc finger domains in the C terminus that functionally bind to a DNA sequence. A proline-rich transactivation domain with a PY motif (PPSY328) was found before the ZF domains [60, 61]. Also, KLF5 undergoes four types of posttranslational modifications; phosphorylation at S153 [62], acetylation at K369 [63], ubiquitination in the TAD domain [64], and sumoylation at K162 and K209 [65, 66] (Figure 1.4).

1.4.2 KLF5 in normal tissue

KLF5 is widely expressed in different tissues, and is best known for its stimulatory role in the proliferation of different types of cells. KLF5 is highly expressed in actively proliferating cells rather than differentiated cells [67]. Specifically, KLF5 levels are high in human and mouse digestive tract tissues such as the intestine and colon [61, 67]. Also, KLF5 is a crucial mediator of epithelial differentiation and homeostasis. KLF5 levels were also found elevated in the base of intestinal crypts where cells are actively proliferating and differentiating but not in the differentiated epithelial cells in the intestinal villi [68, 69]. Knockout of one KLF5 allele reduced villi size in the mouse intestine [70], suggesting that KLF5 is essential in the mouse intestine development. Moreover, KLF5 is strongly expressed during proliferation of epithelial cells

such as immortal but untransformed epithelial cell lines and primary epithelial cell cultures, the bulk of which are progenitor cells [71, 72]. Elevated KLF5 levels contribute to regulating tissue development during embryogenesis [68, 73]. In the mouse prostate, knocking out one allele of Klf5 in epithelial cells promoted cell proliferation and induced hyperplasia; however, knocking out both alleles caused apoptosis, suggesting that Klf5 plays a major role in the proliferation of prostatic epithelial cells [74]. Moreover, Klf5 maintains mouse prostate basal progenitors, which contributes to postnatal prostate development and regeneration via differentiating into luminal cells [75].

1.4.3 KLF5 in cancerous cells

KLF5 has been shown to have a context-dependent function in cancer cells. Due to its role in promoting cell proliferation, KLF5 was considered to have an oncogenic role in some intestine and colon cancers [76-78]. Moreover, in bladder cancer, KLF5 promoted tumor growth in a mouse xenograft model of TSU-Pr1 cells [79]. Also, in salivary gland cancer, *KLF5* had copy number gain, which leads to increased expression of KLF5 [80]. However, in prostate cancer cell lines, *KLF5* mRNA levels were lower and gene copy number loss was detected, and overexpressed KLF5 reduced colony formation in prostate cancer cell lines DU145 and 22RV1 [72, 81]. The *KLF5* gene is rarely mutated in prostate cancers [72], but *KLF5* is located in 13q21 which is the second most frequently deleted chromosomal region in multiple types of human cancers including prostate cancer [82]. Deletion at 13q21 correlated with metastases and higher tumor grade in prostate cancer [83, 84].

KLF5 was reported to promote cell proliferation through facilitating the G1/S and G2/M cell cycle progression [85]. KLF5 overexpression in the TSU-Pr1 bladder cancer line promoted

the progression of the G1/S cell cycle and tumorigenesis [86]. KLF5 increased cell proliferation in primary mouse cultures of esophageal keratinocytes by upregulation of EGFR and MEK / ERK signaling [87]. Moreover, KLF5 mediated the proliferative and transforming function of oncogenic Ras [77]. In H-Ras-transformed NIH3T3 cells, overexpression of KLF5 induced a significant increase in cell proliferation [88]. KLF5 was also found to mediate K-Ras (V12G) induced IEC-6 intestinal epithelial cell proliferation [89]. On the other hand, in DU145 and PC-3 cells, the proliferation promoting function of KLF5 was mediated by its deacetylated form, while acetylated KLF5 inhibits cell proliferation [90].

1.4.4 KLF5 in EMT

As a transcription factor regulating various biological processes, KLF5 helps to mediate the epithelial to mesenchymal transition (EMT). In human hepatocellular carcinoma (HCC), KLF5 induces EMT via activating PI3K/AKT/Snail signaling and plays a crucial role in HCC progression [91]. However, it has also been reported that KLF5 functions as an epithelial factor that inhibits EMT induction by maintaining the transcription of miR-200 in human epithelial cells, and that downregulation of KLF5 is essential for TGF-β to induce EMT [92]. Activation of the TGF-β signaling pathway recruits p300 acetyl-transferase to acetylate KLF5 at lysine 369 and regulates downstream targets via acetylated KLF5 and Smad complexes [93].

1.5 Transforming growth factor-β (TGF-β)

1.5.1 TGF-β signaling pathway

TGF-β ligands are disulfide-linked dimers. In an activated form, TGF-β ligands include two subfamilies sharing similar sequences: the TGF-β-activin-nodal subfamily and the BMP

subfamily [94]. Ligand binding requires a receptor complex consisting of two type I receptors and two type II components. As Ser/Thr protein kinases, type II receptors phosphorylate the type I components [95]. Phosphorylation of type I receptor propagates activating signals by phosphorylating Smad proteins [96]. Smad proteins contain two globular domains; the MH1 domain mediates DNA-binding ability while the MH2 domain mediates interaction with other co-factors [94]. Upon phosphorylation by TGF-β type I receptor (TGFBR1), Smad2/3 binds with SMAD4 in the MH2 domain and the Smad protein complex translocates to the nucleus where it binds with other co-factors for target gene transcriptional regulation [97-99]. On the other hand, TGF-β ligand-occupied receptors directly activate several non-canonical, non-Smad pathways to enhance, attenuate, or otherwise modulate downstream cellular responses. There are various branches of MAP kinase pathways [100], Rho-like GTPase signaling pathways [101], and phosphatidylinositol-3-kinase/AKT pathways in these non-Smad pathways [102 103] (Figure 1.5).

1.5.2 TGF-β function in normal tissue

As a crucial modulator of the immune system, TGF-β promotes growth arrest and apoptosis in human and mouse lymphocytes [104, 105]. Additionally, TGF-β treatment also induced apoptosis in two interleukin-2-dependent T-cell lines [106]. Moreover, TGF-β inhibited cell proliferation and induced apoptosis in the development and maintenance of the digestive system. In rat liver cells, TGF-β induced p53 and Bax dependent apoptosis [107], while in human gastric cancer cells, TGF-β induced p53 independent apoptosis [108]. In addition, Smad family proteins have been reported to mediate TGF-β induced cell apoptosis. In MDCK cells, transiently transfected SMAD4 induced apoptosis, and co-expression of SMAD3 and SMAD4 led to enhanced TGF-β-induced apoptosis [109]. In prostate cancer cells DU145 and PC-3U,

overexpression of SMAD7 induced apoptosis while knockdown of SMAD7 in DU145 and HaCaT cells inhibited TGF-β-mediated cell apoptosis [110].

1.5.3 TGF-β function in cancerous tissue

TGF-β plays dual functions in human cancers [111, 112]. As a tumor promoter, TGF-β ligands are upregulated in various cancer types including breast [113], colorectal [114], and lung cancers [115]. In these cancers, increases in the TGF-β ligand levels with elevated circulating levels have been observed both locally and systemically. In lymph node metastasis, higher levels of TGF-β were shown compared to primary tumors or in tumors that eventually metastasize. Also, TGF-β contributes to invasiveness, metastasis, and poorer prognosis [116, 117]. In triple-negative breast cancer, TGF-β regulates cancer stem cell and metastatic properties to mediate paclitaxel resistance [53, 118, 119]. In addition, TGF-β induced SMAD activity mediates lung relapse of breast tumors via regulating angiopoietin-like 4 [120].

As a tumor suppressor, disruption of TGF-β receptors, or their downstream effectors are frequently observed in cancer. For example, TβRII deletions or mutations are seen in colon [121], stomach [122], and breast cancers [123], and TβRI receptor modifications are often commonly seen in cancers of the ovaries, head and neck, breast, liver, and prostate [124]. Downstream mediators of TGF-β signal transduction, including Smad2 and Smad3, are mutated in colorectal cancer [125], hepatocellular carcinoma [126], and gastric cancer [127]. Moreover, we previously reported that TGF-β induces growth inhibition via acetylation on KLF5 lysine 369 in HaCaT cells [128, 129], and prostate cancer cells [90].

1.5.4 TGF-β function in EMT

TGF-β induces EMT in various cell types including breast epithelial cells, wound healing, and renal fibrosis[130]. Use of a dominant negative TGFBR2 in squamous cell carcinoma and breast cancer abrogated their ability to undergo EMT and migration and metastasize to distant sites [131]. Meanwhile, the restoration of TGFBR2 in colorectal cancer cells that are normally TβRII-null and non-invasive induced invasive behavior [132]. Transgenic mice with activated expression of TGFB1 in keratinocytes showed an increased propensity to form spindle cell carcinomas, suggesting that this keratinocyte-to-spindle cell transition involves TGFB1 [133]. Furthermore, TGF-β induced the formation of a mutant p53, Smad, and p63 complex in cancers where p53 is mutated. In this complex, p63 loses its tumor-suppressive function allowing for the initiation of EMT and metastasis by both TGF-β and mutant p53 [134]. Similarly, in epithelial cells, the Smad protein complex activated by canonical TGF-β signaling transcriptionally activated SNAIL1 and TWIST1[135, 136]. High levels of TGF-β are also seen on the invasive front, indicating TGF-β is involved in EMT, tumor cell migration, and invasion [131].

1.5.5 TGF-β function in apoptosis

TGF-β triggers apoptosis through both Smad-dependent and independent pathways in various cell types. In a Smad-dependent manner, TGF-β induces pro-apoptotic protein expression including TGF-β inducible early response gene (TIEG1) [137], death-associated protein kinase (DAPK) [138], and inositol-5-phosphatase (SHIP) [139]. TGF-β is also linked via DAXX to the Fas-mediated apoptosis pathway, an adaptor protein that mediates the signaling of the Fas receptor. DAXX stabilizes TGFBR2, which results in JNK activation and Fas apoptosis signaling [140].

1.5.6 TGF-β and acetylated KLF5

The pro-proliferative KLF5 becomes anti-proliferative upon TGF-β-mediated acetylation in epithelial homeostasis. In the HaCaT epidermal cell line, KLF5 mediates cell proliferation. Under TGF-β treatment, KLF5 is also indispensable for TGF-β-induced anti-proliferation function [128]. KLF5 inhibited the expression of p15 (CDKN2B), a cell cycle inhibitor, but became a coactivator in TGF-β-induced p15 expression[93]. Furthermore, KLF5 acetylation deficiency prevented p300-assembled Smad4-KLF5 complex formation on the p15 promoter, and affected Smad4 and FOXO3 binding on the p15 promoter *in vivo* [93]. In brief, TGF-β induces the acetylation of KLF5 at lysine 369 (K369) via Smad-recruited p300 acetyl-transferase. Acetylated KLF5 forms a transcriptional complex different from that of deacetylated KLF5, exerting distinct functions in gene regulation, cell proliferation, and tumorigenesis.

1.6 Figures

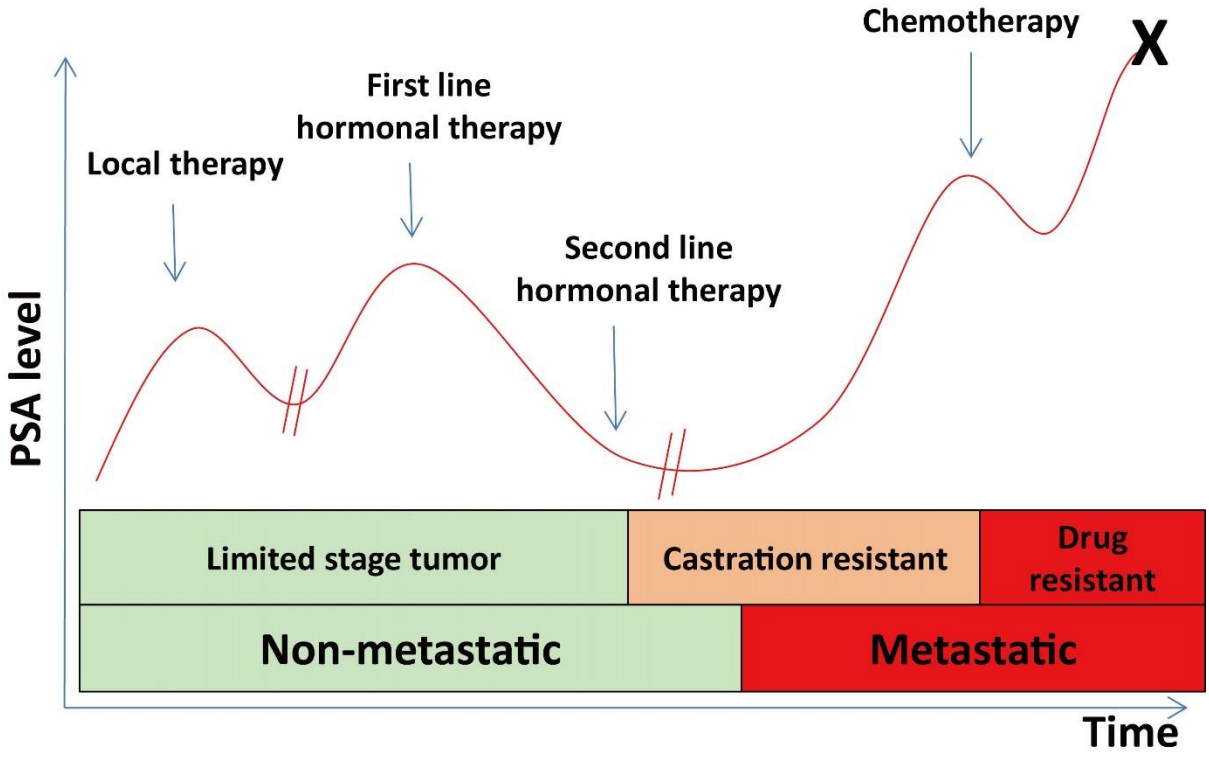

Figure 1.1: Natural History of Prostate Cancer.

Adapted from Figg WD, et al., eds. *Drug Management of Prostate Cancer.* New York, NY, 2010

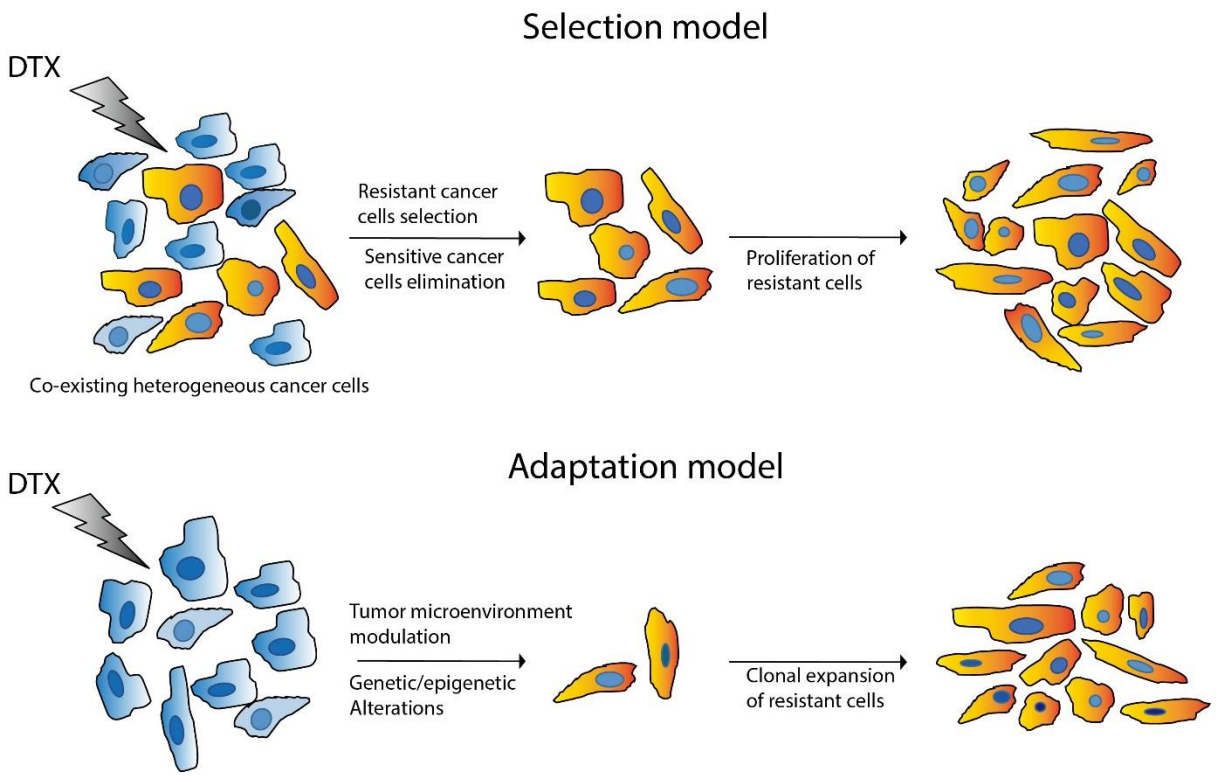

Figure 1.2: CRPC Models. The clonal selection model indicates that prostate cancer consists of heterogeneous cells of which a minority is a pre-existing clone of castration-resistant cells (orange cells) with predominant androgen-dependent cells (blue cells) after ADT in an androgen-deprived environment; castration-resistant cells are selected for their survival and proliferative advantages; Whereas the adaptation model indicates that primary prostate cancer is initially homogeneous, consisting of only androgen-dependent cells and that castration resistance occurs as an adaptive transition after androgen deprivation through genetic/epigenetic transfer to castration-resistant cells of some of the previously androgen-dependent cells. Adapted from Ahmed M, et al., *Adaptation and clonal selection models of castration‐resistant prostate cancer: Current perspective*, International Journal of Urology, 2012

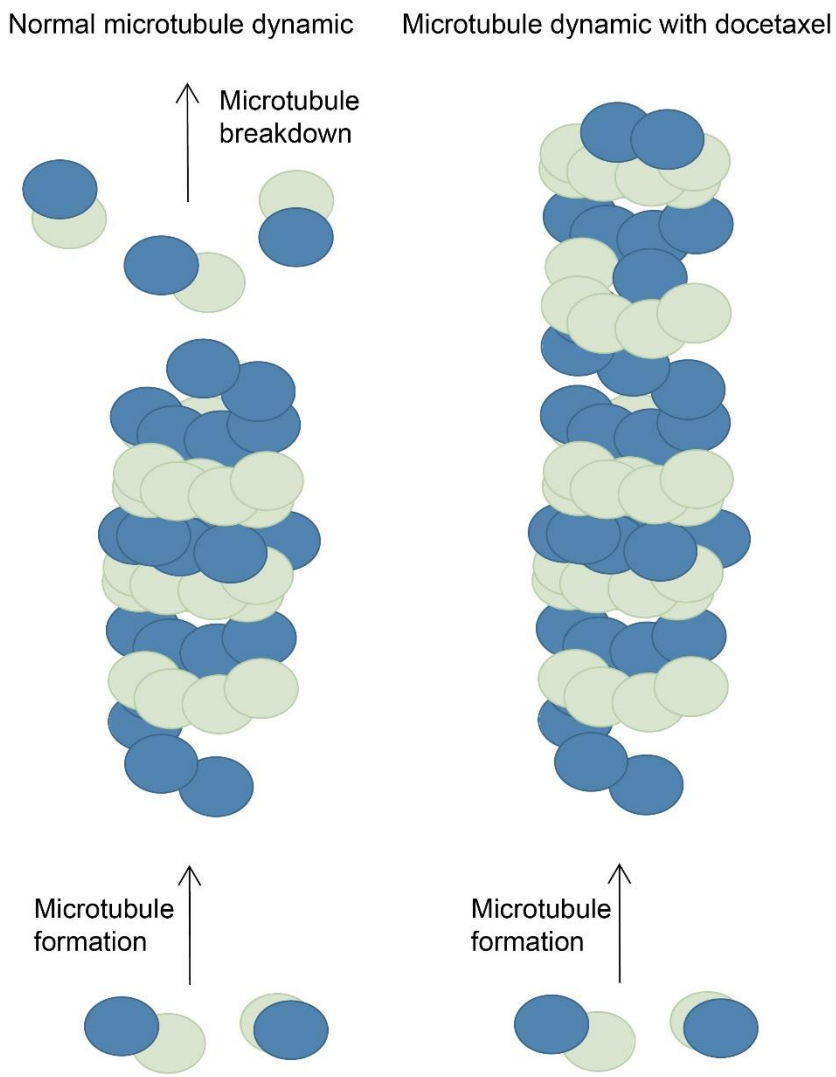

Figure 1.3: Docetaxel effect on microtubule dynamic. As a microtubule-stabilizing agent, docetaxel disrupts microtubule function by inhibition of tubulin depolymerization. Adapted from Burbank KS, et al., *Microtubule dynamic instability*, Current Biology, 2006

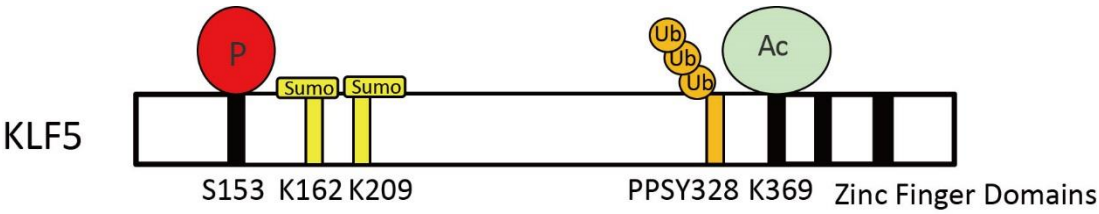

Figure 1.4: The structure of KLF5. KLF5 protein contains 457 amino acid polypeptide with three zinc finger domains in C terminus to functionally bind to DNA sequence; a proline-rich transactivation domain with a PY motif (PPSY328) the ZF domains. KLF5 undergoes four types of posttranslational modifications: phosphorylation at S153, acetylation at K369, ubiquitination in the TAD domain, and sumoylation at K162 and K209. Adapted from Dong JT, et al., *Essential role of KLF5 transcription factor in cell proliferation and differentiation and its implications for human diseases*, Cellular and Molecular Life Science, 2009

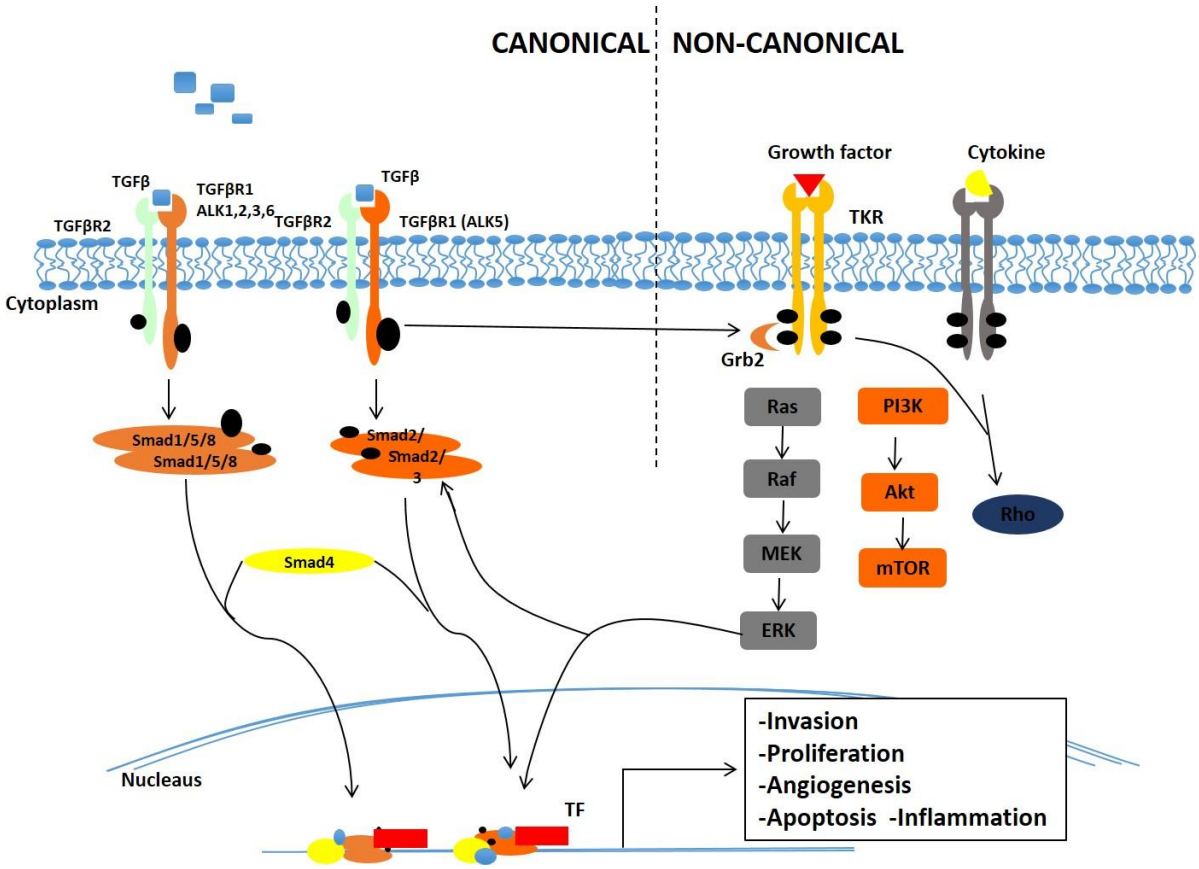

Figure 1.5: Canonical and non-canonical TGF-β signaling pathways.

Adapted from Neuzullet C, et al., *Perspectives of TGF-β inhibition in pancreatic and hepatocellular carcinomas*, Oncotarget, 2013.

Chapter 2: TGF-β/acetylated KLF5 axis mediates docetaxel drug resistance

2.1 Introduction

Prostate cancer is the second leading cause of cancer-related deaths in American males and was expected to cause more than 30,000 deaths in the year 2019 [2]. As a lethal form of prostate cancer, castration-resistant prostate cancer (CRPC) is the prostate cancer has developed resistance to androgen deprivation therapy. CRPC patients initially benefit from docetaxel (DTX) as a first-line treatment with prolonged survival time and improved rates of response [29, 36]. Unfortunately, most patients receiving DTX ultimately develop resistance [141, 142]. Therefore, novel therapeutic strategies are needed for DTX-resistant prostate cancer treatment.

DTX stabilizes microtubules in actively proliferating cells to induce cytotoxicity. It preferably binds to β-tubulin to inhibit the depolymerization of microtubules [42]. Extensive research has demonstrated that the upregulation of the drug efflux pump contributes to DTX resistance and inhibition of multidrug resistance sensitizes cells to chemotherapy [43-45]. Also, several studies have reported that multiple mutations and overexpression of β-tubulin induce DTX resistance by reducing the binding affinity between DTX and β-tubulin [46-48]. Epithelial-mesenchymal transition (EMT) has emerged as a critical mechanism mediating DTX resistance by coordinating various intracellular signaling pathways and biological processes, including phosphatidylinositol-3-kinase (PI3K/Akt) signaling and cancer stem cell properties [49-53].

TGF-β activates various cellular processes in human cancer [111, 112, 143]. Among multiple TGF-β targets, cancer stem cell properties are reported to mediate TGF-β–induced paclitaxel resistance in triple-negative breast cancer [53]. Human Krüppel-like factor 5 (KLF5) was

identified as an indispensable factor for TGF-β to regulate gene transcription and cell proliferation in epithelial cells [92, 93, 128, 129]. The activated TGF-β signaling pathway recruits p300 acetyl-transferase to acetylate KLF5 at lysine 369 and regulates downstream targets with an acetylated KLF5 and Smads complex [93]. Moreover, as a dual functional growth factor, TGF-β induces growth inhibition via acetylation on KLF5 lysine 369 in HaCaT cells [128, 129], and prostate cancer cells [90]. It is unclear whether TGF-β–induced KLF5 acetylation is required for DTX resistance of prostate cancer cells.

2.2 Material and methods

Cell culture and reagents

Human prostate cancer cell lines (DU145, PC-3, and C4-2) were obtained from the American Type Culture Collection (ATCC, Manassas, VA, USA), and cultured according to ATCC's instructions. Human recombinant TGF-β1 was purchased from R&D Systems, Inc. (Minneapolis, MN, USA). Docetaxel and SB-505124 were purchased from MilliporeSigma (St. Louise, MO, USA). ABT-199 and S63845 were purchased from Cayman Chemical (Ann Arbor, MI, USA). The jetPRIME transfection reagent (Polyplus transfection, New York, NY, USA) was used for plasmid transfection according to the manufacturer's protocol.

Knockout of *KLF5* in prostate cancer cell lines

The CRISPR-cas9 system was used to eliminate KLF5 protein according to the protocol from the Feng Zhang laboratory [144]. Briefly, sgRNA-encoding DNA was designed and synthesized as DNA oligos specific for the KLF5 genome: 5'-CACCGACGGTCTCTGGGATTTGTAG-3' and 5'-AAACCTACAAATCCCAGAGACCGTC-3', annealed and then cloned into the CRISPR-cas9 lentivirus backbone lentiCRISPRv1 vector (Addgene, Boston, MA, #49535), and lentiviruses were generated following the protocols described on the Addgene website (http: //www.addgene.org/lentiviral/protocols-resources/). Prostate cancer cells infected with lentiviruses were selected in the medium containing puromycin (1 μg/ml) for 72-96 hours before seeding and screening for single clones. KLF5-null clones were identified by Western blotting and confirmed by sequencing the targeted genome region after PCR amplification with primers 5'-CACAATCGACAAAATAAGCCTG-3' and 5'-

CAGTAGCTGGTACAGGTGGCCC-3'.

Retroviral expression of KLF5, KLF5^{K369R,} and KLF5^{K369Q}

The coding regions of wild type *KLF5* and the acetylation-deficient *KLF5^{K369R}* mutant were amplified by PCR from the plasmids described in a previous study [90] with primers 5'-CCAAGCTTATGGACTACAAGGACGACGATGACAAGATGGCTACAAGGGTGCTGAG-3' and 5'-CCATCGATTCAGTTCTGGTGCCTCTTCAT-3', except that a FLAG-tag was added to the N-terminus of KLF5 or KLF5^{KR}. PCR products were digested with HindIII and ClaI restriction enzymes, purified, and subsequently cloned into the pLHCX vector (Clontech, MountainView, CA). The *KLF5^{K369Q}* mutant, which encodes the Ac-KLF5-mimicking KLF5^{KQ}, was generated by site-directed mutagenesis with primers 5'-AACCCCGATTTGGAGCAACGACGCATCCACTA-3' and 5'-TAGTGGATGCGTCGTTGCTCCAAATCGGGGTT-3' following standard procedures. In addition, the sgRNA targeting site was also mutated with primers 5'-TCACTCACCTGAGAACTGGGCTGTATAAATCCCAGAGACCGTG-3' and 5'-CACGGTCTCTGGGATTTATACAGCCCAGTTCTCAGGTGAGTGA-3' to introduce nonsense mutations, which helped to avoid cas9-mediated interference. Retroviruses were packaged and applied to infect prostate cancer cells according to the protocol described in a previous study [90]. All plasmids were sequenced to confirm the expected mutations.

Cytotoxicity assay

Cytotoxicity was evaluated with water-soluble tetrazolium salt in the Cell Counting Kit-8 (Dojindo Molecular Technologies, Inc., Rockville, MD, USA). Approximately $3x10^3$ cells were seeded in 96-well plates with indicated TGF-β and/or SB-505124 treatments 24 hours

before docetaxel and/or ABT-199 treatment. After 72 hours of docetaxel treatment, CCK-8 was added to each well, and the plates were incubated for 3 hours, followed by absorbance measurement at 450 nm using the Synergy H1 Hybrid Multi-Mode Reader (BioTek, Winooski, VT, USA).

Colony formation assay

Thick layers of Matrigel matrix (Corning) were used for colony formation assay (3D culture) by adding 50 μl Matrigel in each well on a 96-well plate. After 30 minutes incubation in a 37°C incubator, 200 cells mixed with 100 μl medium containing 5% Matrigel and indicated TGF-β and/or SB-505124 treatments were seeded in each well. DTX treatment was scheduled in 24 hours. Change medium every 2 days. In 15 days for DU145 cells and 7 days for PC-3 cells, colony images were captured using Olympus IX51 Inverted Microscope (Hunt Optics & Imaging, Inc., Pittsburgh, USA) and colonies with a diameter greater than 50 μm were counted.

Xenograft mouse tumorigenesis model

Male BALB/c nude mice (3–4 weeks old) were purchased from Charles River (San Diego, CA), and closely monitored and handled at an Emory University Division of Animal Resources facility according to the policies of the Institutional Animal Care and Use Committee. Equal volumes of PBS and Matrigel were first used to suspend DU145 cells at 2×10^7 cells/ml, and 100 μl cell-containing mixture was subcutaneously injected into both flanks of mice. Four mice were used in each group, and DTX was administered daily in a concentration of 1.8 mg/(kg*day) starting from the 7th day. Tumor volume of eight tumors from four mice was measured every two days, and tumors were surgically isolated on the 23rd day followed by weighting and photographing.

Realtime qPCR

Trizol reagent (Invitrogen, Carlsbad, CA, USA) was used to isolate total RNA. The first strand cDNA was synthesized from total RNA with the RT-PCR kit from Promega. Realtime qPCR with SYBR Green master mix was used to measure *BCL2* mRNA level in Applied Biosystems^{TM} 7500 Real-Time PCR System (Thermo Fisher Scientific). Primer sequences for *BCL2:* Forward: 5'-GAGAAATCAAACAGAGGCCG-3', Reverse: 5'-CTGAGTACCTGAACCGGCA-3'

Tibial tumorigenesis assay

Nude mice were anesthetized with 3% isoflurane and maintained by 2.5% isoflurane, and no toe reflex of muscle tone was present at this point. Both legs were cleaned with a 10% povidone/iodine swab/solution, followed by ethanol, repeating 3 times. Lateral malleolus, medial malleolus, and lower half of tibia with forefinger and thumb was gently grasped, and then leg combination of flexion and lateral rotation was bent, such that the knee was visible and accessible. While firmly grasping the ankle/leg of the mouse, 27g ½ needle was inserted under the patella, through the middle of the patellar ligament, and into the anterior intercondylar area in the top of the tibia. When inserting the needle into the tibia, the syringe was carefully guided through the growth plate using steady and firm pressure with slight drilling action. Upon penetration of the tibial growth plate, the needle was encountered markedly less resistance. We also used a gentle, lateral movement of the needle to ensure the needle was in the tibia and through the growth plate. The movement was limited because the needle was in the proper place within tibia. A volume of 20 μl of cell solution Little (1 million cells) was injected into the tibia, and no resistance was felt at this point. The needle was then

extracted slowly. The mice were placed on a heating pad during the recovery period and monitored every day until the fifth day after injection.

Histological procedure for bone and TRAP staining

The mouse bones were fixed in 10% neutral-buffered formalin for 24 hours and then decalcified with 10% ethylenediaminetetraacetic acid (EDTA) for 10 days. After decalcification, they were processed in a Tissue-Tek VIP processor and embedded in paraffin for sectioning. Lateral sections (5 μm-thick) were cut to include the tibia, knee joint, and the distal femur. Hematoxylin & eosin (H&E) staining and the tartrate-resistant acidic phosphatase (TRAP) staining were done on consecutive sections from each tissue block. For TRAP staining, deparaffinized bone sections were incubated first in 0.2 M acetate buffer for 20 minutes and then in the same buffer with naphthol AS-MX phosphate (0.5 mg/ml) and fast red TR salt (1.1 mg/ml) for 30-45 min in a 37℃ oven. The color change was monitored every 15 min (TRAP-positive area turns red). Slides were then counterstained with hematoxylin and mounted for analysis with Immu-Mount (Thermo Scientific, Waltham, MA).

Statistical analysis

Data were expressed as means ± standard errors of the mean (SEM). The statistical significance of the difference in means of two groups was determined with the two tail unpaired Student *t*-test. Two-way ANOVA test was used to analyze mouse xenograft tumor volume curves. *P*-values greater than 0.05 were considered statistically insignificant (ns), *p*-values less or equal to 0.05 were considered statistically significant (*). *P*-values less or equal to 0.01 were labeled as **; *p*-value less or equal to 0.001 were labeled as ***.

2.3 Results

KLF5 is required by TGF-β to induce DTX resistance in prostate cancer cells

Some earlier studies have reported that TGF-β induces resistance to DTX[53, 145, 146]. To measure the level of DTX resistance of prostate cancer cell lines DU145 and PC-3, we conducted *in vitro* cell survival assays following treatment with DTX and TGF-β. We found that treatment with 10 ng/μl TGF-β led to a two-fold increase in DTX IC50 (from 1.13 to 2.40 nM) in DU145 prostate cancer cells. Specifically, starting at 2.5 nM DTX treatment, cell survival was more than 2-fold greater in cells treated with 10 ng/μl TGF-β (p-value < 0.001), while TGF-β inhibition with 2.5 μM SB-505124 led to a decrease in cell survival of more than 50% (p-value < 0.05), with an IC50 of 0.96 nM (Figure 2.1A). Moreover, increasing the concentration of DTX led to a greater difference in the percentage of cells surviving (Figure 2.1A, right panel). At a DTX concentration lower than 1 nM, the percentage of cell survival after treatment with TGF-β and SB-505124 was similar, while with DTX concentrations higher than 1 nM, we began to observe significant differences in cell survival (Fig 2.1A). Similar trends were observed in PC-3 cells. Treatment with 10 ng/μl TGF-β induced a three-fold increase in IC50 (from 1.87 nM to 5.22 nM) and higher cell survival percentages at DTX concentrations of 0.5, 1, 5, and 100 nM (p-value<0.001). On the other hand, the IC50 decreased from 5.22 nM to 2.03 nM in cells treated with the combination of TGF-β and SB-505124 (Figure 2.1B). These results further show that TGF-β induced DTX resistance, and inhibition of TGF-β signaling by SB-505124 sensitized cells to DTX treatment.

Next, we explored whether TGF-β–induced DTX resistance depends on KLF5 expression. We first knocked out KLF5 endogenously using the CRISPR-Cas9 system in DU145 and PC-

3 cells and measured the DTX sensitivity of these cells with an *in vitro* cell survival assay. Interestingly, TGF-β or SB-505124 treatment did not change the DTX sensitivity when KLF5 was endogenously knocked out (Figure 2.1C-D). In contrast, after the restoration of KLF5 expression in DU145 and PC-3 KLF5-null cells, TGF-β treatment alone increased DTX resistance, with an increase in IC50 from 1.1 to 5.8 nM in DU145 cells, and from 0.9 to 3.9 nM in PC-3 cells (Figure 2.1C-D). In cells treated with the combination of SB-505124 and TGF-β, IC50 values were 1.1 nM in DU145 cells and 0.88 nM in PC-3 cells, which were similar to those of the control group. Notably, cell survival was more than 2-fold greater after 2.5, 5, 10, and 100 nM DTX treatment in the TGF-β treatment group than in the control group or the TGF-β and SB505124 combination treatment group (Figure 2.1C-D).

Colony formation assay in 3D Matrigel was used to simulate an *in vivo* environment with DTX treatment. After 1 nM DTX treatment for 15 days, colonies with diameters greater than 50 μm were counted. DTX treatment effectively inhibited growth and killed KLF5-null cells regardless of TGF-β treatment (Figure 2.1E-F). Furthermore, KLF5 restoration in DU145 and PC-3 KLF5-null cells contributed to TGF-β–induced DTX resistance. In DU145 KLF5 -/- cells with restored wild-type KLF5, treatment with DTX in the absence of TGF-β inhibited growth and caused cell death, but in the presence of TGF-β DTX did not reduce colony numbers significantly (p-values > 0.05) (Figure 2.1E), although TGF-β decreased colony numbers. In PC-3 KLF5 -/- cells with restored wild-type KLF5, although DTX treatment significantly reduced colony numbers in the presence and absence of TGF-β, this effect was greater in the absence of TGF-β (p-value < 0.01) (Figure 2.1F). Using *in vitro* cytotoxicity assay and three-dimensional colony formation assay with Matrigel, we concluded that KLF5 is essential for

TGF-β to induce DTX resistance in DU145 and PC-3 cells.

KLF5 acetylation mediates TGF-β induced DTX resistance

Previously, we found that TGF-β induced KLF5 acetylation at lysine 369 by recruiting P300 acetyltransferase. Therefore, we wanted to know if KLF5 lysine 369 mediates TGF-β–induced DTX resistance. We utilized the lentivirus system to restore wild-type KLF5 and acetylation deficient mutant $KLF5^{K369R}$ (KR) in KLF5-null DU145 cells before treatment with TGF-β and/or its inhibitor. We found that point mutation at KLF5 lysine 369 blocked TGF-β–induced DTX resistance (Figure 2.2A). In addition, we wondered if acetylated KLF5 mediates TGF-β–induced DTX resistance. Using the lentivirus system, we restored acetylation deficient mutant $KLF5^{K369R}$ (KR) and acetylation mimicking mutant $KLF5^{K369Q}$ (KQ) in KLF5 -/- DU145 and PC-3 cells. The IC50 of DTX was more than 2-fold greater in cells expressing the KQ mutant than in cells expressing the KR mutant (IC50 4.7 vs. 2.0 nM, respectively) (Figure 2.2B). KQ expression led to a more than 20% increase in cell survival percentage starting from 1 nM DTX concentration. In addition, we performed a 3D colony formation assay with Matrigel for 15 days. We found that, although DTX significantly decreased colony numbers in both KQ and KR cells, cells expressing KQ had greater colony formation than those expressing KR with 1 nM DTX treatment (Figure 2.2B). These results suggest that KLF5 acetylation at K369 induced DTX resistance in DU145 cells.

We next studied whether TGF-β–induced DTX resistance depends on acetylated KLF5. *In vitro*, 72 hours of 10 ng/μl TGF-β treatment induced a 5-fold increase in DTX IC50 (from 3.15 nM to 15.04 nM) in DU145 KQ cells and more than 7-fold increase (from 0.72 nM to 5.29 nM) in PC-3 KQ cells (Figure 2.3A-B). Moreover, TGF-β inhibition by SB-505124 successfully

eliminated the increase in IC50 induced by TGF-β treatment in both DU145 and PC-3 cells (Figure 2.3A-B). Colony formation assay in Matrigel was performed to measure DTX resistance in a three-dimensional (3D) environment (Figure 2.3C-D). In control DU145 and PC-3 KQ cells, treatment with 1 nM DTX reduced colony numbers by more than 50%. While TGF-β demonstrated a growth inhibitory effect, DTX did not inhibit colony formation of KQ cells in the presence of TGF-β. Inhibition of TGF-β by its receptor inhibitor SB-505124 sensitized KQ cells to DTX, as shown by a drastic decrease in the number of colonies surviving DTX treatment (Figure 2.3C-D left panels). Additionally, we assessed whether TGF-β induces DTX resistance in acetylation deficient mutant $KLF5^{K369R}$ (KR) cells. Interestingly, in both DU145 and PC-3 KR cells, TGF-β and its inhibition failed to change IC50 significantly (Figure 2.3A-B). Moreover, in the colony formation assay, TGF-β and its inhibition did not affect colony survival under DTX treatment (Figure 2.3C-D right panels). These results show that TGF-β requires acetylated KLF5 to induce DTX resistance.

Acetylated KLF5 induces DTX resistance *in vivo*.

Next, we conducted xenograft mouse tumorigenesis assays to explore the function of acetylated KLF5 in a pre-clinical setting. DTX was administered to nude mice 7 days after subcutaneous injection of DU145 empty vector (EV), KLF5, KR, and KQ cells in the context of KLF5 knockout as we described above. The EV and KQ groups had smaller tumor burden than the KLF5 and KR groups in the absence of DTX treatment. Consistent with a previous report [90], this suggests wild type KLF5 and acetylation deficient KLF5 promote tumor growth while acetylated KLF5 inhibits tumor growth. In DTX treated mice, we observed the largest reduction in tumor burden (tumor volume and weight) in the KR group, and no significant

reduction in the KQ group (Figure 2.3E - G). Consistent with the *in vitro* study, data from the xenograft mouse model suggests that KLF5 acetylation induces DTX resistance while acetylated deficient KLF5 sensitizes cells to DTX treatment.

Furthermore, using the tibial injection mouse model of bone metastasis, we treated mice carrying tibial tumors of KQ or KR with DTX. Tumor cells expressing KQ gave rise to more severe bone lesions than those expressing KR as indicated by radiographs of tumor-bearing tibias (Figure 2.4A). As shown with X-ray radiographs and tumor areas, we found that DTX treatment inhibited metastatic growth of KR tumors but not KQ tumors (Figure 2.4) which is consistent with findings in Figure 2.3F. As shown by radiographs at 5 weeks after the tibial inoculation of cells in Figure 2.4A, bone lesion induced by KR was significantly inhibited by DTX treatment, but not in the group injected with KQ cells. Moreover, cells with KQ rendered larger tumor areas in the bone than those with KR, as indicated by H&E staining of bones with tumors and quantitative analyses of tumor areas. DTX also suppressed the bone lesion of KR tumors but not that of KQ tumors in H&E staining of the bone lesion (Figure 2.4B, C). Interestingly, in the condition of DTX treatment, TRAP staining showed significantly reduced TRAP-positive cells in the KR group but not in the KQ group, suggesting a suppressive role of DTX on osteoclast formation in KR group, but not in the KQ group (Figure 2.4D, E). Also, tumor volume curves showed an inhibitory effect of DTX in the KR group, however, no significant reduction was observed in the KQ group under DTX treatment (Figure 2.4F, G). These findings show that KLF5 acetylation at K369 is essential in the DTX resistance of the metastatic bone lesion.

TGF-β/acetylated KLF5 signaling in prostate cancer patients

Furthermore, we performed survival analysis in prostate cancer patients conditioned on TGF-β signaling and *KLF5* mRNA status. We defined a high level of TGF-β signaling as greater than median mRNA levels of *TGFB1* and either *TGFBR1* or *TGFBR2*. We found a high level of TGF-β signal was associated with a shortened disease-free survival time (log-rank p-value = 0.018) (Figure 2.5A). Next, we performed survival analysis stratified on the *KLF5* mRNA level and TGF-β signal strength. In the 247 patients with *KLF5* mRNA level greater than the median, a higher TGF-β signal correlated with significantly shorter disease-free survival time (log-rank p-value < 0.0001) (Figure 2.5B). In contrast, in patients with a lower *KLF5* mRNA level, the TGF-β signal did not correlate with significant survival changes (log-rank ep-values > 0.05). We further performed similar Kapan-Meier analysis in a 57 patient cohort [147] in which all patients had metastatic CRPC (mCRPC). We found that high-level TGF-β was not associated with overall survival time (log-rank p-value = 0.516) (Figure 2.5C). However, in the 43 patients with *KLF5* mRNA level greater than the first quartile, a high TGF-β signal was associated with significantly shorter overall survival time (log-rank p-value = 0.019) (Figure 2.5D). This shows that TGF-β reduces overall survival time in an mCRPC patient group with a high level of *KLF5* mRNA. In short, based on the findings in two prostate cancer patient datasets, a high level of TGF-β induced a shorter survival time in patients with a high *KLF5* mRNA level.

2.4 Discussion

This chapter has revealed a phenotype that acetylated KLF5 mediate DTX resistance in advanced prostate cancer. Based on previous reports that TGF-β induces acetylation on KLF5 lysine 369 in HaCaT cells [128, 129], and prostate cancer cells [90], we found by *in vitro* and *in vivo* studies that TGF-β induced DTX resistance through the acetylation of KLF5.

TGF-β is a ubiquitously-expressed cytokine that exhibits dual function in various biological processes. Long term, high dose inhibition of the TGF-β pathway may induce increased expression of oncoproteins that were sequestered by TGF-β in the initial stages of tumor formation [148]. Indeed, a recent clinical trial evaluating the effects of TGF-β blockade by GC-1008 in metastatic breast cancer (clinical trial ID NCT01401062) has shown that blocking TGF-β alone is insufficient in controlling tumor growth even when combined with radiation [149]. Therefore, targeting the TGF-β signaling pathway for therapeutic benefit requires consideration of multimodal therapeutic strategies and biomarkers for stratification of patients based on predicted response.

We found that prostate cancer cells with acetylated KLF5 expression induced severe bone lesions and generated larger bone metastases, and were resistant to docetaxel treatment. Our findings further suggest that KLF5 acetylation could be an alternative drug target for overcoming DTX resistance in prostate cancer. In the absence of acetylated KLF5, TGF-β was compromised in inducing DTX resistance. Considering that paracrine TGF-β is present in the tumor microenvironment, the findings from the xenograft mouse model and tibial injection mouse model further support a critical role of acetylated KLF5 in DTX resistance, which thus suggests acetylated KLF5 as an alternative target of TGF-β's tumor promoter function. Notably,

as a basic transcription factor, KLF5 regulates a broad spectrum of biological processes including cell cycle progression, migration, and differentiation [85]; and inhibition of KLF5 function may induce significant off-target effect [71, 150]. At present, the taxanes docetaxel and cabazitaxel are the only chemotherapeutic agents that have a survival benefit for mCRPC patients, but virtually all mCRPCs eventually develop resistance [151], and patients with bone metastasis still have poor prognoses under docetaxel therapies [152]. Therefore, acetylated-KLF5 could be a pivotal mediator that causes the resistance of chemotherapy on bone metastases of prostate cancer patients. Therapies targeting acetylated KLF5 could provide effective strategies to harness prostate cancer bone metastasis. Therefore, KLF5 acetylation could be an alternative drug target that is more specific for inhibiting KLF5 function in drug resistance.

2.5 Figures

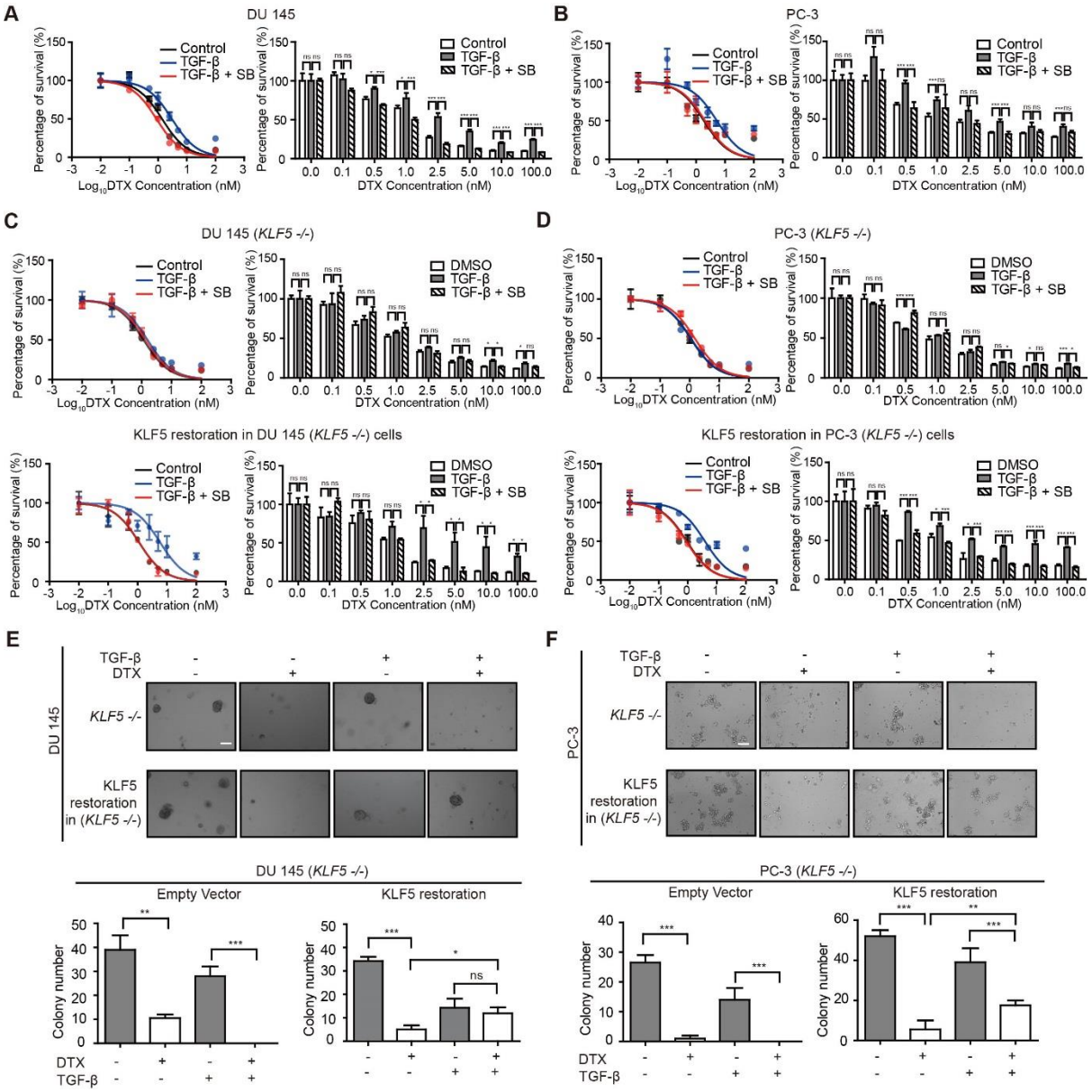

Figure 2.1. KLF5 is required by TGF-β to induce DTX resistance in prostate cancer cells. (A, B) Cytotoxicity assay in prostate cancer DU145 and PC-3 cells with concomitant treatment with docetaxel (DTX) and TGF-β1 (10 ng/μl) and/or TGF-β receptor I inhibitor, SB505124 (SB, 2.5 μM). (C, D) Cytotoxicity assay in DU145 and PC-3 cell variants with concomitant treatment with DTX and TGF-β1 (10 ng/μl) and/or SB505124 (2.5 μM). *KLF5* -/-, endogenous *KLF5* knockout. (E, F) Colony formation assay of *KLF5* -/- DU145 and PC-3

cells with or without wild type *KLF5* restoration in Matrigel treated with DTX (1 nM) and/or TGF-β1 (10 ng/μl). Cytotoxicity assay and Matrigel colony formation assay were performed in triplicate, and error bars represent the standard errors of the means. ns, $p > 0.05$; *, $p \leq 0.05$; **, $p \leq 0.01$; ***, $p \leq 0.001$. Scale bars, 100 μm. Magnification, X10. DTX: docetaxel; SB: SB-505124.

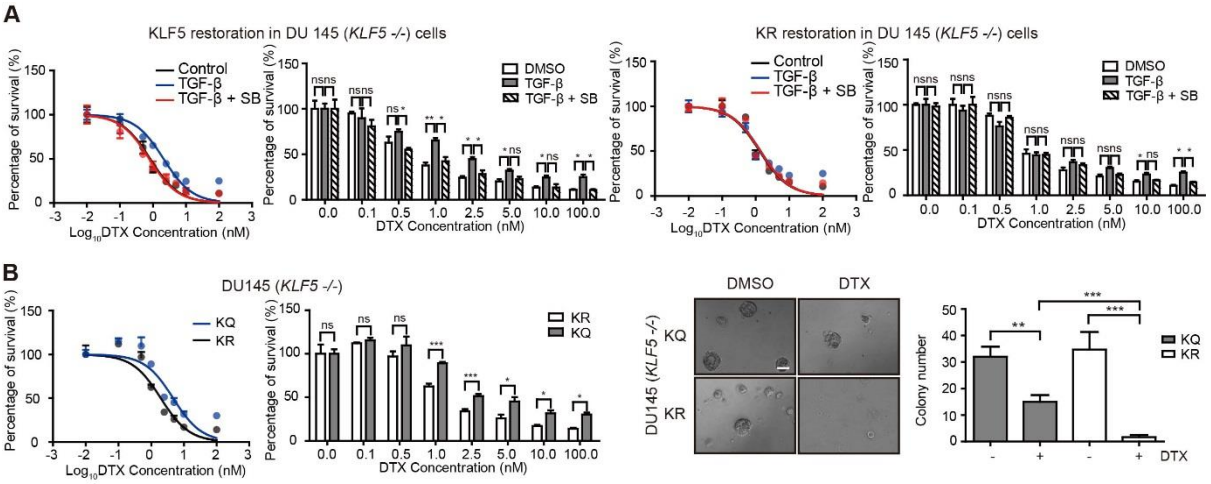

Figure 2.2. KLF5 acetylation at K369 mediates DTX resistance in prostate cancer cells. (A) Cytotoxicity assay in DU145 (*KLF5*-/-) cells expressing wild type *KLF5* and acetylation deficient mutant KLF5^{K369R} (KR) with concomitant treatment with DTX and TGF-β1 (10 ng/μl) and/or SB505124 (2.5 μM). (B) Cytotoxicity assay (left) and colony formation assay in Matrigel (right) of DU145 (KLF5-/-) cells expressing acetylation deficient mutant KLF5^{K369R} (KR) and acetylation mimicking mutant KLF5^{K369Q} (KQ) treated with DTX (1 nM). Cytotoxicity assays were performed in triplicate, and error bars represent the standard errors of the means. ns, $p > 0.05$; *, $p \leq 0.05$; **, $p \leq 0.01$; ***, $p \leq 0.001$. DTX: docetaxel; SB: SB-505124.

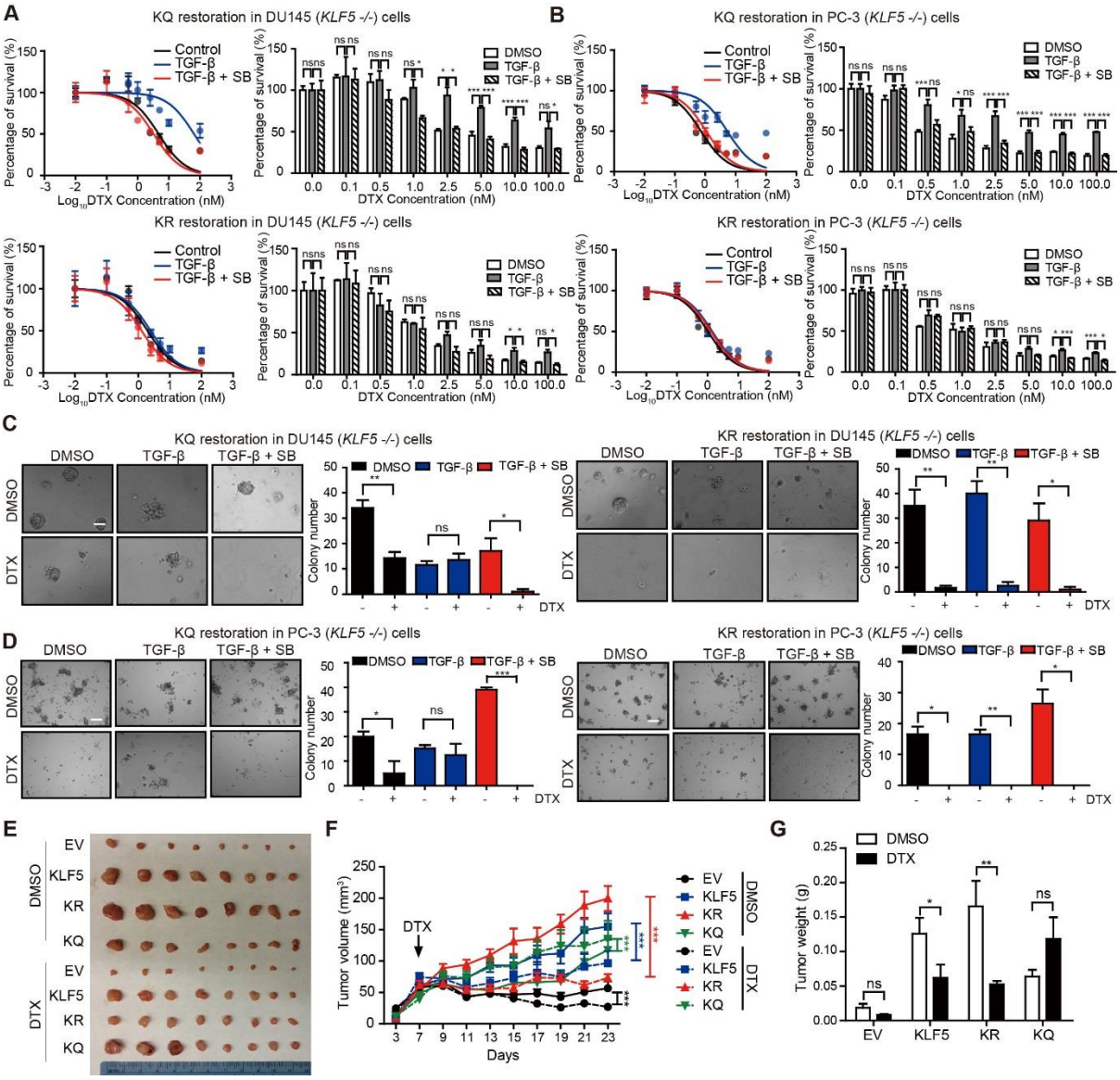

Figure 2.3. KLF5 acetylation at K369 mediates DTX resistance in prostate cancer cells. (A - D) Cytotoxicity assay of DTX (A, B) and colony formation assay with 1 nM DTX (C, D) in DU145 and PC-3 (KLF5-/-) cells expressing KR and KQ with concomitant treatment of TGF-β1 (10 ng/μl) and/or SB505124 (2.5 μM). (E - G) Xenograft tumorigenesis assay with DU145 KLF5 -/- (EV), wild-type KLF5 (KLF5), KR, KQ cells. Eight tumors from 4 nude mice were available for each group. Cytotoxicity assay and Matrigel colony formation assay were performed in triplicate, and error bars represent the standard errors of the means. ns, $p > 0.05$; *, $p \leq 0.05$; **, $p \leq 0.01$; ***, $p \leq 0.001$. DTX: docetaxel; SB: SB-505124.

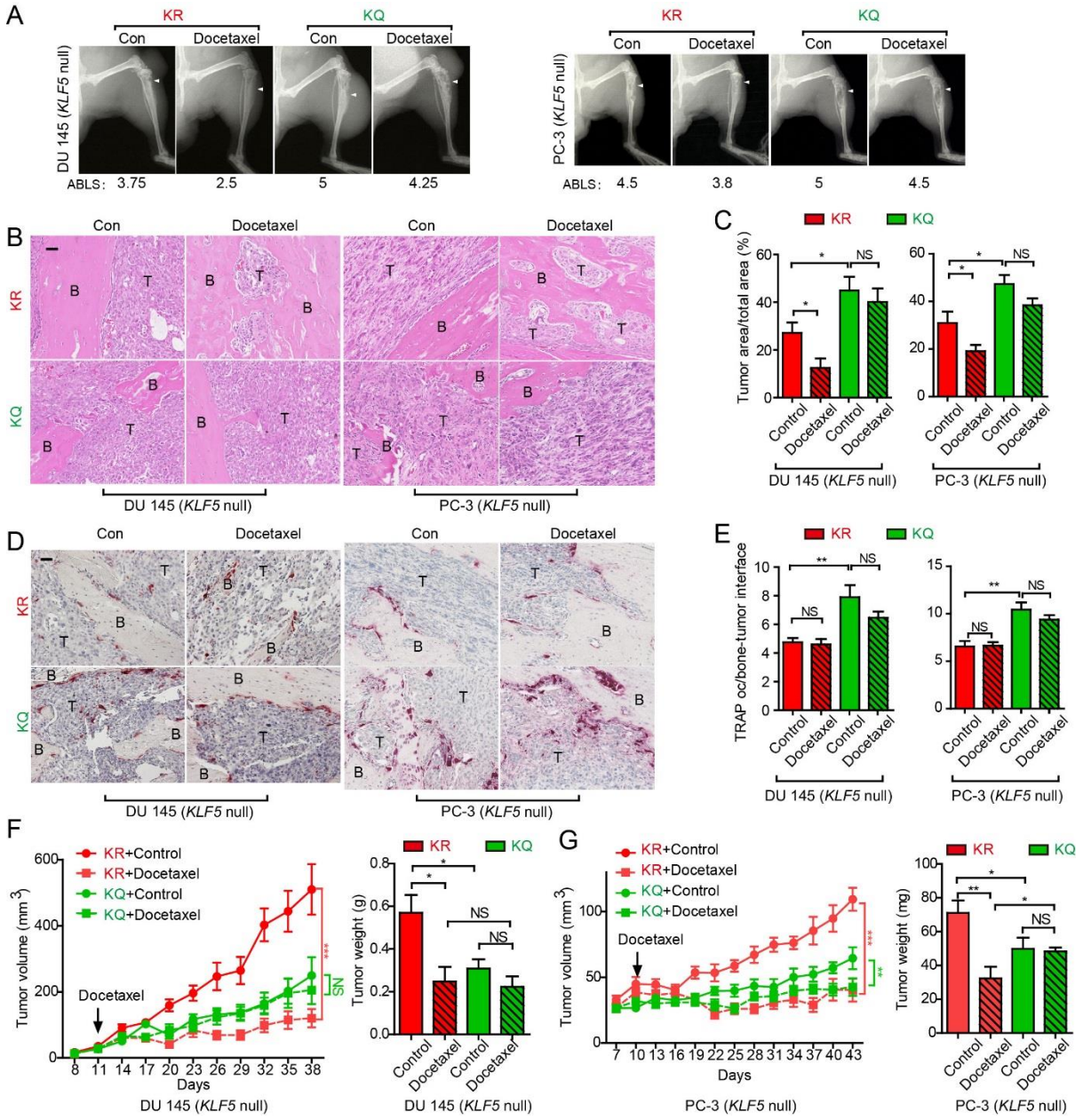

Figure 2.4. Acetylation of KLF5 mediates DTX resistance of prostate cancer cell-induced bone metastatic lesions. (A) Bone metastatic inhibition by DTX on prostate cancer cells (DU145 and PC-3) expressing different forms of KLF5 (KR and KQ), indicated by radiographs at 5 weeks after tibial inoculation of cells. DU145 and PC-3 cells with KLF5 knockout (KLF5 null) were infected with lentiviruses to express acetylation-deficient mutant KLF5K369R (KR) and acetylation-mimicking mutant KLF5K369Q (KQ). White arrows point to bone lesion areas. (B) H&E staining of tibial tumor samples from prostate cancer cells with indicated forms of

KLF5. B, trabecular bone regions; BM, bone marrow regions; T, tumor regions. (C) The ratio of tumor area to a total sample area of DU145 (Left) and PC-3 cells (right) with different forms of KLF5 in the bone conditioned on DTX treatment status. Each group had 5-8 samples. (D) TRAP staining of bone samples bearing DU145 (left) and PC-3 (right) cancer cells with different KLF5 statuses. TRAP occurrence at the interface of bone (B) and tumor (T) areas. Scale bar, 100 μm. (E) Statistical analyses of the TRAP occurrence at the bone-tumor interface in the bone samples bearing DU145 and PC-3 prostate cancer cells. For DU145 tibia tumors, KR and KQ contains 4 and 8 samples respectively. For PC-3 tiba tumors, each group contains 6 samples. (F, G) Tumor volume curves and tumor weight of tumor area in tibia in KR and KQ group conditioned on DTX treatment status.

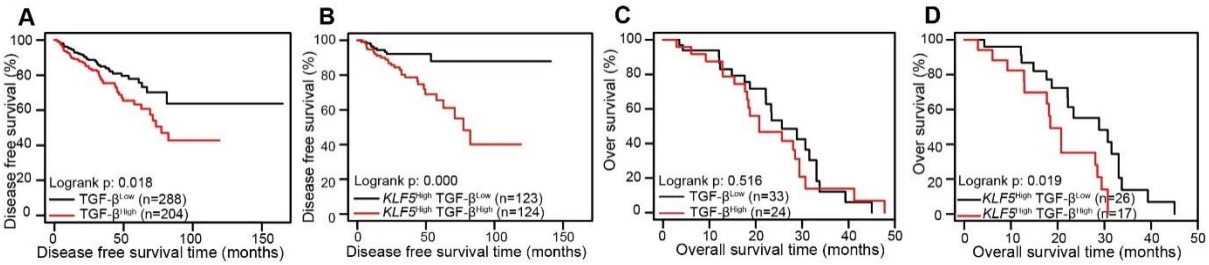

Figure 2.5. Higher TGF-β signaling activity and higher *KLF5* mRNA level correlate with poorer survival of prostate cancer patients. (A, B) Kaplan-Meier estimates of disease free survival in 492 (A) and 247 (B) patients with advanced prostate cancer (TCGA, Provisional). (C, D) Kaplan-Meier estimates of overall survival in 57 (C) and 43 (D) patients with castration-resistant prostate cancer. *KLF5*^{low}, mRNA expression z-score less than the median; *KLF5*^{high}, mRNA expression z-score greater than the median, TGF-β^{high}, *TGFB1* and either *TGFBR1* or *TGFBR2* greater than the median; and TGF-β^{low}, *TGFB1* and either *TGFBR1* or *TGFBR2* equal to or smaller than the median.

Chapter 3: Mechanisms mediating the TGF-β/acetylated KLF5 induced drug resistance in prostate cancer

3.1 Introduction

Approximately 20% of prostate cancers progress toward castration-resistant prostate cancer (CRPC) [153], and 90 % of patients with metastatic CRPC (mCRPC) develop bone metastases [154, 155]. While denosumab or zoledronic acid is used to prevent or delay skeletal-related event (SRE) of CRPC with bone metastases [156, 157], no significant cancer-specific and overall survival benefits have been observed [158]. Docetaxel and cabazitaxel are currently the only chemotherapeutic agents with a survival benefit for mCRPC patients, however, patients with bone metastasis often failed to benefit from docetaxel therapies [152]. There is also a shortage of effective treatment approaches for patients with chemoresistant bone metastases that suffer from prostate cancer.

Prostate cancer bone metastases are produced and outgrow as a multi-step process in which tumor cells and other bone marrow cells interact with each other through paracrine signals and cell surface receptors [159]. For example, paracrine signaling from tumor cells like PTHrP stimulates osteoblasts to produce RANKL [160], which promotes osteoclast differentiation and initiates bone resorption [161]. Osteolytic resorption releases more active agents such as TGF-β that promote cancer cell survival and growth, which in turn secrete additional osteolytic factors such as PTHrP, IL-11, VEGF, or MMP [161-165]. This cycle between TGF-β and osteolytic resorption is one of the mechanisms that trigger for prostate cancer bone metastases, and targeting TGF-β signaling can contribute to bone metastasis therapies [166, 167]. Although new

findings have emerged for the molecular mechanisms that underlie bone-metastatic growth of prostate cancer, the process is still poorly understood and effective treatments for patients with bone metastases are limited, in particular for inhibition of key mediators that mediate the progression of bone metastasis and its chemoresistance.

TGF-β is generated by tumor microenvironments, but advanced tumors also acquire an autocrine capacity to secrete TGF-β [168]. Although TGF-β suppresses tumor growth during the early stages of tumorigenesis, in advanced tumors it is a potent inducer of epithelial-mesenchymal transition (EMT) and bone metastasis [97, 116, 169-172].

As an apoptosis suppressor, Bcl-2 dimerizes with pro-apoptotic proteins to sequester mitochondrial outer membrane permeabilization [173]. With its pro-survival function, Bcl-2 is indispensable in the transition of prostate cancer cells from androgen-dependence to androgen-independence and correlates with the androgen-independent phenotype [174]. Bcl-2 is also reported to mediate chemotherapy resistance in various malignancies including those of the lung, lymphoid, and thyroid [175-177]. Moreover, as a result of apoptosis induced by DTX, Bcl-2 was phosphorylated and inactivated [178-180]. However, the mechanism by which Bcl-2 mediates TGF-β and acetylated KLF5-induced DTX resistance remain unknown. The present study shows that the KLF5 and TGF-β signaling axis mediates DTX resistance through transcriptionally upregulating Bcl-2 and inhibiting DTX-induced Bcl-2 degradation.

In this chapter, we explored mechanism mediating TGF-β and KLF5 acetylation induced chemoresistant of prostate cancer. Utilizing *in vitro* and bioinformatics methods, showing that TGF-β mediates docetaxel resistance by transcriptionally upregulation of Bcl-2 and inhibiting Bcl-2 degradation induced by DTX. Using small molecule inhibitor, inhibition of Bcl-2

partially reverses TGF-β induced DTX resistance. Moreover, CXCR4 could be another direct downstream target of acetylated KLF5. These findings identify an acetylation-modified transcription factor KLF5 as a key modulator of prostate cancer drug resistance and provide a rationale for the use of docetaxel plus ABT-199 in the treatment of drug resistant prostate cancer expressing Ac-KLF5.

3.2 Material and methods

Cell lines and mouse strains

PC-3 and DU145 cell lines were purchased from the American Type Culture Collection (ATCC, Manassas, VA) and propagated as described [90]. Male BALB/c nude mice (3–4 weeks old) were purchased from Charles River (San Diego, CA), and closely monitored and handled at an Emory University Division of Animal Resources facility according to the policies of the Institutional Animal Care and Use Committee.

Apoptosis and necrosis assay

Apoptosis and necrosis experiments were conducted with the RealTime-Glo™ Annexin V Apoptosis and Necrosis Assay (Promega, Madison, WI, USA) following the manufacturer's instruction.

Caspase-3/7 enzymatic activity was measured using the Caspase-Glo® 3/7 Assay System from Promega following manufacturer's instruction.

Early apoptosis was measured by staining cells with Annexin V-FITC and PI as previously described [181]. Briefly, after indicated treatments for 20 hours, cells were collected, washed with cold PBS, resuspended in 100 µl of 1 x Annexin V binding buffer, incubated with 5 µl of Annexin V and PI (BD Pharmingen) for 15 min at room temperature in the dark, and analyzed by flow cytometry. Data were analyzed with FlowJo 7.6 software.

Western blotting analysis and immunoprecipitation assay

Subconfluent cells were scraped and collected with medium, and washed with cold phosphate-buffered saline (PBS), harvested with 2x Laemmli Sample Buffer (Bio-Rad, Hercules, CA, USA) and heated at 98 °C for 5 minutes. The whole cell lysate was separated

by SDS-PAGE and blotted with nitrocellulose membranes (Bio-Rad). The membrane was blocked with 5% non-fat milk in a TBS buffer (PH 8.0) with 0.1% Tween-20, and further incubated overnight at 4 °C with primary antibody (Bcl-2 antibody: 15071, Bax antibody: 2772, Bak antibody: 12105, Bcl-xL antibody: 2764, PARP antibody: 9542, Cell Signaling Technology, Danvers, MA, USA. B-actin antibody: sc-47778, Santa Cruz Biotechnology, Dallas, TX, USA. Mcl-1 antibody: AB2910, MilliporeSigma, St. Louise, MO, USA). The membrane was rinsed 3 x 5 minutes with TBS buffer (PH 8.0) with 0.1% Tween-20 and incubated with secondary antibody (Anti-rabbit IgG, HRP-linked Antibody: 7074, Anti-mouse IgG, HRP-linked Antibody: 7076, Cell Signaling Technology) for 2 hours in room temperature. The membrane was then washed for 3 x 5 minutes in TBS buffer (PH 8.0) with 0.1% Tween-20 followed by visualization using the ECL detection system and LAS-4000 (GE Healthcare Buckinghamshire, UK).

In the immunoprecipitation assay, whole cell lysate was collected by incubating 4 hours with RIPA buffer (MilliporeSigma) supplemented with 0.5% Protease Inhibitor Cocktail (Sigma), and centrifuged at 12,000 rpm for 2 minutes at 4 °C. Cell lysate, the supernatant, was incubated with HA-Tag antibody (3724; Cell Signaling Technology) or KLF5 antibody (AF 3758; R&D Systems) overnight at 4 °C. Protein and antibody were then incubated with Protein G Sepharose beads (MilliporeSigma) for 2 hours at 4 °C. Samples were rinsed three times with 500 μl RIPA buffer before 4 °C 1,800 rpm centrifuge. Protein G pellet was suspended with 2x Laemmli Sample Buffer (Bio-Rad) and heated at 98 °C for 5 minutes.

Luciferase reporter system

BCL2 promoter LB322 plasmid (Bcl-2 from ATG to -3934) was a gift from Linda Boxer

(Addgene plasmid # 15381; http://n2t.net/addgene:15381; RRID: Addgene_15381) [182]. The jetPRIME transfection reagent (Polyplus transfection) was used for plasmid transfection according to the manufacturer's protocol. Forty-eight hours after transfection, cells were lysed with 100 µl of Passive Lysis Buffer (Promega, Madison, WI, USA), and luciferase activities were measured with the Luciferase Assay System (Promega) on a Berthold FB12 Luminometer (Berthold, Bad Wildbad, Germany). Luciferase activities were normalized by protein concentration measured by Pierce™ BCA Protein Assay Kit (Thermo Fisher Scientific, Waltham, MA, USA). Each data point was repeated in triplicate.

RNA-Seq and ChIP-Seq analyses

For RNA-Seq, DU145 cells expressing different forms of KLF5 were collected for RNA isolation and proceeded to library construction using a SE50 protocol, and the libraries were sequenced using single-end 50 bp reads on a BGISEQ-500 at BGI (Shenzhen, Guangzhou, China). PC-3 with different forms of KLF5 were collected for RNA isolation at Emory Integrated Genomics Core and proceeded to library construction and RNA-Seq at Novogene (Sacramento, CA) using paired-end 150 bp reads on a NovaSeq. FASTQ files from sequencing were quality controlled and adapter trimmed using FASTQC (v0.11.5) and mapped to the HG19 reference genome using the STAR aligner (v2.5.0a) [183]. Putative PCR duplicates were marked and removed with SAMtools (v1.7) for downstream analysis [184]. Gene expression levels were determined by the number of fragments per kilobase per million reads (FPKM), similar to a previously described procedure [185]. Briefly, reads overlapping exonic regions of UCSC HG19 known genes were determined using the 'summarizeOverlaps' function of the 'GenomicAlignments'_(v1.20.1) package in the R/Bioconductor (v3.6.1). Differentially

expressed genes were determined using edgeR (v3.26.5) with an FDR ≤0.05 determining significance [186].

DU145 cells with different forms of KLF5 (40 million cells for each) were used for ChIP assay following the procedures of SimpleChIP® Enzymatic Chromatin IP Kit (Magnetic Beads) (Cell Signaling, #9003). The CelLytic NuCLEAR Extraction Kit (Sigma, # NXTRACT) was used for nuclear extraction to enhance ChIP efficiency. The nuclear fraction of cells were digested by micrococonuclease (provided in the kit of ChIP assay) at 37°C for 20 minutes. The KLF5 antibody from R&D (#AF3758) (60 μg) was used to pull down KLF5 bound sequences. The DNA samples were sent to BGI for quality control, library construction (SE50), and sequencing with the BGISEQ-500 sequencer. FASTQ files of sequencing were quality controlled and adapter trimmed using FASTQC (v0.11.5) before mapping them to the HG19 reference genome using Bowtie (v2.2.6) [187]. Enriched regions were determined using MACS2 (v2.1.0.20151222) relative to input files with a q value (FDR adjusted p-value) of 0.05 [188]. The union of all enriched regions was determined and coverage in these regions was determined using the 'summarizeOverlaps' function in R/Bioconductor (v3.6.1) before differential analysis using edgeR (v3.26.5) where regions with an FDR ≤0.05 were considered significant [186].

Docetaxel resistant cell lines

Docetaxel resistant cell lines were established following a dose-escalation strategy. DU145 parental cells were initially cultured in medium containing 0.5 nM DTX, and then the cells were subcultured every two weeks in medium with a 50% increase in DTX concentration. DDR50 tolerated final DTX concentrations of 50 nM, and DDR100 tolerated final DTX concentrations of 100 nM.

Statistical analysis

Readings in all experiments were expressed as means ± standard errors. The statistical significance of differences between the two groups was determined by using the unpaired Student *t*-test, and *p*-values of 0.05 or smaller were considered statistically significant. Two-way ANOVA tests were used for the analysis of tumor volume curves.

3.3 Results

Acetylation of KLF5 upregulates the transcription of Bcl-2 to desensitizes cells to DTX.

We aimed to explore the mechanism of DTX resistance mediated by acetylated KLF5 and TGF-β in prostate cancer cells. First, we tested if DTX caused DU145 cell death through an apoptotic pathway. As an early indicator of apoptosis, the level of phosphatidylserine (PS) was measured using the RealTime-Glo Annexin V Apoptosis and Necrosis Assay. In DU145 cells, 10 nM DTX treatment induced a sharp increase in Annexin V signal after 24 hours of treatment as detected by luminescence; however, cell permeability was not elevated until 36 hours (Figure 3.1A). This observation shows that, rather than PS exposure and cell permeability occurring at the same time, PS exposure was observed 12 hours before cell membrane breakdown. This further indicates that DTX is an apoptosis inducer. Second, with the same assay, we found that de-acetylated KLF5 mutant induced a 1.5-fold greater level of Annexin V signal starting from 24 hours of DTX treatment (Figure 3.1B). This indicates that DTX treatment induced a stronger early apoptosis response in KR cells than in KQ cells. To identify the molecule mediating this early apoptosis event, Bcl-2, Bak, Mcl-1, Bcl-xL, Bax levels were measured in cells with different KLF5 acetylation status via Western blotting. Isogenic DU145 KLF5-null cells restored with EV, wild type KLF5, KR, and KQ had similar expression levels of Bak and Bcl-xL, while none of them expressed Bax, as confirmed by previous reports of Bax missense mutation in DU145 cells [189]. Interestingly, KQ cells had a significantly higher level of Bcl-2, while KLF5 and KQ cells had slightly increased Mcl-1 levels (Figure 3.2A).

We used a luciferase reporter system to test if acetylated KLF5 regulates Bcl-2 at the

transcriptional level. We found two predicted KLF5 binding elements (KBE) in the Bcl-2 promoter region at -1601~-1611 with sequence: CCCCTCCGCCC and -40~-50 with sequence: GCTCCCACCCC [190, 191]. Truncation mutants (KBE1: *BCL2* (-1626)-Luc and KBE2: *BCL2* (-750)-Luc) were constructed before the firefly luciferase sequence to measure relative luminance in DU145 cells (Figure 3.2B). DU145 *KLF5* null cells were first overexpressed with EV, wild type KLF5, KR, or KQ. The relative luminance in the KLF5 group was 1.2-fold greater than that in the EV group (p-values < 0.05 comparing both truncation mutants separately). Compared to the EV group, the KR group showed similar luminance (p-value < 0.05 with *BCL2* (-1626)-Luc, p value>0.05 with *BCL2* (-750)-Luc), while the KQ group showed an increase in luminance of more than 2-fold (p-values < 0.0001 comparing both truncation mutants separately). The two truncation mutants showed similar luminance, indicating that KBE1 is not the potential acetylated KLF5 regulating region. Furthermore, we knocked down KLF5 with KLF5 siRNA and found decreased luminance level to 50% of the siRNA control group (Figure 3.2C). To test if Bcl-2 mRNA levels were increased, we conducted quantitative RT-PCR. We found that relative BCL2 mRNA expression was increased by 8-fold compared to the vehicle control group and more than 4-fold compared to the wild-type KLF5 and de-acetylated KLF5 mimic groups (Figure 3.2D). In addition, as detected by Western Blotting, knockdown of KLF5 in KQ cells downregulated Bcl-2 protein level but did not affect that in KR cells (Figure 3.2E). Therefore, as a transcriptional factor, acetylated KLF5 upregulates Bcl-2 transcriptionally.

To test whether Bcl-2 upregulation plays a role in DTX resistance, we assessed the ability of a small molecule inhibitor specific to Bcl-2, ABT-199, to sensitize prostate cancer cells to

DTX treatment. Interestingly, treatment with 500 nM ABT-199 sensitized KQ cells to DTX treatment. A significantly smaller percentage of cells survived DTX treatment, and the IC50 decreased by 30% (from 3.0 nM to 1.1 nM) after ABT-199 treatment combined with DTX (Figure 3.2F). However, treatment with 500 nM ABT-199 failed to sensitize KR cells to DTX treatment (Figure 3.2G). Thus, Bcl-2 inhibition by ABT-199 successfully inhibits DTX resistance induced by acetylated KLF5.

In addition, we used an Mcl-1 specific inhibitor, S63845, to treat KR and KQ cells in the DTX cytotoxicity assay. The concentration of S63845 selected was the maximum that cells could tolerate. We found that S63845 did not significantly shift the survival curve in either KR or KQ cells (Figure 3.1C-D), suggesting that Mcl-1 does not play a significant role in TGF-β induced DTX resistance in KQ cells.

TGF-β induces KLF5 acetylation and Bcl-2 expression.

Next, we further explored the role of TGF-β in regulating Bcl-2 expression. DU145 KLF5 null cells restored with wild-type KLF5 were treated with TGF-β1 for 72 hours. Protein samples were harvested at 0, 24, 48, and 72 hours after treatment. As shown by Western blotting, TGF-β induced upregulation of acetylated KLF5 as early as 24 hours, and Bcl-2 expression starting from 48 hours (Figure 3.3A). Moreover, luciferase reporter assay showed an increase in relative luciferase activity in cells restored with wild-type KLF5 after transfection of *BCL2* (-1626)-Luc, which was further augmented by TGF-β treatment (Figure 3.3B). Real-time qPCR assay showed that TGF-β treatment increased *BCL2* mRNA level in KLF5 cells but not in EV, KR, or KQ cells (Figure 3.3C-D). These results indicate that induction of KLF5 acetylation by TGF-β is essential for TGF-β to induce *BCL2* mRNA. In cells with KLF5 null or KLF5

acetylation deficient mutant, TGF-β failed to initiate BCL2 transcription. As a TGF-β activated form of KLF5 mimic, KQ cells did not respond to TGF-β treatment. However, TGF-β inhibition by SB-505124 decreased *BCL2* mRNA level in KQ cells and decreased luciferase activity in KQ cells transfected with *BCL2* (-1626)-Luc, suggesting that TGF-β signaling is indispensable in the transcriptional activation of BCL2 by acetylated KLF5 (Figure 3.3E-F). These results further showed that TGF-β induces KLF5 acetylation, and acetylated KLF5 activated BCL2 expression depends on TGF-β signaling.

TGF-β inhibits DTX-induced Bcl-2 degradation

Inactivation of Bcl-2 is a recognized mechanism of apoptosis [192, 193], which is essential for DTX-induced cell death [194]. We thus further investigated the role of Bcl-2 induced by the TGF-β/acetylated KLF5 axis in DTX resistance. Western blotting and quantitative RT-PCR were used to measure Bcl-2 protein level and mRNA level, respectively, after DTX treatment with or without TGF-β. We observed that 10 nM DTX treatment slightly upregulated BCL2 mRNA level at 8 and 16 hours of treatment, and then downregulated it starting from 24 hours of treatment; however, the protein level was decreased starting from 16 hours of treatment (Figure 3.4A), which is ahead of the decrease in BCL2 mRNA level, suggesting that the effects of DTX on Bcl-2 protein could be attributed to reason other than transcriptional regulation. Surprisingly, the combined treatment of TGF-β and DTX failed to decrease the Bcl-2 protein level, although a lower mRNA level was observed starting from 8 hours of combined treatment (Figure 3.4B).

To further test if the increased protein level in the TGF-β and DTX combined treatment group was due to TGF-β's ability to inhibit degradation, we used cycloheximide (CHX) to block protein synthesis in KQ cells. Under protein synthesis blockade by CHX, DTX treatment

decreased Bcl-2 protein level starting from 8 hours in DU145 KQ cells, and combined treatment with TGF-β maintained the Bcl-2 protein level (Figure 3.4C). This further shows that DTX led to Bcl-2 degradation and TGF-β can inhibit the degradation induced by DTX. At the same time, the Bcl-2 protein level was not affected by CHX alone or combined with TGF-β (Figure 3.4D). TGF-β did not affect the Bcl-2 protein level, therefore, the aforementioned decrease in Bcl-2 protein level under TGF-β treatment is not due to degradation. On the other hand, although KR cells have much lower Bcl-2 level, Bcl-2 was downregulated by DTX, but maintained by treatment with TGF-β alone or the DTX and TGF-β combination in a pattern similar to KQ (Figure 3.5A-B). This result further suggests that TGF-β stabilized Bcl-2 under DTX treatment in an acetylated KLF5 independent manner.

Given the Bcl-2 stabilizing role of TGF-β under DTX treatment, we wondered if inhibition of Bcl-2 suppresses DTX resistance induced by TGF-β. As shown in Figure 3.3C-D, 10 ng/μl TGF-β treatment increased the DTX IC50 2-fold in KQ cells. Interestingly, the addition of 1000 nM ABT-199 abolished the increase in IC50 induced by TGF-β treatment (Figure 3.4E). In the early apoptosis detection assay, instead of a sharp increase of Annexin V signal at 18 hours under DTX treatment, TGF-β treatment attenuated the upregulation of the Annexin V signal. However, the addition of ABT-199 restored the induction of Annexin V signal by TGF-β (Figure 3.4F). We further measured the expression of PARP and its cleaved form in KQ cells via Western blotting and found that DTX treatment at 10 nM for 20 hours induced PARP cleavage (Figure 3.6A). However, when the cells were co-treated with DTX and TGF-β, DTX showed a weaker effect on PARP cleavage. Interestingly, combined treatment of DTX, TGF-β and ABT-199 successfully rescued the downregulation of cleaved PARP by TGF-β (Figure

3.6A). Furthermore, flow cytometry detected early apoptosis signal induced after DTX treatment in KQ cells of DU145 (Figure 3.6B). With the Annexin V+/PI- cell percentage as an indicator of early apoptosis, we observed that TGF-β alone decreased, while DTX alone increased, early apoptosis; DTX-induced early apoptosis was attenuated by TGF-β treatment, and addition of ABT-199 overcame the effect of TGF-β on DTX-induced early apoptosis (Figure 3.6B). These findings suggest that, as a potent Bc-2 selective inhibitor, ABT-199 sensitizes cells to DTX treatment by reversing the effect of TGF-β.

TGF-β stabilizes Bcl-2 during DTX treatment via inhibition of ubiquitin-dependent protein degradation.

Next, we aimed to identify the mechanism by which TGF-β inhibited DTX-induced Bcl-2 degradation. A thorough literature review reveals that Bcl-2 is degraded via ubiquitination-mediated proteasome degradation (Figure 3.5C). Therefore, we used 10 μM MG-132, a 26S proteasome inhibitor, to block proteasome-dependent degradation. MG-132 maintained the Bcl-2 protein level by reversing the downregulating effect of DTX (Figure 3.4G, 3.5D). This finding indicates that protein degradation by the 26S proteasome is the major process mediating Bcl-2 degradation. Furthermore, we explored whether poly-ubiquitination mediated the proteasome-dependent degradation of Bcl-2. We first overexpressed HA-tagged ubiquitin and Bcl-2 in 293T cells, then performed an immunoprecipitation assay to pull down Bcl-2 after 3 hours of MG-132 treatment. HA-tagged ubiquitination was detected in Western blotting assay with the HA-tag antibody. DTX treatment increased the poly-ubiquitination of Bcl2 (Figure 3.4H, Lane 1 and 2), and this was reversed by treatment with the combination of TGF-β and DTX (Figure 3.4H, Lane 2 and 3). Together, DTX induced poly-ubiquitination of Bcl-2 and

proteasome degradation, and TGF-β stabilized Bcl-2 via inhibition of Bcl-2 poly-ubiquitination.

We established two DTX-resistant DU145 cell lines, DU145 DTX Resistant 50 (DDR50), and DU145 DTX Resistant 100 (DDR100) by selection under increasing DTX concentration. DDR50 and DDR100 survived and grew in 50 nM and 100 nM DTX containing medium, respectively. Interestingly, Western blotting showed that both resistant cell lines expressed a higher level of KLF5, acetylated KLF5, and Bcl-2 (Figure 3.7A). Treatment with 500 nM ABT-199 significantly reduced cell survival with DTX treatment at 50, 100, 500, 1000 nM (Figure 3.7B). In addition, siRNA-mediated KLF5 silencing in DDR50 cells sensitized them to DTX treatment by inhibiting cell survival with DTX treatment at 100, 500, and 1000 nM (Figure 3.7C). Therefore, Bcl-2 mediated DTX resistance, and the Bcl-2 inhibitor ABT-199 significantly sensitized DDR50 cells to DTX treatment. These data also suggest that acetylated KLF5/Bcl-2 signaling could be a fundamental mechanism mediating DTX resistance.

BCL2 associates with unfavorable clinical outcomes in prostate cancer patients

Prostate cancer patient data from two datasets were used to identify the roles of TGF-β, Bcl-2, and KLF5 in prostate cancer. First, we analyzed mRNA and protein levels of BCL2 in the TCGA provisional prostate adenocarcinoma dataset with clinical information. Among the 499 patient samples, there were 187 stage I/II prostate cancer patient samples, 304 stage III, and higher prostate cancer patient samples, and 8 missing values. In addition, there were 345 samples without lymph node metastasis, 80 with lymph node metastasis, and 74 missing values. There were 458 samples without distant metastasis (M0), 1 sample with distant metastasis (M1), and 40 missing values. Moreover, there were 292 samples with a Gleason score lower or equal to 7, 206 with a Gleason score higher than 7, and 1 missing value. We found that higher BCL2

mRNA and protein levels were associated with older age, higher tumor stage, and higher Gleason score (Table 1).

In the TCGA provisional prostate adenocarcinoma dataset, KLF5 mRNA levels co-expressed with that of BCL2 with Pearson co-efficient value equal to 0.49 (p-value < 0.0001), which indicates an intermediate correlation (Figure 3.8A). Disease-free survival data obtained from the same cohort found that a higher level of Bcl-2 protein correlated with significantly shorter disease-free survival time (log-rank p-value = 0.02) (Figure 3.8B). Moreover, in two individual prostate cancer studies [147, 195], we found that in patients with previous taxane treatment, higher levels of prostate-specific antigen (greater than the median) correlated with a higher level of BCL2 mRNA (Figure 3.8C). In a prostate cancer tissue microarray, we performed immunohistochemistry staining of Bcl-2 and acetylated KLF5. We found the nuclear fraction stained with acetylated KLF5 co-localized and strongly correlated with the cytoplasmic fraction stained with Bcl-2 (Spearman co-efficient = 0.71, p-value < 0.0001) (Figure 3.8D). These findings further show that Bcl-2 and KLF5 play pivotal roles in prostate cancer progression not only *in vitro* but also in clinical prostate cancer samples.

Direct downstream targets of acetylated KLF5

In another approach to identify direct downstream target of acetylated KLF5, we performed RNA-Seq and ChIP-Seq in EV, KLF5, KR, and KQ expressing prostate cancer cells to characterize downstream genes regulated by acetylated KLF5. Overexpression of KLF5 in both DU145 and PC-3 cells induced 294 and 62 differential expressed genes respectively (Figure. 3.9A, C). While many genes were similarly regulated by KR and KQ, 84 and 32 genes were up- and down-regulated explicitly by KQ in DU145 cells (Figure. 3.9B), and the

respective numbers were 71 and 35 in PC-3 cells (Figure. 3.9D). Overlapping genes between PC-3 and DU145 cells were also observed for KLF5 (Figure. 3.9E, Table S1) and $KLF5^{KQ}$ (Figure. 3.9F, Table S2).

Furthermore, 4007 potential KLF5 bound promoter regions in DU145 cells were identified by the ChIP-Seq assay (Figure. 3.10A, Table S3). Although the majority of the binding regions were shared by KQ and KR, KQ and KR had 424 and 11 non-overlapping peaks respectively (Figure. 3.10B, Table S3), suggesting stronger binding affinities of KQ. Overlapping genes between ChIP-Seq and RNA-Seq analyses in DU145 cells revealed that promoters of some differentially expressed genes were directly bound by KLF5 (Figure. 3.10C, Table S4), and some were selectively bound by KQ (Figure. 3.10D, Table S5), identifying several directly targeted genes of KLF5 (Figure. 3.10C) and KQ (Figure. 3.10D). Some genes with differential expression in RNA-Seq did not overlap with ChIP-Seq results, suggesting that some genes are indirectly regulated by KLF5 (Figure. 3.10E, Table S6) and KQ (Figure. 3.10F, Table S7).

Integrating RNA-Seq data from DU145 and PC-3 cells, we found five genes that were upregulated and 2 downregulated by KQ in all 3 analyses (RNA-Seq in both PC-3 and DU145 and ChIP-Seq in DU145) (Figure. 3.11A). Although the promoters of *CXCR4* and *LGR6* were bound by KLF5, as revealed by the ChIP-Seq analysis, only the *CXCR4* promoter showed a differential binding between KQ and KR (Figure 3.11B). Therefore, future study should focus on CXCR4 and further characterized the transcriptional activation of CXCR4 by KQ.

3.4 Discussion

In this chapter, we uncovered the function of TGF-β and acetylated KLF5 in Bcl-2 transcriptional regulation and stabilization. Using multiple patient datasets with expression profiles and clinicopathological information, we also found that BCL2 was a potential biomarker with both prognostic and predictive functions. Lastly, we found that inhibition of Bcl-2 by ABT-199 overcomes DTX resistance. Moreover, utilizing RNA-seq and ChIP-seq techniques, we identified CXCR4 as a potential acetylated KLF5 direct target that mediates osteolytic tumor growth of prostate cancer in bone and osteoclast differentiation to promote DTX resistance. These findings establish a novel signaling pathway TGF-β/acetylated-KLF5/BCL2 that participate in DTX resistance in prostate cancer and provide a therapeutic strategy to target acetylated KLF5-expressing drug resistant prostate cancer.

Drug resistance can lead to untreatable and lethal malignancies, and thus has been investigated extensively. Among various resistance mechanisms, EMT induced by modulation of the tumor microenvironment is a prominent contributor to drug resistance [49], mainly through cancer stem cell properties [196-198] and prolonged cell cycle [199]. Notably, EMT, as a process critical for invasive and migratory phenotypes, can be activated by paracrine and autocrine TGF-β signaling [118, 200]. Moreover, TGF-β induces taxane family drug resistance in various types of cancer including prostate cancer [53, 142]. In addition to its tumor promoting properties, TGF-β is also known as a tumor suppressor due to its ability to inhibit cell proliferation [201, 202] and induce cell death [137, 138]. Similarly, in the present study, we identified a novel mechanism of TGF-β dual function regulation. We found that DTX treatment acts as a “switch” for TGF-β dual function, and Bcl-2 is a critical factor to “turn on” the adaptive resistance promoting

function of TGF-β. In the absence of DTX, TGF-β inhibits cell apoptosis by an intrinsic mechanism in which transcriptional activation of Bcl-2 was regulated via KLF5. In contrast, in the context of DTX treatment, TGF-β inhibits cell apoptosis by stabilizing Bcl-2.

Our findings suggest that the use of one or more currently available agents targeting the TGF-β/acetylated KLF5/BCL2 signaling axis is beneficial to patients with DTX-resistant prostate cancer. We demonstrated that TGF-β and Bcl-2 had potential prognostic values in prostate cancer patients (Figure 3.8B-C) and that the Bcl-2 inhibitor, ABT-199, blocked DTX resistance *in vitro* mediated by TGF-β (Figure 3.4E) and acetylated KLF5 mediated DTX resistance *in vitro* (Figure 3.2B), which warrant *in vivo* studies to test TGF-β receptor 1 inhibitor (e.g., SB-505124) and Bcl-2 inhibitor (e.g., ABT-199) for their therapeutic value in overcoming DTX resistance. Interestingly, a recent epidemiological study has shown that naftopidil, a naphthalene-based α1-adrenoceptor antagonist, reduces prostate cancer incidence due to its blocking effect on TGF-β signaling and Bcl-2 expression [203], which is consistent with our finding that lower levels of TGF-β signaling and Bcl-2 expression correlated with prolonged disease-free survival in patients with advanced prostate cancer. Therefore, as a single agent inhibiting TGF-β signaling and Bcl-2 expression, naftopidil could be an effective inhibitor of the TGF-β/acetylated KLF5 signaling axis for overcoming DTX resistance in prostate cancer.

Furthermore, our study identified several candidate biomarkers for advanced prostate cancer. Analysis of 499 prostate cancer samples and 57 mCRPC samples demonstrated that higher TGF-β signaling activity is prognostic of shorter overall survival in patients with higher *KLF5* mRNA levels. With high levels of KLF5, TGF-β could exert its function through the

acetylation of KLF5. Also, higher Bcl-2 protein level was also prognostic of worse disease-free survival. Analysis of two datasets of mCRPC patients showed that *BCL2* expression could potentially predict treatment responses in prostate cancer patients, as in patients with the history of taxane treatment, higher *BCL2* levels correlated with an elevated prostate specific antigen (PSA) level, which is the indicator of prostate cancer biochemical recurrence [204]. The bone is a major metastatic site of advanced prostate cancer, and enriched TGF-β in the bone promotes bone destruction and metastasis [205]. It is thus possible that *BCL2* expression in the primary tumor and bone metastasis could be predictive of taxane treatment response.

Considering the non-specificity of targeting a transcription factor, we identified an acetylated KLF5-downstream effector CXCR4 (Figure 3.11A-B), which was reported to mediate DTX treatment resistance [206, 207]. Therefore, further study could focus on characterizing the transcriptional activation of CXCR4 by KQ. Moreover, therapeutic inhibition of CXCR4 by its inhibitor Plerixafor (AMD3100), an FDA-approved drug for non-Hodgkin lymphoma and multiple myeloma, could be of value in determining CXCR4's function in drug resistance mediated by acetylated KLF5.

In summary, findings in this chapter have revealed that TGF-β induced DTX resistance in both intrinsic and adaptive pathways. Intrinsically, TGF-β acts through the acetylation of KLF5 to transcriptionally upregulate Bcl-2. Adaptively, with the presence of DTX, TGF-β stabilizes Bcl-2 through ubiquitination to mediate DTX resistance. Inhibition of Bcl2 by ABT-199 overcame DTX resistance. Accordingly, these results suggest that the TGF-β/acetylated KLF5/BCL2 signaling axis mediates DTX resistance in prostate cancer and that targeting this signaling axis might be a novel therapeutic approach for the treatment of chemo-resistant

prostate cancer.

3.5 Figures

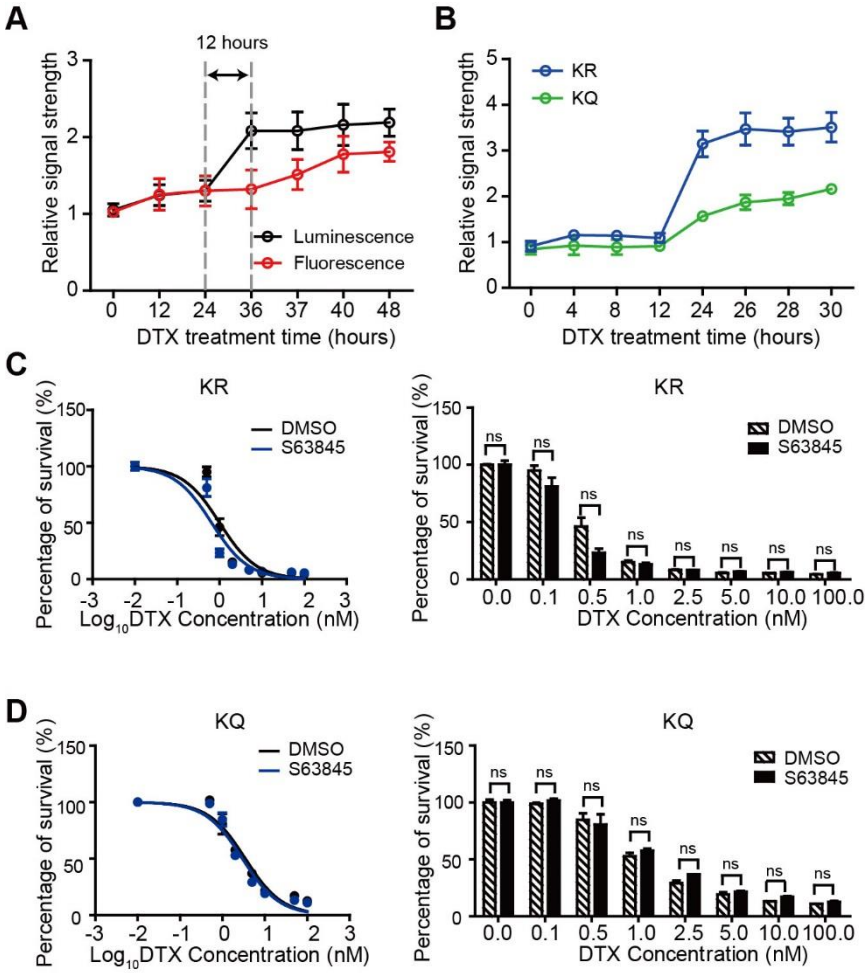

Figure 3.1. DTX is less effective in inducing early apoptosis in cells expressing acetylated KLF5, and Mcl-1 did not play an apparent role in TGF-β induced DTX resistance in KQ cells. (A, B) Apoptosis and necrosis assays were used to measure early apoptosis response in DU145 parental cells (A) and KR and KQ cells (B) with DTX treatment (10 nM). (C, D) Cytotoxicity assay of DTX-treated DU145 (KLF5-/-) cells expressing KR and KQ with or without concomitant treatment of S63845 (1 μM). Cytotoxicity assay was performed in triplicate, and error bars represent the standard errors of the means. ns, $p > 0.05$; *, $p \leq 0.05$; **, $p \leq 0.01$; ***, $p \leq 0.001$. DTX: docetaxel.

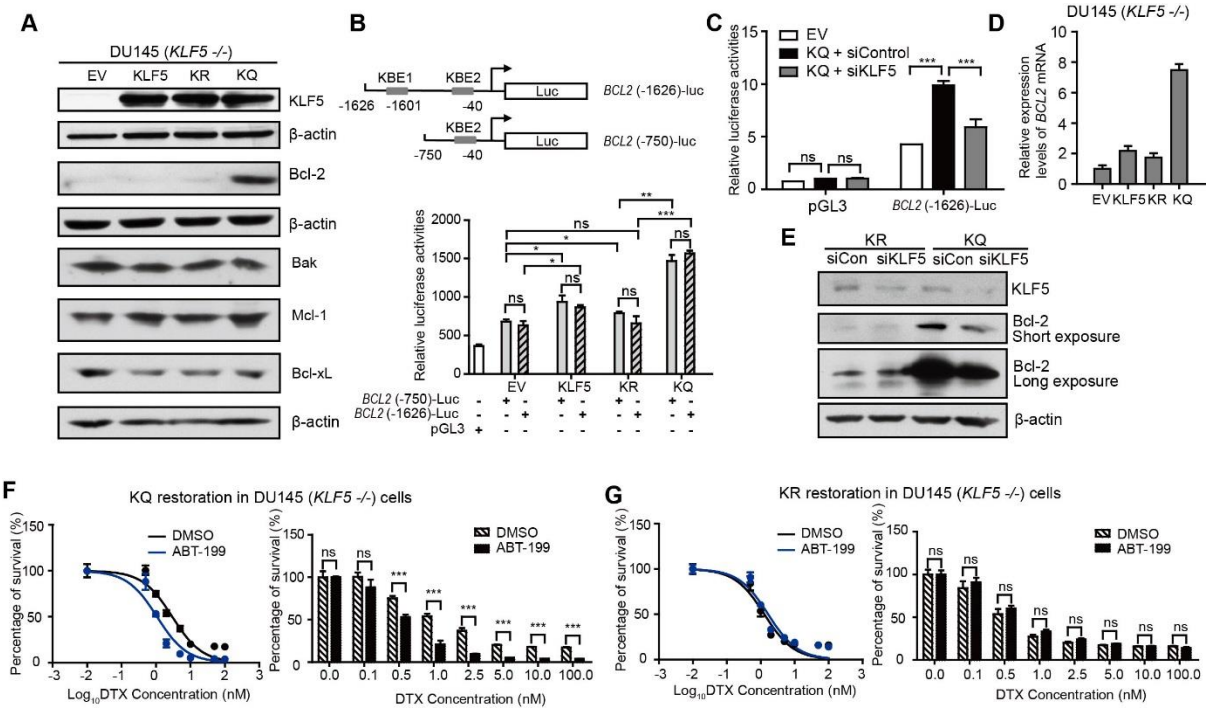

Figure 3.2. Acetylated KLF5 induces DTX resistance by upregulating Bcl-2. (A) Western blotting analysis of Bcl-2 family proteins in isogenic *KLF5* null (*KLF5* -/-) DU145 cells expressing empty vector (EV), $KLF5^{WT}$ (KLF5), $KLF5^{K369R}$ (KR), and $KLF5^{K369Q}$ (KQ). β-actin is used as an endogenous control. (B) Mapping of the promoter of *BCL2* mRNA regulated by acetylated KLF5 by transfecting *BCL2* promoter truncations with pGL3 plasmid backbone in DU145 EV, KLF5, KR, KQ cells. (C) Relative luciferase activities in EV, KQ, and KQ cells transfected with *KLF5* siRNA. (D) Relative mRNA levels of *BCL2* in DU145 EV, KLF5, KR, and KQ cells, as detected by real-time qPCR with GAPDH as an endogenous control. (E) Detection of Bcl-2 and β-actin (endogenous control) proteins by Western blotting after *KLF5* knockdown by siRNA in DU145 KR and KQ cells. (F, G) Cytotoxicity assay of DTX in DU145 KQ and KR cells treated with Bcl-2 inhibitor, ABT-199 (500 nM). Real-time qPCR assay and cytotoxicity assay were performed in triplicate, and error bars represent the standard errors of the means. ns, $p > 0.05$; *, $p \leq 0.05$; **, $p \leq 0.01$; ***, $p \leq 0.001$. DTX: docetaxel.

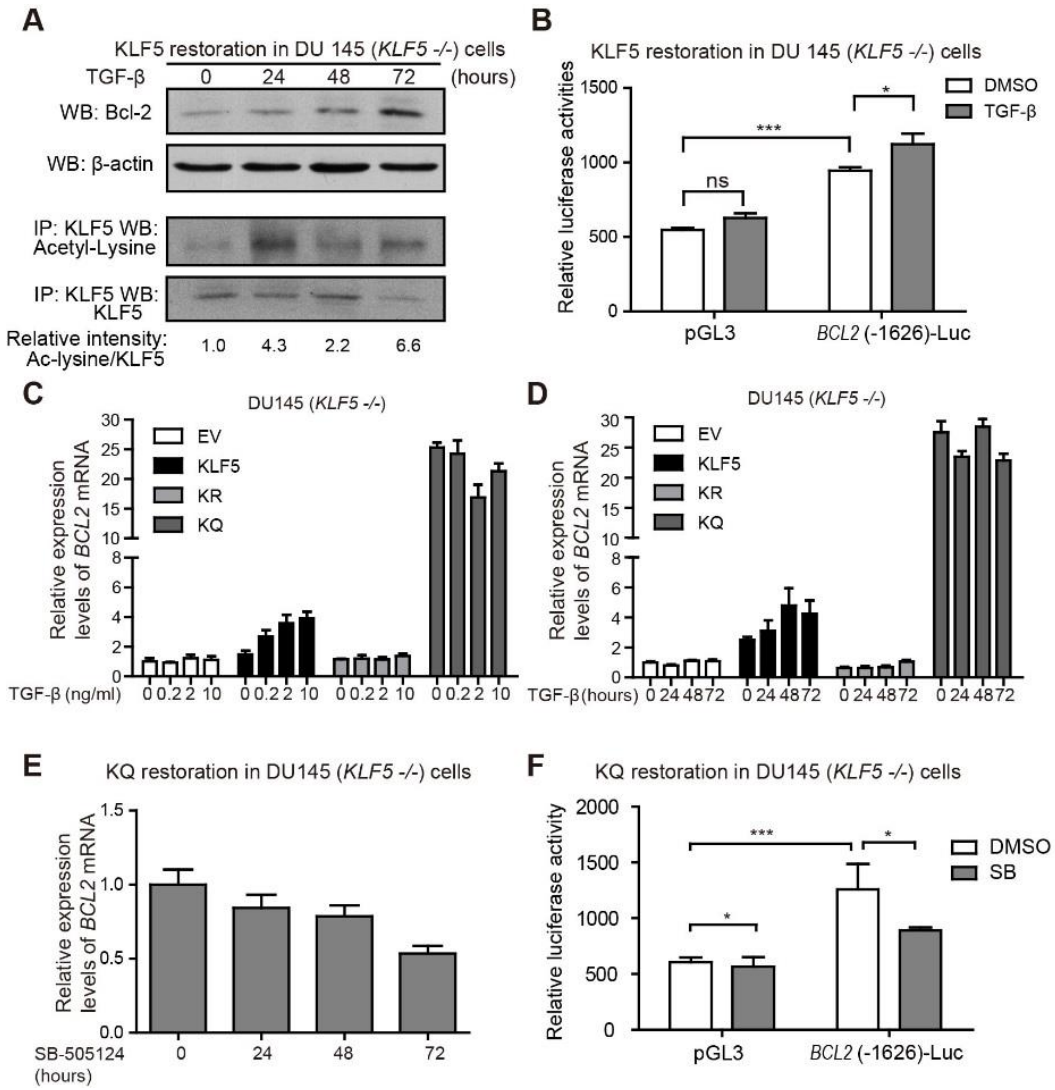

Figure 3.3. TGF-β induces KLF5 acetylation and upregulates Bcl-2 expression. (A) Western blotting analyses of KLF5 and Bcl-2 in whole cell protein lysates and acetylated lysine in KLF5 immunoprecipitated protein lysates, after 0, 24, 48, 72 hours treatment with 10 ng/ml TGF-β1. (B) Relative luciferase activities in KLF5 cells transfected with *BCL2* promoter and treated with TGF-β1. (C, D) Relative mRNA levels of *BCL2* in DU145 EV, KLF5, KR, and KQ cells treated with 0, 0.2, 2, 10 ng/μl TGF-β1 for 48 hours (C), TGF-β1 (10 ng/μl) for 0, 24, 48, 72 hours (D), as detected by real-time qPCR with GAPDH as an endogenous control. (E) Relative mRNA level of *BCL2* in DU145 KQ cells treated with 2.5 nM SB-505124 for 0, 24, 48, 72 hours, as detected by real-time qPCR with GAPDH as an endogenous control. (F)

Relative luciferase activities in KQ cells transfected with *BCL2* promoter and treated with SB-505124 (SB, 2.5 μM). Real-time qPCR assay, and luciferase activity assay were performed in triplicate, and error bars represent the standard errors of the means. ns, $p > 0.05$; *, $p \leq 0.05$; **, $p \leq 0.01$; ***, $p \leq 0.001$.

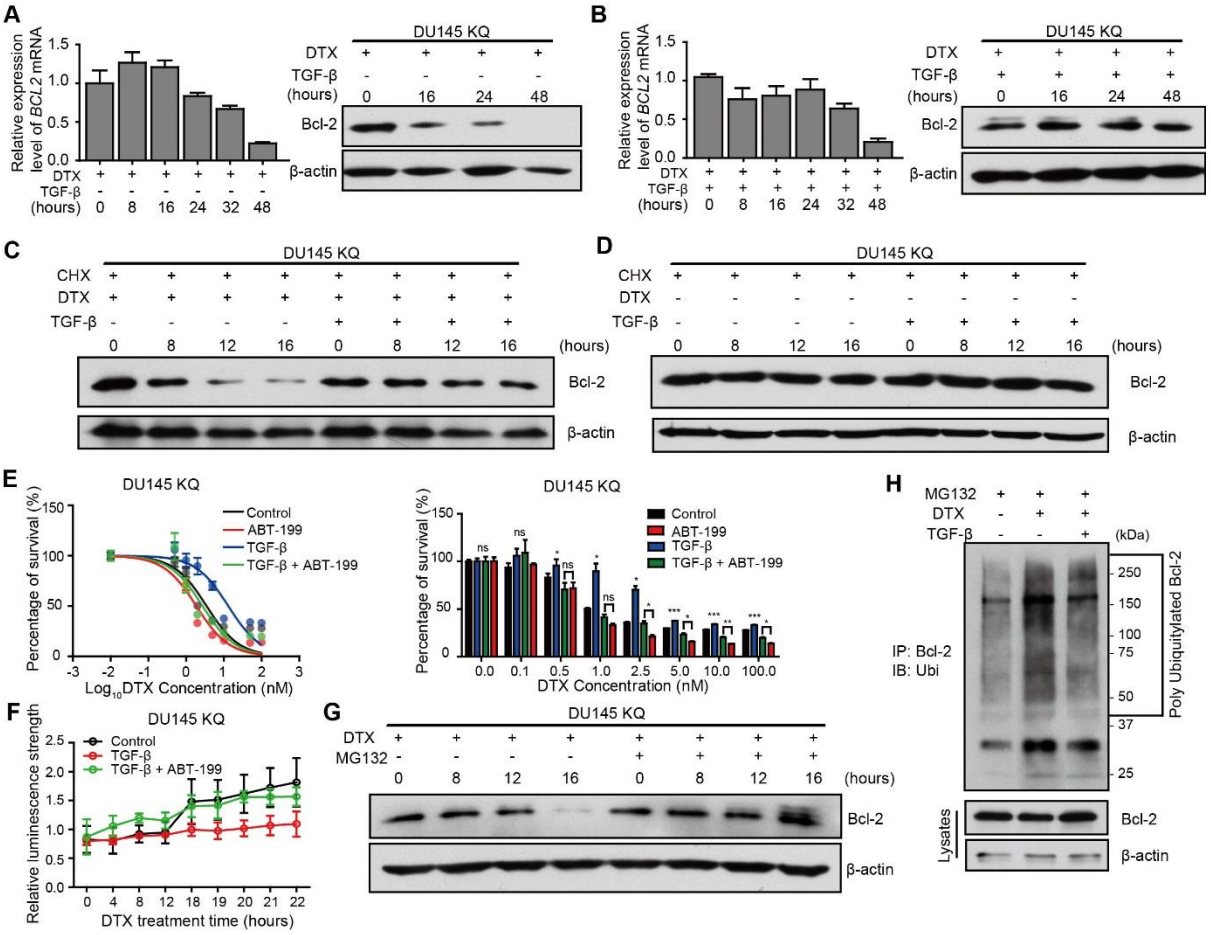

Figure 3.4. TGF-β induces DTX resistance through stabilizing Bcl-2 protein. (A, B) Detection of Bcl-2 mRNA and protein levels in DU145 KQ cells treated with DTX (10 nM) alone (A), a combination of TGF-β (10 ng/ml) and DTX (10 nM) (B) for different times as indicated by real-time qPCR (left panel) and Western blotting (middle panel) respectively. β-actin and GAPDH were used as internal controls for Western blotting and real-time qPCR, respectively. (C, D) Detection of Bcl-2 protein level by Western blotting in DU145 KQ cells treated with different combinations for different times as indicated. DTX, 10 nM; TGF-β, 10 ng/μl; Cycloheximide (CHX), 10 μM. (E) Cytotoxicity assay measuring DTX resistance in DU145 KQ cells after 72 hours of combined treatment with TGF-β (10ng/μl) and ABT-199 (1 μM). (F) Apoptosis and necrosis assay measuring DTX induced Annexin V staining in DU145 KQ cells with combined treatment with TGF-β (10ng/μl) and ABT-199 (1 μM). (G) Western

blotting analysis of Bcl-2 protein level in DU145 KQ cells over 16 hours, MG-132 (10 μM) treatment 3 hours before protein collection. (H) Western blotting analysis of HA-tagged polyubiquitination in Bcl-2 antibody precipitated protein in 293T cells overexpressing Bcl-2 and HA-tagged ubiquitin. 16 hours of DTX (10 nM), TGF-β (10 ng/μl), 3 hours of MG-132 (10 μM) prior to protein collection. Cytotoxicity assay and real-time qPCR assay were performed in triplicate, and error bars represent the standard errors of the means. ns, $p > 0.05$; *, $p \leq 0.05$; **, $p \leq 0.01$; ***, $p \leq 0.001$. DTX: docetaxel.

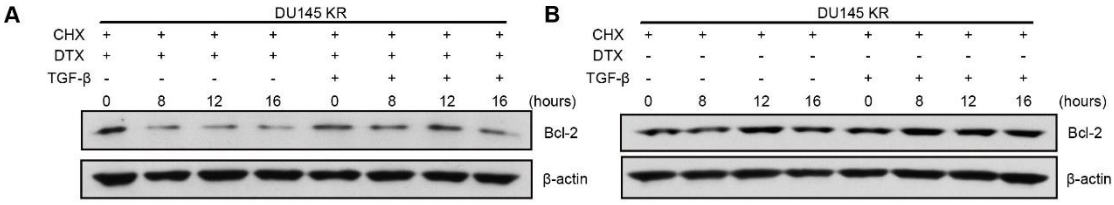

C

Mechanisms Regulating Bcl-2 Stablity.

Function	Regulation Type	Findings	Referrence
Stablize	S-nitrosylation	In H460 cells, nitric oxide induced S-nitrosylation on cystein residues.	Chanvorachote et al., 2006
		In H460 cells, Cys158 and Cys229 of Bcl-2 were nitrosylated.	Azade et al., 2006
	Phosphorylation	In HeLa cells,the MAP kinase sites Thr74 and Ser87 of Bcl-2 are phosphorylated by MAP kinase.	Breitschopf et al., 2000
	Mono-ubiquitination	In 293 cells, Parkin induced monoubiquitination on C-terminus of Bcl-2.	Chen et al., 2010
Destablize	S-denitrosylation	In HeLa, A375, and 7860, MDA-7/IL24 induced s-denitrosylation on Bcl-2.	Tian et al., 2012
	Dephosphorylation	In HUVEC cells, TNF-alpha induced dephosphorylation on Thr 56, Thr 74, and Ser 87 (major role) of Bcl-2.	Dimmeler et al., 1999
		In H460 cells , Cisplatin/hydrogen peroxide/hydroxyl radical induced dephosphorylation of Bcl-2.	Wang et al., 2008 Luanpotpong et al., 2011
	Poly-ubiquitination	In H460 cells, Cr(VI)-I induced ROS led to polyubiquintinated Bcl-2.	Azad et al., 2008
		In SW480, PPAR-alpha induced polyubiquintination on Lysine 22 with Bcl-2.	Gao et al., 2015
		In HeLa and MEF, lysine 17 of Bcl-2 was ubiquintinated by E3 ligase XIAP.	Edison et al., 2017
		In HEK293, Keap1:Cul3-Rbx1 induced polyubiquintnation on lysine 17.	Niture et al., 2011
		In 293T, FBXO10 polyubiquintinated Bcl-2.	Chiorazzi et al., 2013
	Caspases Cleavage	In Huh7, caspase 3 (major role) and caspase 9 cleaved Bcl-2, FKBP38 prevented the cleavage by binding to flexible loop domain of Bcl-2.	Choi et al., 2010

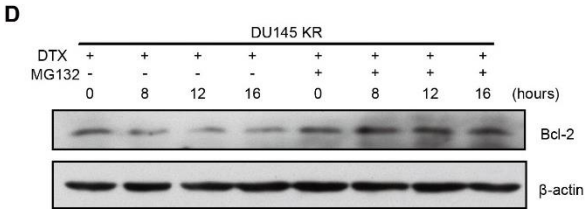

Figure 3.5. TGF-β induces DTX resistance by stabilizing Bcl-2 protein in DU145 cells expressing acetylation-deficient KLF5. (A, B) Detection of Bcl-2 protein level by Western blotting in DU145 KR cells treated with different combinations of DTX (10 nM), TGF-β (10 ng/μl), and cycloheximide (CHX, 10 μM) for the indicated time. (C) A literature review of molecular mechanisms that regulate Bcl-2 stability. (D) Western blotting analysis of Bcl-2 protein in DU145 KR cells after 16 hours of DTX treatment. MG-132 treatment was applied at 10 μM for 3 hours before protein collection. Cytotoxicity assays were performed in triplicate, and error bars represent the standard errors of the means. ns, $p > 0.05$; *, $p \leq 0.05$; **, $p \leq 0.01$; ***, $p \leq 0.001$. DTX: docetaxel.

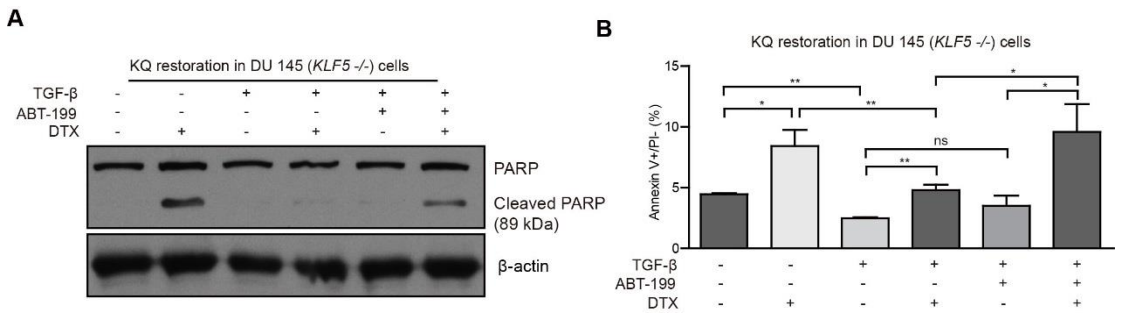

Figure 3.6. TGF-β induces DTX resistance through apoptosis inhibition. Detection of PARP and cleaved PARP protein levels by Western blotting (A) and Annexin V +/PI – cell percentage by flow cytometry analysis (B) in DU145 KQ cells treated with different combinations of DTX (10 nM), TGF-β (10 ng/μl), and ABT-199 (1000 μM) for 20 (A) or 16 hours (B). Flow cytometry analysis was performed in triplicate, and error bars represent the standard errors of the means. ns, $p > 0.05$; *, $p \leq 0.05$; **, $p \leq 0.01$; ***, $p \leq 0.001$. DTX: docetaxel.

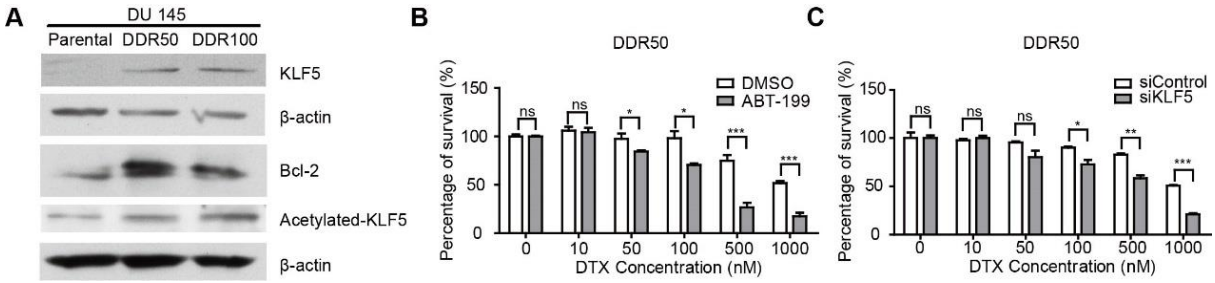

Figure 3.7. Bcl-2 mediates DTX resistance in prostate cancer cells. (A, B) Detection of KLF5, Bcl-2, and acetylated-KLF5 in parental cells and Docetaxel Resistant 50 and 100 (DDR50 and DDR100) cells of the DU145 cell line. (B) Cytotoxicity assay of DTX in DDR50 cells with or without ABT-199 treatment (500 nM). (C) Cytotoxicity assay of DTX in DDR50 cells with or without *KLF5* silencing by siRNA. Cytotoxicity assays were performed in triplicate, and error bars represent the standard errors of the means. ns, $p > 0.05$; *, $p \leq 0.05$; **, $p \leq 0.01$; ***, $p \leq 0.001$. DDR50: DTX-resistant cell lines tolerated a final DTX concentration of 50 nM; DDR100: DTX-resistant cell lines tolerated a final DTX concentration of 100 nM.

Table 1. Association of BCL2 Expression with Clinical and Pathologic Variables in 499 Primary Tumors from Prostate Cancer

		BCL2 mRNA expression (M/Y)					Bcl-2 protein expression (M/Y)		
Variable	Total Cases	Lower	Higher	*P* value (M/Y)*		Total Cases	Lower	Higher	*P* value (M/Y)*
Age (years)									
<61	223	115/49	108/174	0.428/0.009 #		139	50/50	89/89	0.002/0.002
>=61	275	132/36	143/239			126	60/60	66/66	
Stage									
I/II	187	101/116	86/71	0.198/0.035 #		85	49/40	36/45	0.009/0.003
III/IV	304	146/159	158/145			180	83/59	97/121	
Lymph node									
-	345	170/267	175/78	0.626/0.163		156	97/87	59/69	0.768/0.032 #
+	80	37/56	43/24			38	24/14	14/24	
Gleason score									
<=7	292	149/238	143/54	0.585/0.005 #		147	86/94	61/53	0.001/0.000
>7	206	100/146	106/60			118	46/50	72/68	

Data are given as number of tumors. Higher or lower BCL2 expression was relative to the median (M) of 409.17 (mRNA, TPM) and -0.13 (p, z-scores) or

* *P* values were determined by using the Pearson X2 test

The *P* value became smaller than 0.05 after the optimal cutoff point determined by the Youden Index was applied.

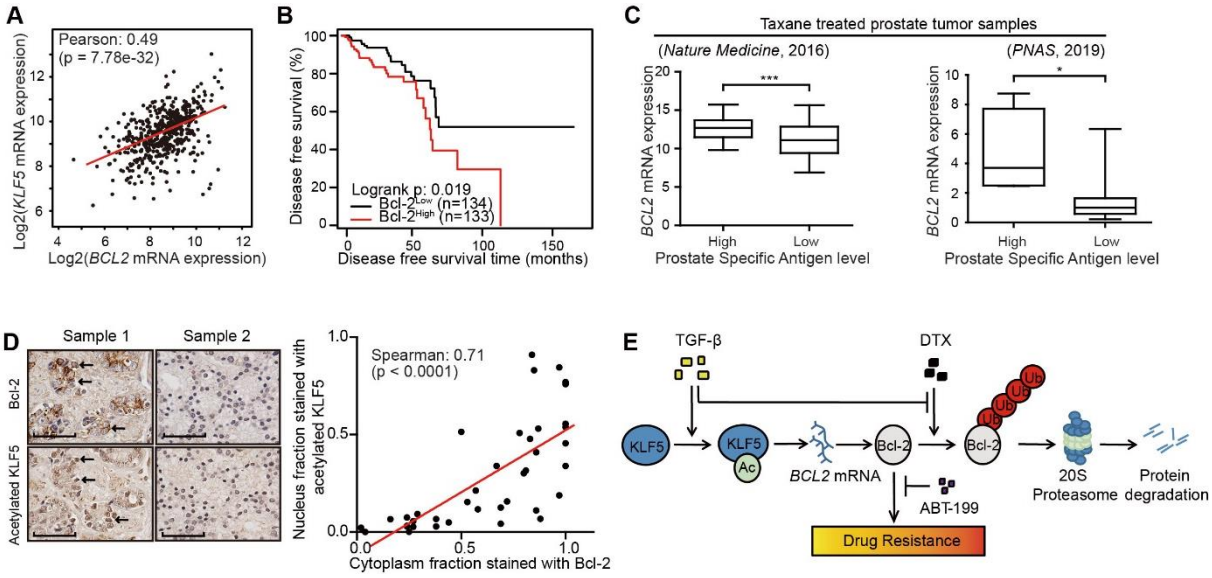

Figure 3.8. Higher acetylated KLF5 correlates with higher Bcl-2 expression and the latter associated with poorer survival of prostate cancer patients. (A) mRNA expression analysis and correlation of *BCL2* and *KLF5* from 499 prostate cancer patient samples (TCGA, Provisional). (B) Kaplan-Meier estimates of disease-free survival in 267 patients with prostate cancer (TCGA, Provisional). Bcl-2^{low}: protein expression z-score less than mean. Bcl-2^{high}: protein expression z-score greater than mean. (C) *BCL2* mRNA expression level in taxane treated prostate cancer patients with high and low prostate specific antigen (PSA) level. (D) Prostate cancer tissue arrays stained for acetylated KLF5 and Bcl-2 pictured to show the correlation of acetylated KLF5 and Bcl-2. Two representative tumor samples are shown. (E) A schematic model shows that TGF-β and acetylated KLF5 signaling axis induce DTX resistance through Bcl-2 upregulation and stabilization. Error bars represent the standard errors of the means. ns, $p > 0.05$; *, $p \leq 0.05$; **, $p \leq 0.01$; ***, $p \leq 0.001$. Scale bars, 100 μm. Magnification, X40. DTX: docetaxel.

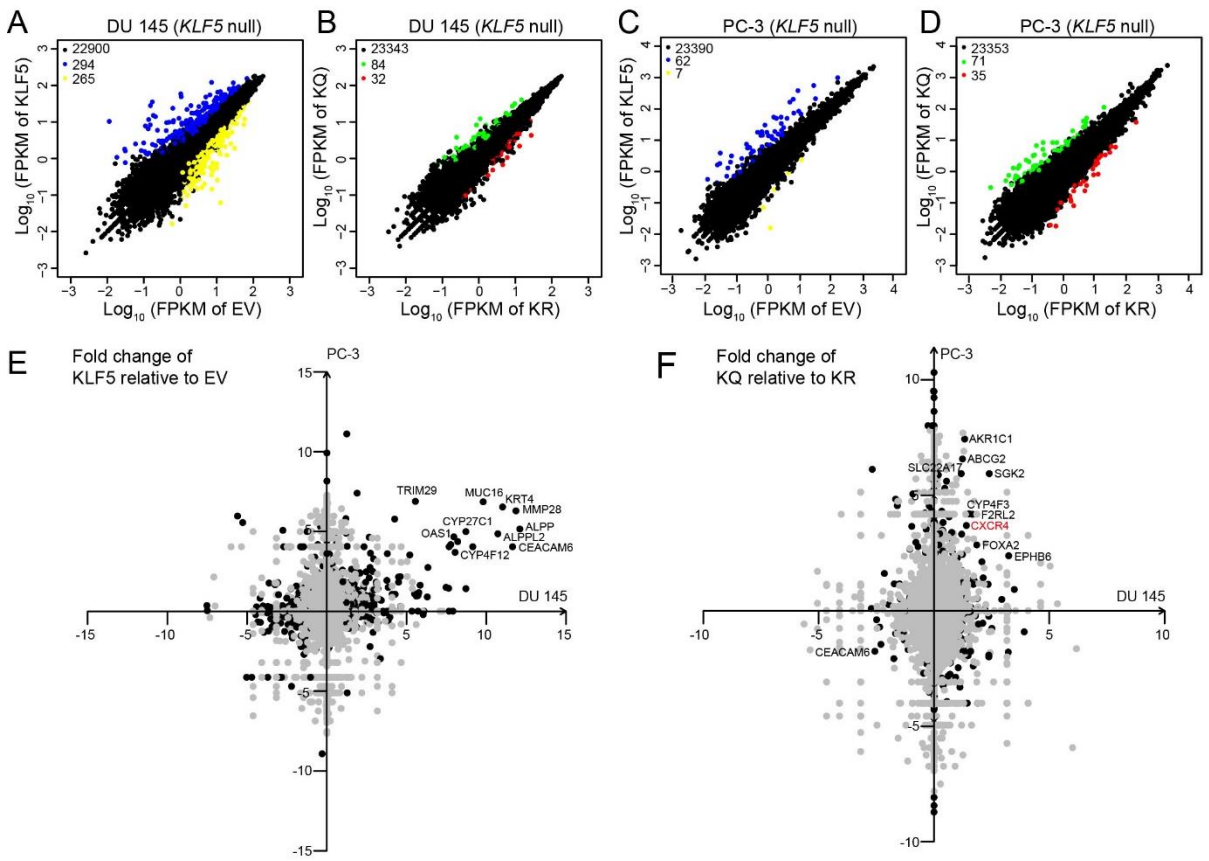

Figure 3.9. KQ and KR regulate distinct sets of genes expression in prostate cancer cells. RNA-Seq and ChIP-Seq analyses were performed using KLF5-null DU145 and PC-3 cells that ectopically expressed empty vector (EV), wildtype KLF5 (KLF5); acetylation deficient mutant KLF5K369R (KR), and acetylation mimicking mutant KLF5K369Q (KQ). (A-D) Differentially expressed genes between EV and KLF5 (A, C) or between KR and KQ (B, D) in DU145 (A, B) or PC-3 (C, D) cells. Details are available in Table S1 for DU145 and in Table S2 for PC-3 cells. Blue and yellow dots in A and C indicate the genes that were upregualted and downregulated, respectively, by KLF5 by at least 2 folds; while green and red dots in B and D indicate genes that were upregulated by KQ and KR, respectively, by at least 2 folds. The FDR adjusted p-value for the changes between EV and KLF5 or between KR and KQ was no greater than 0.001. Black dots indicate other genes. FPKM, fragments per kilobase of exon per million mapped reads. (E, F) Overlap of differentially expressed genes between EV and

KLF5 (E, details are available in Table S3) and between KR and KQ (F, details are available in Table S4.). Black dots here indicate differentially expressed genes with FDR adjusted p-value less than 0.001, and grey dots indicate others. The top ten differential genes with the same trends between DU145 and PC-3 cell lines are shown in the figures.

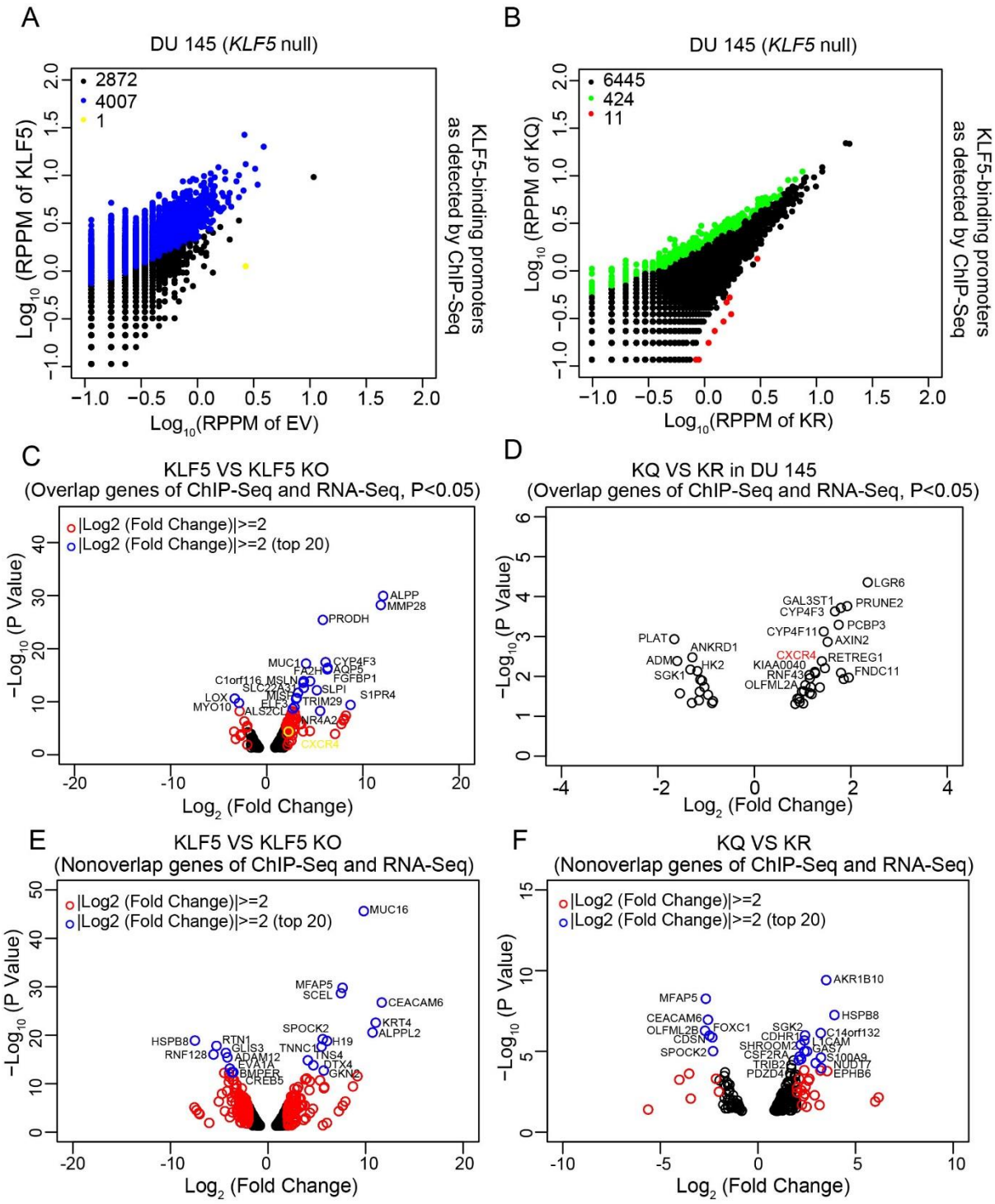

Figure 3.10. KQ and KR bind to the promoter region of distinct sets of genes in prostate cancer cells. (A, B) Promoter regions (-2500~+500) bound by KLF5 (A) and differentially bound promoter regions between KR and KQ (B), as detected by ChIP-Seq analysis using the KLF5 antibody. Blue dots and yellow dots in A indicate the enriched peaks in KLF5 and EV

group respectively, while green and red dots in B indicate KQ- and KR-enriched binding peaks respectively. All dots with the 4 colors indicate binding peaks with P values not greater than 0.01 and fold changes not less than 1.5. Black dots indicate other peaks that occurred in the promoter regions in the ChIP-Seq analysis. RPPM reads per peak per million. Details are available in Table S5. (C, D) Overlapped genes between RNA-Seq and ChIP-Seq analyses in the EV and KLF5 comparison of DU145 cells (C), in the KR and KQ comparison of DU145 cells (D). Circles indicate the genes that had both binding peaks in their promoter regions and expression changes with a P-value no more than 0.05. Details are available in Table S6. (E, F) Non-overlapped genes between RNA-Seq versus ChIP-Seq for the EV and KLF5 comparison (E, details are available in Table S8) and the KR and KQ comparison (F, details are available in Table S9) of DU145 cells. Circles indicate genes that did not have binding peaks in the ChIP-Seq analysis but had expression changes with p-values no more than 0.05. In C-F, blue and red dots indicate genes with expression changes no less than 4 fold, and blue dots indicate the 20 genes with the greatest fold changes.

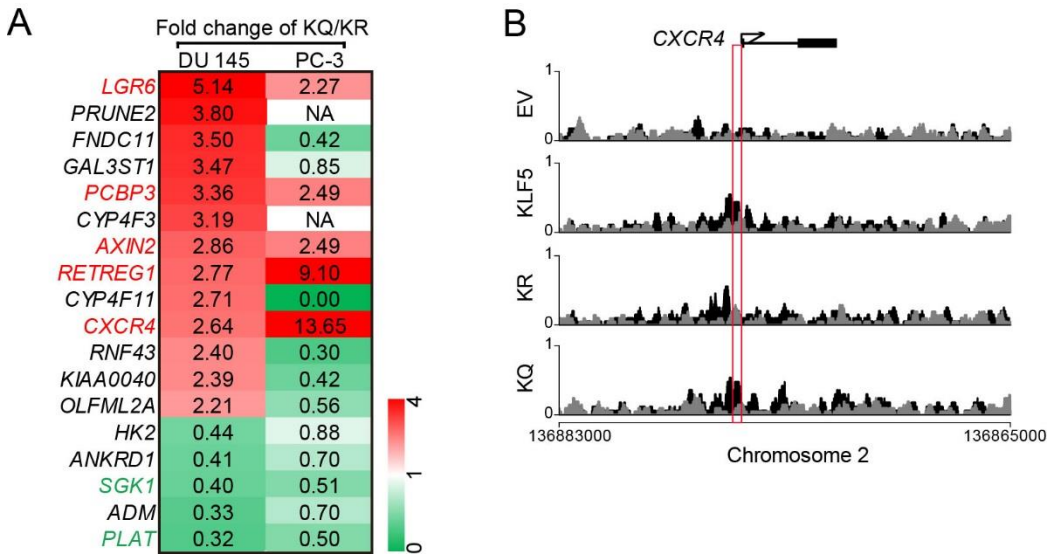

Figure 3.11. Identification of CXCR4 as a functional effector of acetylated KLF5 in the induction of osteoclast differentiation. (A) Heatmap of genes in panel A with fold changes between KQ and KR in both DU145 and PC-3 cells, as revealed by RNA-Seq analysis. Names in red and green indicate genes that are upregulated and downregulated, respectively, by KQ in both cell lines. (B) A region in the CXCR4 promoter, indicated by a red box, is specifically bound by KQ and KLF5 but not by KR, as demonstrated by ChIP-Seq analysis.

Chapter 4: Discussion

4.1 Summary and conclusions

This dissertation focused on function and molecular mechanisms associated with the KLF5 transcription factor and prostate cancer chemoresistance. Taken together (Figure 4.1), our work has shown the role of the TGF-β/acetylated KLF5 signaling axis in docetaxel resistance of prostate cancer. In Chapter 2, we demonstrated that KLF5 is indispensable in TGF-β–induced DTX resistance. Moreover, KLF5 acetylation at lysine 369 mediates DTX resistance *in vitro* and *in vivo*. In Chapter 3, we showed that the TGF-β/acetylated KLF5 signaling axis activates Bcl-2 expression transcriptionally. Furthermore, DTX-induced Bcl-2 degradation depends on a proteasome pathway, and TGF-β inhibits DTX-induced Bcl-2 ubiquitination. Moreover, utilizing RNA-seq and ChIP-seq analysis, we showed that CXCR4, which is indispensable in bone metastasis growth and docetaxel resistance, could be another direct downstream target of acetylated KLF5. At the beginning of this dissertation project, there was a gap in prostate cancer research regarding the mechanism and therapeutic strategy of docetaxel resistance in mCRPC patients. The taxanes docetaxel and cabazitaxel are the only chemotherapeutic agents that have a survival benefit for mCRPC patients, but virtually all patients with mCRPCs eventually develop resistance [151], and patients with bone metastasis still have poor prognoses with docetaxel based therapeutic regimens [152]. Our study deepened the understanding of prostate cancer biology and demonstrated that the TGF-β/acetylated KLF5 signaling axis mediates DTX resistance in prostate cancer. Pharmacological blockade of this pathway via inhibition of Bcl-2 could provide clinical insights into chemoresistance of prostate cancer.

4.2 Novel role of TGF-β/Acetylated KLF5 signaling in DTX resistance in prostate cancer

Generally, anti-cancer drug resistance mechanisms include intrinsic and adaptive mechanisms (Figure 4.2). Intrinsically, cells display properties that provide survival benefits before therapeutic intervention. Reportedly, these properties include poor drug influx or excessive efflux; drug inactivation or lack of activation; drug target alterations; and a lack of cell death induction due to dysfunctional apoptosis, which is a hallmark of cancer [208]. Specifically, major reported mechanisms that mediate DTX resistance include upregulation of the drug efflux pump that interrupts pharmacological dynamic (PD) factors such as DTX distribution in human bodies [43-45]. Docetaxel binds to β-tubulin to inhibit the depolymerization of microtubules [42]. Mutations and overexpression of β-tubulin induce docetaxel resistance by suppressing binding affinity between DTX and β-tubulin [46-48]. Also, it is reported that evasion of apoptosis via p38/p53/p21 signaling induces DTX resistance in prostate cancer [54], and alteration of mitochondrial apoptotic pathway mediates DTX resistance in breast cancer cells [55]. Our study found that TGF-β mediates DTX resistance through both intrinsic and adaptive pathways. Intrinsically, extracellular TGF-β signals act through acetylation of KLF5 to transcriptionally activate Bcl-2 to enhance its intrinsic anti-apoptotic ability. Adaptively, in response to DTX treatment, prostate cancer cells utilize TGF-β signals to stabilize Bcl-2. As an anti-apoptotic molecule, Bcl-2 accumulates in the cell due to upregulated expression and inhibition of degradation. Therefore, TGF-β mediates DTX resistance through both intrinsic and adaptive pathways.

KLF5 is indispensable for tumor formation and chemo-resistance, and its acetylation modifies the state of tumor cells. Our study found that knockout of KLF5 in prostate cancer

cells dramatically inhibited the tumor formation both subcutaneously and in the tibia, indicating a necessity of KLF5 in tumorigenesis of prostate cancer cells. The KLF5-knockout cells hardly form tumors in xenograft models and exhibit a drug-sensitive cell state. Overexpression of KLF5 rendered significant drug resistance in the context of TGF-β treatment *in vitro* and *in vivo*. Collectively, KLF5 is indispensable for prostate cancer cells to tumor formation and chemo-resistance.

Our study also showed that acetylated KLF5 is a crucial cell state modifier. We found that acetylated KLF5 mediates docetaxel resistance in *in vitro* assays, xenograft and orthotopic mouse models. As a downstream effector of the TGF-β pathway, acetylated KLF5 activates the expression of BCL2 and CXCR4, in addition to other reported genes including p15 and MYC [63, 90, 93, 129, 209]. Functionally, acetylated KLF5 modifies the prostate cancer cell state by promoting an anti-apoptotic cell state in response to DTX and pro-survival cell state in bone metastasis.

4.3 Clinical implications

Our findings suggest that targeting the TGF-β/acetylated KLF5 signaling axis is beneficial to patients with DTX-resistant prostate cancer. First, we found that pharmacological inhibition of Bcl-2 overcame DTX resistance *in vitro*. We further found that ABT-199, a BCL2 inhibitor, exerts cytotoxic effects in combination with docetaxel, which is consistent with our finding that TGF-β/acetylated KLF5 signaling played a major role in DTX resistance. Therefore, our study provides a candidate inhibitor that could effectively inhibit DTX resistance in prostate cancer.

Emphasizing the indispensable role of KLF5 in prostate cancer chemo-resistance, our findings further suggest that KLF5 acetylation status could be an alternative drug target to overcome DTX resistance in prostate cancer. In the absence of acetylated KLF5, TGF-β was prevented from inducing DTX resistance and facilitating tumor bone metastasis formation. Considering that paracrine TGF-β signaling in the tumor microenvironment, the findings from the xenograft and orthotopic mouse models further support a critical role of acetylated KLF5 in DTX resistance. As a basic transcription factor, KLF5 regulates many biological processes including migration, cell cycle progression, and differentiation [85]; and inhibition of KLF5 function may interrupt normal tissue homeostasis [71, 150]. Therefore, KLF5 acetylation could be an alternative drug target specific to drug resistance.

Additionally, our study identified several candidate biomarkers for advanced prostate cancer. Using clinical patient sample expression profiles, we demonstrated that higher TGF-β signaling activity is prognostic of shorter overall survival in patients with higher *KLF5* mRNA levels. Also, higher Bcl-2 protein levels were prognostic of worse disease-free survival. We also found that *BCL2* mRNA expression could potentially predict treatment responses in patients with mCRPC. In patients with a history of taxane treatment, higher levels of BCL2 correlated with higher levels of PSA, the biochemical recurrence indicator for prostate cancer [204]. As a major site of metastasis for advanced prostate cancer, the bone has a high level of TGF-β which was reported to promote bone destruction and metastasis [205]. It is thus possible that BCL2 expression in the primary tumor and bone metastases could be a predictor of taxane treatment response.

4.4 Future directions

The overarching goal of this research was to characterize mechanisms mediating TGF-β/acetylated KLF5 induced docetaxel resistance in advanced-stage prostate cancer. This goal was built on the clinical problem that almost all prostate cancer patients receiving docetaxel eventually develop docetaxel resistance.

Regarding the roles of Bcl-2 in TGF-β/acetylated KLF5 induced docetaxel resistance, one future direction would be to determine whether Bcl-2 inhibition can overcome prostate cancer docetaxel resistance in a preclinical mouse model with xenograft and tibial injection of prostate cancer cells. To observe the potential therapeutic effect of inhibition of Bcl-2, we would measure the tumor growth and perform survival analysis of mice treated with the Bcl-2 inhibitor ABT-199 and DTX. We could also explore the combined effect of the two drugs to further characterize the interaction of ABT-199 and DTX *in vivo*. Such a preclinical study would also inform future clinical trials.

We reported that CXCR4 could be a direct downstream target of the TGF-β/acetylated KLF5 signaling axis. CXCR4 is a key player in the retention and survival of human acute myeloid leukemia blasts and other type of human cancer cells, and inhibition of CXCR4 is reported to downregulate BCL2 via altered miR-15a/16-1 expression [210]. One future direction would be to determine the interaction between Bcl-2 and CXCR4 in the context of mCRPC. It is plausible that inhibition of CXCR4 would downregulate Bcl-2 to further sensitize cells to docetaxel treatment.

Furthermore, we used H&E staining to explore the role of growth-factor angiogenesis *in vivo*. Xenograft tumors from mice injected with DU145 EV, KLF5, KR, and KQ cells were

H&E stained to measure microvessel number and area (Figure 4.3). Cells overexpressing KLF5 showed significantly greater vessel numbers and larger vessel areas when compared to the empty vector (EV) group, suggesting that KLF5 mediates angiogenesis *in vivo*. Also, the KQ group also had larger vessel numbers and vessel areas when compared to the KR group, even though vessel number and area in the KQ group were smaller than that in the KLF5 group (Figure 4.3B, C). These findings suggest that acetylated KLF5 rather than deacetylated KLF5 mediates angiogenesis *in vivo*. The reason for KQ being less effective in inducing angiogenesis than KLF5 remains to be determined, but one possibility is that KQ cells proliferate at a much lower rate. Considering that KR tumors are larger than KQ tumors yet KQ tumor-induced more angiogenic (Figure 4.3), it would be interesting to examine whether and how prostate cancer cells use both acetylated and de-acetylated forms of KLF5 in angiogenesis.

Similar to DU145 and PC-3 cells, we established C4-2 (KLF5 -/-) cells using the CRISPR-Cas9 technique. C4-2 cells are AR-positive and express TGF-β receptors. We then ectopically expressed empty vector (EV), wild-type KLF5 (KLF5), acetylation deficient KLF5 (KR), and acetylation mimicking KLF5 (KQ) in the C4-2 (KLF5 -/-) cells. We treated the EV, KLF5, KR, and KQ cells with TGF-β and its inhibitor in DTX cytotoxicity assays. Similar to DU145 and PC-3 cells, we found that wild-type KLF5 and KQ mediated TGF-β induced DTX resistance, but KR did not (Figure 4.4A-D), indicating that the result in AR-positive C4-2 cells is consistent with DU145 and PC-3 cells and suggesting that AR does not play a major role in TGF-β mediated DTX resistance. The interaction of AR and TGF-β/acetylated KLF5 signaling is a meaningful point to investigate in future studies.

In summary, this thesis has revealed that the TGF-β/acetylated KLF5 signaling axis

mediates DTX resistance in prostate cancer through transcription activation and stabilization of Bcl-2. Targeting this signaling axis by ABT-199 might be a novel therapeutic approach for the treatment of chemo-resistant prostate cancer.

4.5 Figures

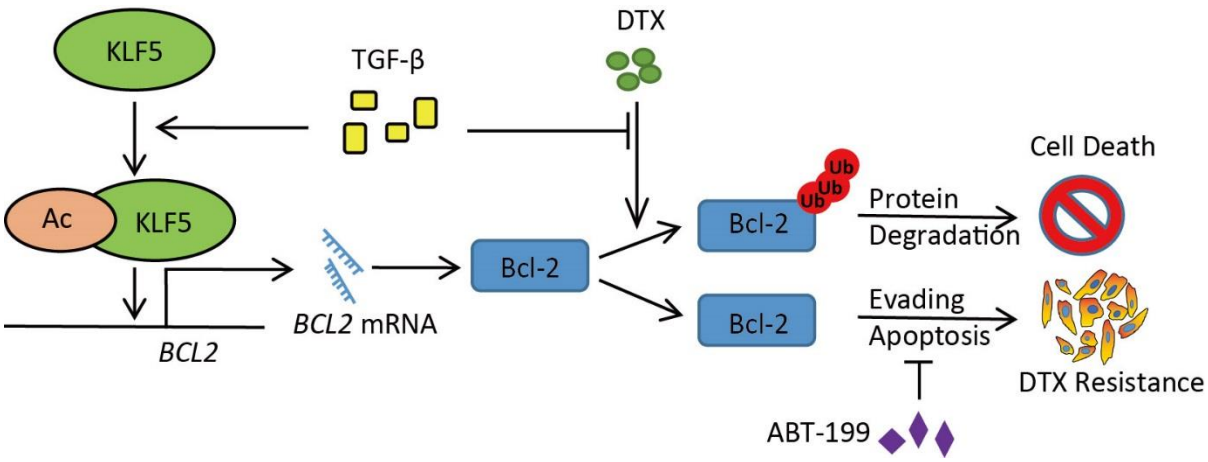

Figure 4.1 Summary of dissertation findings. TGF-β/acetylated KLF5 signaling axis in the docetaxel resistance of prostate cancer.

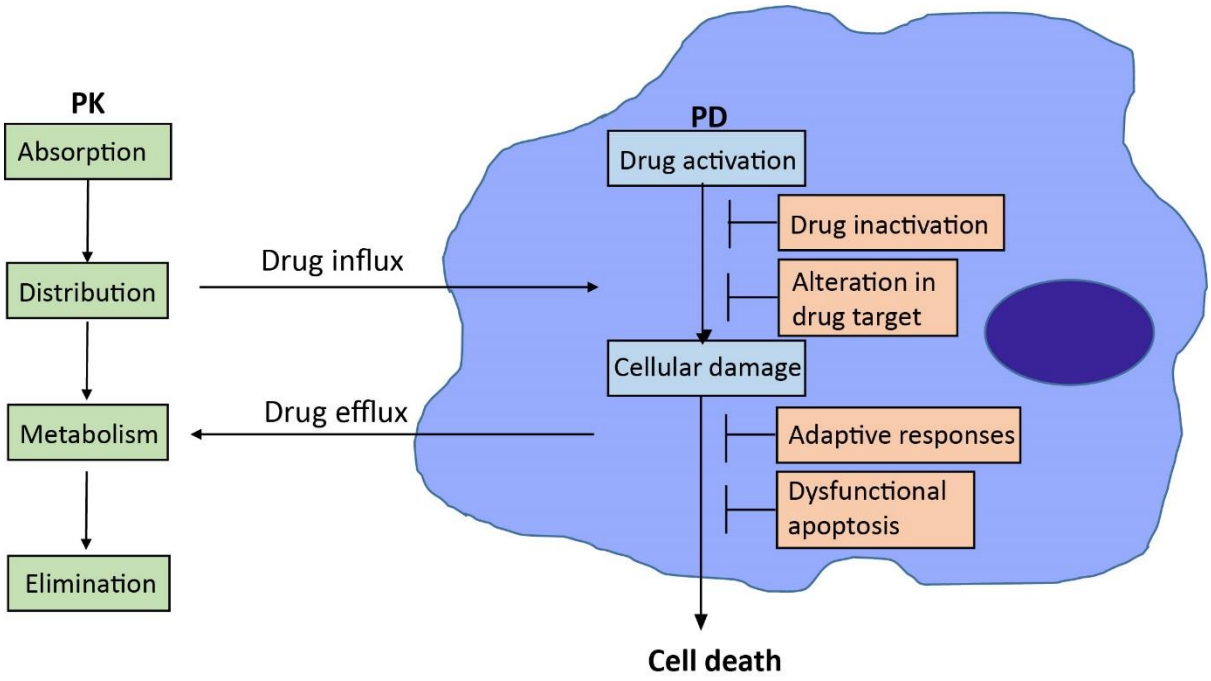

Figure 4.2: Cancer drug resistance mechanism in human cancer. Pharmacokinetic (PK) factors including drug absorption, distribution, metabolism and elimination (ADME) affect treatment efficacy in human cancer. In the tumour, pharmacodynamic (PD) processes mediates drug activation and cellular damage of the drug in cancer cells. Adapted from Holohan C, et al., *Cancer drug resistance: an evolving paradigm*, Nature Reviews Cancer, 2013

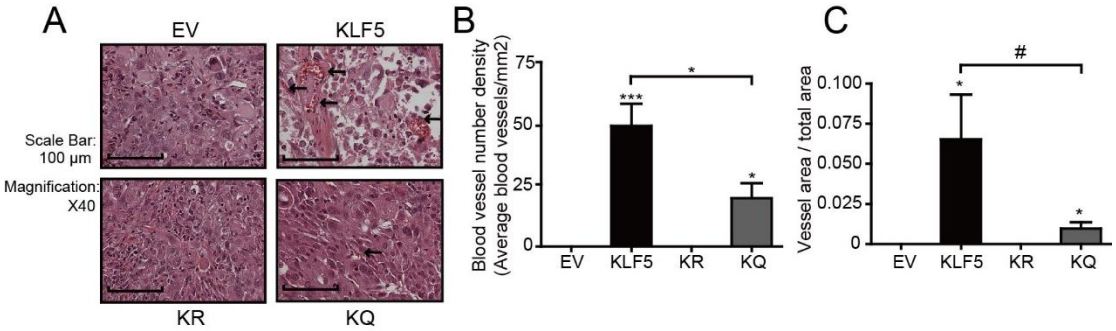

Figure 4.3: KLF5 promotes angiogenesis *in vivo*. (A) H&E staining of xenograft tumor expressing different KLF5 status. (B, C) Quantification of blood vessel number density (B) and vessel area percentage (C).

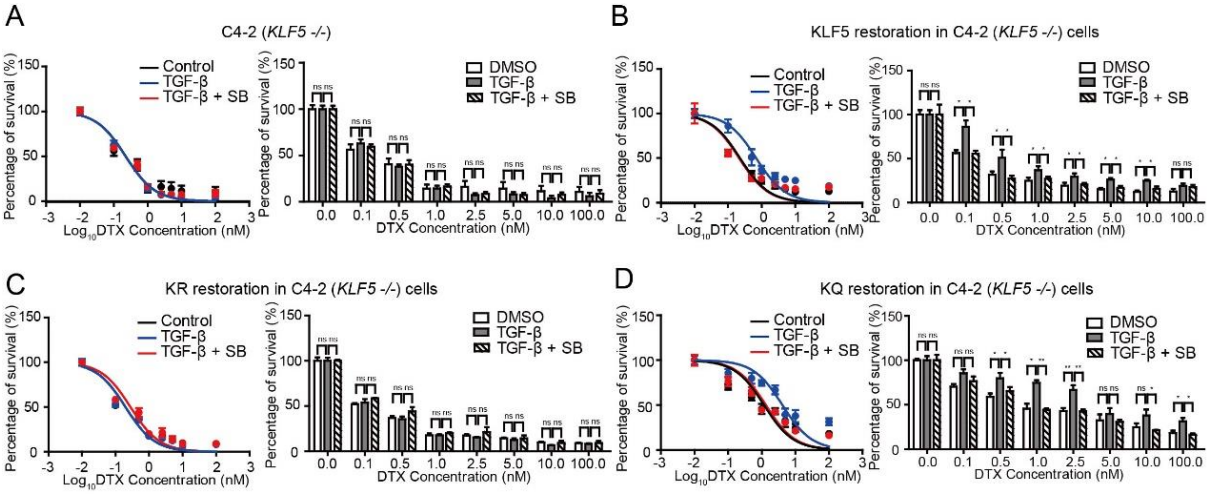

Figure 4.4. KLF5 in its acetylated form is required by TGF-β to induce DTX resistance in prostate cancer AR+ cells. (A-D) Cytotoxicity assay in prostate cancer C4-2 cells with different KLF5 status concomitant treatment with docetaxel (DTX) and TGF-β1 (10 ng/μl) and/or TGF-β receptor I inhibitor, SB505124 (SB, 2.5 μM). *KLF5 -/-*, endogenous *KLF5* knockout. Cytotoxicity assay was performed in triplicate, and error bars represent the standard errors of the means. ns, $p > 0.05$; *, $p \leq 0.05$; **, $p \leq 0.01$; ***, $p \leq 0.001$. DTX: docetaxel; SB: SB-505124.

References

1. The L. GLOBOCAN 2018: counting the toll of cancer. *Lancet* 2018;**392**: 985.

2. Siegel RL, Miller KD, Jemal A. Cancer statistics, 2019. *CA Cancer J Clin* 2019;**69**: 7-34.

3. Hanahan D, Weinberg RA. The hallmarks of cancer. *Cell* 2000;**100**: 57-70.

4. Hanahan D, Weinberg RA. Hallmarks of cancer: the next generation. *Cell* 2011;**144**: 646-74.

5. Couzin-Frankel J. Breakthrough of the year 2013. Cancer immunotherapy. *Science* 2013;**342**: 1432-3.

6. Horne SD, Pollick SA, Heng HH. Evolutionary mechanism unifies the hallmarks of cancer. *Int J Cancer* 2015;**136**: 2012-21.

7. Catalona WJ, Richie JP, Ahmann FR, Hudson MA, Scardino PT, Flanigan RC, DeKernion JB, Ratliff TL, Kavoussi LR, Dalkin BL, Waters WB, MacFarlane MT, et al. Comparison of Digital Rectal Examination and Serum Prostate Specific Antigen in the Early Detection of Prostate Cancer: Results of a Multicenter Clinical Trial of 6,630 Men. *J Urol* 2017;**197**: S200-S7.

8. Moyer VA, Force USPST. Screening for prostate cancer: U.S. Preventive Services Task Force recommendation statement. *Ann Intern Med* 2012;**157**: 120-34.

9. Siegel RL, Miller KD, Jemal A. Cancer statistics, 2016. *CA Cancer J Clin* 2016;**66**: 7-30.

10. Bibbins-Domingo K, Grossman DC, Curry SJ. The US Preventive Services Task Force 2017 Draft Recommendation Statement on Screening for Prostate Cancer: An Invitation to Review and Comment. *JAMA* 2017;**317**: 1949-50.

11. Fenton JJ, Weyrich MS, Durbin S, Liu Y, Bang H, Melnikow J. Prostate-Specific Antigen-Based Screening for Prostate Cancer: Evidence Report and Systematic Review for the US Preventive Services Task Force. *JAMA* 2018;**319**: 1914-31.

12. Force USPST, Grossman DC, Curry SJ, Owens DK, Bibbins-Domingo K, Caughey AB, Davidson KW, Doubeni CA, Ebell M, Epling JW, Jr., Kemper AR, Krist AH, et al. Screening for Prostate Cancer: US Preventive Services Task Force Recommendation Statement. *JAMA* 2018;**319**: 1901-13.

13. Zong Y, Goldstein AS. Adaptation or selection--mechanisms of castration-resistant prostate cancer. *Nat Rev Urol* 2013;**10**: 90-8.

14. Chandrasekar T, Yang JC, Gao AC, Evans CP. Mechanisms of resistance in castration-resistant prostate cancer (CRPC). *Transl Androl Urol* 2015;**4**: 365-80.

15. Lorente D, Mateo J, Perez-Lopez R, de Bono JS, Attard G. Sequencing of agents in castration-resistant prostate cancer. *Lancet Oncol* 2015;**16**: e279-92.

16. Cunha GR, Cooke PS, Kurita T. Role of stromal-epithelial interactions in hormonal responses. *Arch Histol Cytol* 2004;**67**: 417-34.

17. Kalina JL, Neilson DS, Comber AP, Rauw JM, Alexander AS, Vergidis J, Lum JJ. Immune Modulation by Androgen Deprivation and Radiation Therapy: Implications for Prostate Cancer Immunotherapy. *Cancers (Basel)* 2017;**9**.

18. Dalal K, Che M, Que NS, Sharma A, Yang R, Lallous N, Borgmann H, Ozistanbullu D, Tse R, Ban F, Li H, Tam KJ, et al. Bypassing Drug Resistance Mechanisms of Prostate Cancer with Small Molecules that Target Androgen Receptor-Chromatin Interactions. *Mol Cancer Ther* 2017;**16**: 2281-91.

19. Lawson DA, Zong Y, Memarzadeh S, Xin L, Huang J, Witte ON. Basal epithelial stem cells are efficient targets for prostate cancer initiation. *Proc Natl Acad Sci U S A* 2010;**107**: 2610-5.

20. Penning TM. Mechanisms of drug resistance that target the androgen axis in castration resistant prostate cancer (CRPC). *J Steroid Biochem Mol Biol* 2015;**153**: 105-13.

21. Pal SK, Patel J, He M, Foulk B, Kraft K, Smirnov DA, Twardowski P, Kortylewski M, Bhargava V, Jones JO. Identification of mechanisms of resistance to treatment with abiraterone acetate or enzalutamide in patients with castration-resistant prostate cancer (CRPC). *Cancer* 2018;**124**: 1216-24.

22. Isaacs JT, Coffey DS. Adaptation versus selection as the mechanism responsible for the relapse of prostatic cancer to androgen ablation therapy as studied in the Dunning R-3327-H adenocarcinoma. *Cancer Res* 1981;**41**: 5070-5.

23. Feldman BJ, Feldman D. The development of androgen-independent prostate cancer. *Nat Rev Cancer* 2001;**1**: 34-45.

24. Scher HI, Sawyers CL. Biology of progressive, castration-resistant prostate cancer: directed therapies targeting the androgen-receptor signaling axis. *J Clin Oncol* 2005;**23**: 8253-61.

25. de Bono JS, Logothetis CJ, Molina A, Fizazi K, North S, Chu L, Chi KN, Jones RJ, Goodman OB, Jr., Saad F, Staffurth JN, Mainwaring P, et al. Abiraterone and increased survival in metastatic prostate cancer. *N Engl J Med* 2011;**364**: 1995-2005.

26. Scher HI, Fizazi K, Saad F, Taplin ME, Sternberg CN, Miller K, de Wit R, Mulders P, Chi KN, Shore ND, Armstrong AJ, Flaig TW, et al. Increased survival with enzalutamide in prostate cancer after chemotherapy. *N Engl J Med* 2012;**367**: 1187-97.

27. Small EJ, Schellhammer PF, Higano CS, Redfern CH, Nemunaitis JJ, Valone FH, Verjee SS, Jones LA, Hershberg RM. Placebo-controlled phase III trial of immunologic therapy with sipuleucel-T (APC8015) in patients with metastatic, asymptomatic hormone refractory prostate cancer. *J Clin Oncol* 2006;**24**: 3089-94.

28. Kantoff PW, Higano CS, Shore ND, Berger ER, Small EJ, Penson DF, Redfern CH, Ferrari AC, Dreicer R, Sims RB, Xu Y, Frohlich MW, et al. Sipuleucel-T immunotherapy for castration-resistant prostate cancer. *N Engl J Med* 2010;**363**: 411-22.

29. Tannock IF, de Wit R, Berry WR, Horti J, Pluzanska A, Chi KN, Oudard S, Theodore C, James ND, Turesson I, Rosenthal MA, Eisenberger MA, et al. Docetaxel plus prednisone or mitoxantrone plus prednisone for advanced prostate cancer. *N Engl J Med* 2004;**351**: 1502-12.

30. Berthold DR, Pond GR, Soban F, de Wit R, Eisenberger M, Tannock IF. Docetaxel plus prednisone or mitoxantrone plus prednisone for advanced prostate cancer: updated survival in the TAX 327 study. *J Clin Oncol* 2008;**26**: 242-5.

31. de Bono JS, Oudard S, Ozguroglu M, Hansen S, Machiels JP, Kocak I, Gravis G, Bodrogi I, Mackenzie MJ, Shen L, Roessner M, Gupta S, et al. Prednisone plus cabazitaxel or mitoxantrone for metastatic castration-resistant prostate cancer progressing after docetaxel treatment: a randomised open-label trial. *Lancet* 2010;**376**: 1147-54.

32. Hoskin P, Sartor O, O'Sullivan JM, Johannessen DC, Helle SI, Logue J, Bottomley D, Nilsson S, Vogelzang NJ, Fang F, Wahba M, Aksnes AK, et al. Efficacy and safety of radium-223 dichloride in patients with castration-resistant prostate cancer and symptomatic bone metastases, with or without previous docetaxel use: a prespecified subgroup analysis from the randomised, double-blind, phase 3 ALSYMPCA trial. *Lancet Oncol* 2014;**15**: 1397-406.

33. Komura K, Sweeney CJ, Inamoto T, Ibuki N, Azuma H, Kantoff PW. Current treatment strategies for advanced prostate cancer. *Int J Urol* 2018;**25**: 220-31.

34. Horwitz SB. Taxol (paclitaxel): mechanisms of action. *Ann Oncol* 1994;**5 Suppl 6**: S3-6.

35. Baloglu E, Kingston DG. The taxane diterpenoids. *J Nat Prod* 1999;**62**: 1448-72.

36. Petrylak DP, Tangen CM, Hussain MH, Lara PN, Jr., Jones JA, Taplin ME, Burch PA, Berry D, Moinpour C, Kohli M, Benson MC, Small EJ, et al. Docetaxel and estramustine compared with mitoxantrone and prednisone for advanced refractory prostate cancer. *N Engl J Med* 2004;**351**: 1513-20.

37. Pienta KJ. Preclinical mechanisms of action of docetaxel and docetaxel combinations in prostate cancer. *Semin Oncol* 2001;**28**: 3-7.

38. Desai A, Mitchison TJ. Microtubule polymerization dynamics. *Annu Rev Cell Dev Biol* 1997;**13**: 83-117.

39. Fitzpatrick JM, de Wit R. Taxane mechanisms of action: potential implications for treatment sequencing in metastatic castration-resistant prostate cancer. *Eur Urol* 2014;**65**: 1198-204.

40. Antonarakis ES, Lu C, Wang H, Luber B, Nakazawa M, Roeser JC, Chen Y, Mohammad TA, Chen Y, Fedor HL, Lotan TL, Zheng Q, et al. AR-V7 and resistance to enzalutamide and abiraterone in prostate cancer. *N Engl J Med* 2014;**371**: 1028-38.

41. Zhu ML, Horbinski CM, Garzotto M, Qian DZ, Beer TM, Kyprianou N. Tubulin-targeting chemotherapy impairs androgen receptor activity in prostate cancer. *Cancer Res* 2010;**70**: 7992-8002.

42. Eisenhauer EA, Vermorken JB. The taxoids. Comparative clinical pharmacology and therapeutic potential. *Drugs* 1998;**55**: 5-30.

43. Oprea-Lager DE, Bijnsdorp IV, RJ VANM, AJ VDE, Hoekstra OS, Geldof AA. ABCC4 Decreases docetaxel and not cabazitaxel efficacy in prostate cancer cells in vitro. *Anticancer Res* 2013;**33**: 387-91.

44. Sissung TM, Baum CE, Deeken J, Price DK, Aragon-Ching J, Steinberg SM, Dahut W, Sparreboom A, Figg WD. ABCB1 genetic variation influences the toxicity and clinical outcome of patients with androgen-independent prostate cancer treated with docetaxel. *Clin Cancer Res* 2008;**14**: 4543-9.

45. Geney R, Ungureanu l M, Li D, Ojima I. Overcoming multidrug resistance in taxane chemotherapy. *Clin Chem Lab Med* 2002;**40**: 918-25.

46. Hara T, Ushio K, Nishiwaki M, Kouno J, Araki H, Hikichi Y, Hattori M, Imai Y, Yamaoka M. A mutation in beta-tubulin and a sustained dependence on androgen receptor signalling in a newly established docetaxel-resistant prostate cancer cell line. *Cell Biol Int* 2010;**34**: 177-84.

47. Giannakakou P, Sackett DL, Kang YK, Zhan Z, Buters JT, Fojo T, Poruchynsky MS. Paclitaxel-resistant human ovarian cancer cells have mutant beta-tubulins that exhibit impaired paclitaxel-driven polymerization. *J Biol Chem* 1997;**272**: 17118-25.

48. Terry S, Ploussard G, Allory Y, Nicolaiew N, Boissiere-Michot F, Maille P, Kheuang L, Coppolani E, Ali A, Bibeau F, Culine S, Buttyan R, et al. Increased expression of class III beta-tubulin in castration-resistant human prostate cancer. *Br J Cancer* 2009;**101**: 951-6.

49. Singh A, Settleman J. EMT, cancer stem cells and drug resistance: an emerging axis of evil in the war on cancer. *Oncogene* 2010;**29**: 4741-51.

50. Yang SX, Costantino JP, Kim C, Mamounas EP, Nguyen D, Jeong JH, Wolmark N, Kidwell K, Paik S, Swain SM. Akt phosphorylation at Ser473 predicts benefit of paclitaxel chemotherapy in node-positive breast cancer. *J Clin Oncol* 2010;**28**: 2974-81.

51. Malik SN, Brattain M, Ghosh PM, Troyer DA, Prihoda T, Bedolla R, Kreisberg JI. Immunohistochemical demonstration of phospho-Akt in high Gleason grade prostate cancer. *Clin Cancer Res* 2002;**8**: 1168-71.

52. Creighton CJ, Li X, Landis M, Dixon JM, Neumeister VM, Sjolund A, Rimm DL, Wong H, Rodriguez A, Herschkowitz JI, Fan C, Zhang X, et al. Residual breast cancers after conventional therapy display mesenchymal as well as tumor-initiating features. *Proc Natl Acad Sci U S A* 2009;**106**: 13820-5.

53. Bhola NE, Balko JM, Dugger TC, Kuba MG, Sanchez V, Sanders M, Stanford J, Cook RS, Arteaga CL. TGF-beta inhibition enhances chemotherapy action against triple-negative breast cancer. *J Clin Invest* 2013;**123**: 1348-58.

54. Gan L, Wang J, Xu H, Yang X. Resistance to docetaxel-induced apoptosis in prostate cancer cells by p38/p53/p21 signaling. *Prostate* 2011;**71**: 1158-66.

55. Kutuk O, Letai A. Alteration of the mitochondrial apoptotic pathway is key to acquired paclitaxel

resistance and can be reversed by ABT-737. *Cancer Res* 2008;**68**: 7985-94.

56. Pankov R, Yamada KM. Fibronectin at a glance. *J Cell Sci* 2002;**115**: 3861-3.

57. Govaere O, Wouters J, Petz M, Vandewynckel YP, Van den Eynde K, Van den Broeck A, Verhulst S, Dolle L, Gremeaux L, Ceulemans A, Nevens F, van Grunsven LA, et al. Laminin-332 sustains chemoresistance and quiescence as part of the human hepatic cancer stem cell niche. *J Hepatol* 2016;**64**: 609-17.

58. Han S, Sidell N, Roman J. Fibronectin stimulates human lung carcinoma cell proliferation by suppressing p21 gene expression via signals involving Erk and Rho kinase. *Cancer Lett* 2005;**219**: 71-81.

59. Xing H, Weng D, Chen G, Tao W, Zhu T, Yang X, Meng L, Wang S, Lu Y, Ma D. Activation of fibronectin/PI-3K/Akt2 leads to chemoresistance to docetaxel by regulating survivin protein expression in ovarian and breast cancer cells. *Cancer Lett* 2008;**261**: 108-19.

60. Kojima S, Kobayashi A, Gotoh O, Ohkuma Y, Fujii-Kuriyama Y, Sogawa K. Transcriptional activation domain of human BTEB2, a GC box-binding factor. *J Biochem* 1997;**121**: 389-96.

61. Sogawa K, Imataka H, Yamasaki Y, Kusume H, Abe H, Fujii-Kuriyama Y. cDNA cloning and transcriptional properties of a novel GC box-binding protein, BTEB2. *Nucleic Acids Res* 1993;**21**: 1527-32.

62. Zhang Z, Teng CT. Phosphorylation of Kruppel-like factor 5 (KLF5/IKLF) at the CBP interaction region enhances its transactivation function. *Nucleic Acids Res* 2003;**31**: 2196-208.

63. Miyamoto S, Suzuki T, Muto S, Aizawa K, Kimura A, Mizuno Y, Nagino T, Imai Y, Adachi N, Horikoshi M, Nagai R. Positive and negative regulation of the cardiovascular transcription factor KLF5 by p300 and the oncogenic regulator SET through interaction and acetylation on the DNA-binding domain. *Mol Cell Biol* 2003;**23**: 8528-41.

64. Chen C, Sun X, Ran Q, Wilkinson KD, Murphy TJ, Simons JW, Dong JT. Ubiquitin-proteasome degradation of KLF5 transcription factor in cancer and untransformed epithelial cells. *Oncogene* 2005;**24**: 3319-27.

65. Oishi Y, Manabe I, Tobe K, Ohsugi M, Kubota T, Fujiu K, Maemura K, Kubota N, Kadowaki T, Nagai R. SUMOylation of Kruppel-like transcription factor 5 acts as a molecular switch in transcriptional programs of lipid metabolism involving PPAR-delta. *Nat Med* 2008;**14**: 656-66.

66. Du JX, Bialkowska AB, McConnell BB, Yang VW. SUMOylation regulates nuclear localization of Kruppel-like factor 5. *J Biol Chem* 2008;**283**: 31991-2002.

67. Conkright MD, Wani MA, Anderson KP, Lingrel JB. A gene encoding an intestinal-enriched member of the Kruppel-like factor family expressed in intestinal epithelial cells. *Nucleic Acids Res* 1999;**27**: 1263-70.

68. Ohnishi S, Laub F, Matsumoto N, Asaka M, Ramirez F, Yoshida T, Terada M. Developmental expression of the mouse gene coding for the Kruppel-like transcription factor KLF5. *Dev Dyn* 2000;**217**: 421-9.

69. McConnell BB, Ghaleb AM, Nandan MO, Yang VW. The diverse functions of Kruppel-like factors 4 and 5 in epithelial biology and pathobiology. *Bioessays* 2007;**29**: 549-57.

70. Shindo T, Manabe I, Fukushima Y, Tobe K, Aizawa K, Miyamoto S, Kawai-Kowase K, Moriyama N, Imai Y, Kawakami H, Nishimatsu H, Ishikawa T, et al. Kruppel-like zinc-finger transcription factor KLF5/BTEB2 is a target for angiotensin II signaling and an essential regulator of cardiovascular remodeling. *Nat Med* 2002;**8**: 856-63.

71. Chanchevalap S, Nandan MO, Merlin D, Yang VW. All-trans retinoic acid inhibits proliferation of intestinal epithelial cells by inhibiting expression of the gene encoding Kruppel-like factor 5. *FEBS Lett* 2004;**578**: 99-105.

72. Chen C, Bhalala HV, Vessella RL, Dong JT. KLF5 is frequently deleted and down-regulated but rarely mutated in prostate cancer. *Prostate* 2003;**55**: 81-8.

73. Moore-Scott BA, Opoka R, Lin SC, Kordich JJ, Wells JM. Identification of molecular markers that are expressed in discrete anterior-posterior domains of the endoderm from the gastrula stage to mid-gestation. *Dev Dyn* 2007;**236**: 1997-2003.

74. Xing C, Fu X, Sun X, Guo P, Li M, Dong JT. Different expression patterns and functions of acetylated and

unacetylated Klf5 in the proliferation and differentiation of prostatic epithelial cells. *Plos One* 2013;**8**: e65538.

75. Zhang B, Ci X, Tao R, Ni JJ, Xuan X, King JL, Xia S, Li Y, Frierson HF, Lee DK, Xu J, Osunkoya AO, et al. Klf5 acetylation regulates luminal differentiation of basal progenitors in prostate development and regeneration. *Nat Commun* 2020;**11**: 997.

76. Bateman NW, Tan D, Pestell RG, Black JD, Black AR. Intestinal tumor progression is associated with altered function of KLF5. *J Biol Chem* 2004;**279**: 12093-101.

77. Nandan MO, McConnell BB, Ghaleb AM, Bialkowska AB, Sheng H, Shao J, Babbin BA, Robine S, Yang VW. Kruppel-like factor 5 mediates cellular transformation during oncogenic KRAS-induced intestinal tumorigenesis. *Gastroenterology* 2008;**134**: 120-30.

78. Bialkowska AB, Du Y, Fu H, Yang VW. Identification of novel small-molecule compounds that inhibit the proproliferative Kruppel-like factor 5 in colorectal cancer cells by high-throughput screening. *Mol Cancer Ther* 2009;**8**: 563-70.

79. Ohnishi S, Ohnami S, Laub F, Aoki K, Suzuki K, Kanai Y, Haga K, Asaka M, Ramirez F, Yoshida T. Downregulation and growth inhibitory effect of epithelial-type Kruppel-like transcription factor KLF4, but not KLF5, in bladder cancer. *Biochem Biophys Res Commun* 2003;**308**: 251-6.

80. Giefing M, Wierzbicka M, Rydzanicz M, Cegla R, Kujawski M, Szyfter K. Chromosomal gains and losses indicate oncogene and tumor suppressor gene candidates in salivary gland tumors. *Neoplasma* 2008;**55**: 55-60.

81. Chaib H, Cockrell EK, Rubin MA, Macoska JA. Profiling and verification of gene expression patterns in normal and malignant human prostate tissues by cDNA microarray analysis. *Neoplasia* 2001;**3**: 43-52.

82. Knuutila S, Aalto Y, Autio K, Bjorkqvist AM, El-Rifai W, Hemmer S, Huhta T, Kettunen E, Kiuru-Kuhlefelt S, Larramendy ML, Lushnikova T, Monni O, et al. DNA copy number losses in human neoplasms. *Am J Pathol* 1999;**155**: 683-94.

83. Dong JT, Boyd JC, Frierson HF, Jr. Loss of heterozygosity at 13q14 and 13q21 in high grade, high stage prostate cancer. *Prostate* 2001;**49**: 166-71.

84. Dong JT, Chen C, Stultz BG, Isaacs JT, Frierson HF, Jr. Deletion at 13q21 is associated with aggressive prostate cancers. *Cancer Res* 2000;**60**: 3880-3.

85. Dong JT, Chen C. Essential role of KLF5 transcription factor in cell proliferation and differentiation and its implications for human diseases. *Cell Mol Life Sci* 2009;**66**: 2691-706.

86. Chen C, Benjamin MS, Sun X, Otto KB, Guo P, Dong XY, Bao Y, Zhou Z, Cheng X, Simons JW, Dong JT. KLF5 promotes cell proliferation and tumorigenesis through gene regulation and the TSU-Pr1 human bladder cancer cell line. *Int J Cancer* 2006;**118**: 1346-55.

87. Yang Y, Goldstein BG, Nakagawa H, Katz JP. Kruppel-like factor 5 activates MEK/ERK signaling via EGFR in primary squamous epithelial cells. *FASEB J* 2007;**21**: 543-50.

88. Sun R, Chen X, Yang VW. Intestinal-enriched Kruppel-like factor (Kruppel-like factor 5) is a positive regulator of cellular proliferation. *J Biol Chem* 2001;**276**: 6897-900.

89. Nandan MO, Yoon HS, Zhao W, Ouko LA, Chanchevalap S, Yang VW. Kruppel-like factor 5 mediates the transforming activity of oncogenic H-Ras. *Oncogene* 2004;**23**: 3404-13.

90. Li X, Zhang B, Wu Q, Ci X, Zhao R, Zhang Z, Xia S, Su D, Chen J, Ma G, Fu L, Dong JT. Interruption of KLF5 acetylation converts its function from tumor suppressor to tumor promoter in prostate cancer cells. *Int J Cancer* 2015;**136**: 536-46.

91. An T, Dong T, Zhou H, Chen Y, Zhang J, Zhang Y, Li Z, Yang X. The transcription factor Kruppel-like factor 5 promotes cell growth and metastasis via activating PI3K/AKT/Snail signaling in hepatocellular carcinoma. *Biochem Biophys Res Commun* 2019;**508**: 159-68.

92. Zhang B, Zhang Z, Xia S, Xing C, Ci X, Li X, Zhao R, Tian S, Ma G, Zhu Z, Fu L, Dong JT. KLF5 activates

microRNA 200 transcription to maintain epithelial characteristics and prevent induced epithelial-mesenchymal transition in epithelial cells. *Mol Cell Biol* 2013;**33**: 4919-35.

93. Guo P, Zhao KW, Dong XY, Sun X, Dong JT. Acetylation of KLF5 alters the assembly of p15 transcription factors in transforming growth factor-beta-mediated induction in epithelial cells. *J Biol Chem* 2009;**284**: 18184-93.

94. Shi Y, Massague J. Mechanisms of TGF-beta signaling from cell membrane to the nucleus. *Cell* 2003;**113**: 685-700.

95. Wrana JL, Attisano L, Wieser R, Ventura F, Massague J. Mechanism of activation of the TGF-beta receptor. *Nature* 1994;**370**: 341-7.

96. Huse M, Muir TW, Xu L, Chen YG, Kuriyan J, Massague J. The TGF beta receptor activation process: an inhibitor- to substrate-binding switch. *Mol Cell* 2001;**8**: 671-82.

97. Massague J. TGFbeta signalling in context. *Nat Rev Mol Cell Biol* 2012;**13**: 616-30.

98. Mullen AC, Orlando DA, Newman JJ, Loven J, Kumar RM, Bilodeau S, Reddy J, Guenther MG, DeKoter RP, Young RA. Master transcription factors determine cell-type-specific responses to TGF-beta signaling. *Cell* 2011;**147**: 565-76.

99. Massague J, Seoane J, Wotton D. Smad transcription factors. *Genes Dev* 2005;**19**: 2783-810.

100. Schlessinger J. Cell signaling by receptor tyrosine kinases. *Cell* 2000;**103**: 211-25.

101. Bhowmick NA, Ghiassi M, Bakin A, Aakre M, Lundquist CA, Engel ME, Arteaga CL, Moses HL. Transforming growth factor-beta1 mediates epithelial to mesenchymal transdifferentiation through a RhoA-dependent mechanism. *Mol Biol Cell* 2001;**12**: 27-36.

102. Bakin AV, Tomlinson AK, Bhowmick NA, Moses HL, Arteaga CL. Phosphatidylinositol 3-kinase function is required for transforming growth factor beta-mediated epithelial to mesenchymal transition and cell migration. *J Biol Chem* 2000;**275**: 36803-10.

103. Lamouille S, Derynck R. Cell size and invasion in TGF-beta-induced epithelial to mesenchymal transition is regulated by activation of the mTOR pathway. *J Cell Biol* 2007;**178**: 437-51.

104. Chaouchi N, Arvanitakis L, Auffredou MT, Blanchard DA, Vazquez A, Sharma S. Characterization of transforming growth factor-beta 1 induced apoptosis in normal human B cells and lymphoma B cell lines. *Oncogene* 1995;**11**: 1615-22.

105. Wahl SM, Hunt DA, Wong HL, Dougherty S, McCartney-Francis N, Wahl LM, Ellingsworth L, Schmidt JA, Hall G, Roberts AB, et al. Transforming growth factor-beta is a potent immunosuppressive agent that inhibits IL-1-dependent lymphocyte proliferation. *J Immunol* 1988;**140**: 3026-32.

106. Weller M, Constam DB, Malipiero U, Fontana A. Transforming growth factor-beta 2 induces apoptosis of murine T cell clones without down-regulating bcl-2 mRNA expression. *Eur J Immunol* 1994;**24**: 1293-300.

107. Teramoto T, Kiss A, Thorgeirsson SS. Induction of p53 and Bax during TGF-beta 1 initiated apoptosis in rat liver epithelial cells. *Biochem Biophys Res Commun* 1998;**251**: 56-60.

108. Yamamoto M, Maehara Y, Sakaguchi Y, Kusumoto T, Ichiyoshi Y, Sugimachi K. Transforming growth factor-beta 1 induces apoptosis in gastric cancer cells through a p53-independent pathway. *Cancer* 1996;**77**: 1628-33.

109. Atfi A, Djelloul S, Chastre E, Davis R, Gespach C. Evidence for a role of Rho-like GTPases and stress-activated protein kinase/c-Jun N-terminal kinase (SAPK/JNK) in transforming growth factor beta-mediated signaling. *J Biol Chem* 1997;**272**: 1429-32.

110. Landstrom M, Heldin NE, Bu S, Hermansson A, Itoh S, ten Dijke P, Heldin CH. Smad7 mediates apoptosis induced by transforming growth factor beta in prostatic carcinoma cells. *Curr Biol* 2000;**10**: 535-8.

111. Xu J, Lamouille S, Derynck R. TGF-beta-induced epithelial to mesenchymal transition. *Cell Res* 2009;**19**:

156-72.

112. Huang JJ, Blobe GC. Dichotomous roles of TGF-beta in human cancer. *Biochem Soc Trans* 2016;**44**: 1441-54.

113. !!! INVALID CITATION !!! {}.

114. Shim KS, Kim KH, Han WS, Park EB. Elevated serum levels of transforming growth factor-beta1 in patients with colorectal carcinoma: its association with tumor progression and its significant decrease after curative surgical resection. *Cancer* 1999;**85**: 554-61.

115. Hasegawa Y, Takanashi S, Kanehira Y, Tsushima T, Imai T, Okumura K. Transforming growth factor-beta1 level correlates with angiogenesis, tumor progression, and prognosis in patients with nonsmall cell lung carcinoma. *Cancer* 2001;**91**: 964-71.

116. Massague J. TGFbeta in Cancer. *Cell* 2008;**134**: 215-30.

117. Wikstrom P, Stattin P, Franck-Lissbrant I, Damber JE, Bergh A. Transforming growth factor beta1 is associated with angiogenesis, metastasis, and poor clinical outcome in prostate cancer. *Prostate* 1998;**37**: 19-29.

118. Scheel C, Eaton EN, Li SH, Chaffer CL, Reinhardt F, Kah KJ, Bell G, Guo W, Rubin J, Richardson AL, Weinberg RA. Paracrine and autocrine signals induce and maintain mesenchymal and stem cell states in the breast. *Cell* 2011;**145**: 926-40.

119. Viloria-Petit AM, David L, Jia JY, Erdemir T, Bane AL, Pinnaduwage D, Roncari L, Narimatsu M, Bose R, Moffat J, Wong JW, Kerbel RS, et al. A role for the TGFbeta-Par6 polarity pathway in breast cancer progression. *Proc Natl Acad Sci U S A* 2009;**106**: 14028-33.

120. Padua D, Zhang XH, Wang Q, Nadal C, Gerald WL, Gomis RR, Massague J. TGFbeta primes breast tumors for lung metastasis seeding through angiopoietin-like 4. *Cell* 2008;**133**: 66-77.

121. Markowitz S, Wang J, Myeroff L, Parsons R, Sun L, Lutterbaugh J, Fan RS, Zborowska E, Kinzler KW, Vogelstein B, et al. Inactivation of the type II TGF-beta receptor in colon cancer cells with microsatellite instability. *Science* 1995;**268**: 1336-8.

122. Levy L, Hill CS. Alterations in components of the TGF-beta superfamily signaling pathways in human cancer. *Cytokine Growth Factor Rev* 2006;**17**: 41-58.

123. Chen T, Carter D, Garrigue-Antar L, Reiss M. Transforming growth factor beta type I receptor kinase mutant associated with metastatic breast cancer. *Cancer Res* 1998;**58**: 4805-10.

124. Tokunaga H, Lee DH, Kim IY, Wheeler TM, Lerner SP. Decreased expression of transforming growth factor beta receptor type I is associated with poor prognosis in bladder transitional cell carcinoma patients. *Clin Cancer Res* 1999;**5**: 2520-5.

125. Ohtaki N, Yamaguchi A, Goi T, Fukaya T, Takeuchi K, Katayama K, Hirose K, Urano T. Somatic alterations of the DPC4 and Madr2 genes in colorectal cancers and relationship to metastasis. *Int J Oncol* 2001;**18**: 265-70.

126. Dumont E, Lallemand F, Prunier C, Ferrand N, Guillouzo A, Clement B, Atfi A, Theret N. Evidence for a role of Smad3 and Smad2 in stabilization of the tumor-derived mutant Smad2.Q407R. *J Biol Chem* 2003;**278**: 24881-7.

127. Han SU, Kim HT, Seong DH, Kim YS, Park YS, Bang YJ, Yang HK, Kim SJ. Loss of the Smad3 expression increases susceptibility to tumorigenicity in human gastric cancer. *Oncogene* 2004;**23**: 1333-41.

128. Guo P, Dong XY, Zhang X, Zhao KW, Sun X, Li Q, Dong JT. Pro-proliferative factor KLF5 becomes anti-proliferative in epithelial homeostasis upon signaling-mediated modification. *J Biol Chem* 2009;**284**: 6071-8.

129. Guo P, Dong XY, Zhao K, Sun X, Li Q, Dong JT. Opposing effects of KLF5 on the transcription of MYC in epithelial proliferation in the context of transforming growth factor beta. *J Biol Chem* 2009;**284**: 28243-52.

130. Derynck R, Akhurst RJ. Differentiation plasticity regulated by TGF-beta family proteins in development and disease. *Nat Cell Biol* 2007;**9**: 1000-4.

131. Portella G, Cumming SA, Liddell J, Cui W, Ireland H, Akhurst RJ, Balmain A. Transforming growth factor beta is essential for spindle cell conversion of mouse skin carcinoma in vivo: implications for tumor invasion. *Cell Growth Differ* 1998;**9**: 393-404.

132. Oft M, Heider KH, Beug H. TGFbeta signaling is necessary for carcinoma cell invasiveness and metastasis. *Curr Biol* 1998;**8**: 1243-52.

133. Cui W, Fowlis DJ, Bryson S, Duffie E, Ireland H, Balmain A, Akhurst RJ. TGFbeta1 inhibits the formation of benign skin tumors, but enhances progression to invasive spindle carcinomas in transgenic mice. *Cell* 1996;**86**: 531-42.

134. Adorno M, Cordenonsi M, Montagner M, Dupont S, Wong C, Hann B, Solari A, Bobisse S, Rondina MB, Guzzardo V, Parenti AR, Rosato A, et al. A Mutant-p53/Smad complex opposes p63 to empower TGFbeta-induced metastasis. *Cell* 2009;**137**: 87-98.

135. Tan EJ, Thuault S, Caja L, Carletti T, Heldin CH, Moustakas A. Regulation of transcription factor Twist expression by the DNA architectural protein high mobility group A2 during epithelial-to-mesenchymal transition. *J Biol Chem* 2012;**287**: 7134-45.

136. Thuault S, Tan EJ, Peinado H, Cano A, Heldin CH, Moustakas A. HMGA2 and Smads co-regulate SNAIL1 expression during induction of epithelial-to-mesenchymal transition. *J Biol Chem* 2008;**283**: 33437-46.

137. Tachibana I, Imoto M, Adjei PN, Gores GJ, Subramaniam M, Spelsberg TC, Urrutia R. Overexpression of the TGFbeta-regulated zinc finger encoding gene, TIEG, induces apoptosis in pancreatic epithelial cells. *J Clin Invest* 1997;**99**: 2365-74.

138. Jang CW, Chen CH, Chen CC, Chen JY, Su YH, Chen RH. TGF-beta induces apoptosis through Smad-mediated expression of DAP-kinase. *Nature Cell Biology* 2002;**4**: 51-8.

139. Valderrama-Carvajal H, Cocolakis E, Lacerte A, Lee EH, Krystal G, Ali S, Lebrun JJ. Activin/TGF-beta induce apoptosis through Smad-dependent expression of the lipid phosphatase SHIP. *Nat Cell Biol* 2002;**4**: 963-9.

140. Perlman R, Schiemann WP, Brooks MW, Lodish HF, Weinberg RA. TGF-beta-induced apoptosis is mediated by the adapter protein Daxx that facilitates JNK activation. *Nat Cell Biol* 2001;**3**: 708-14.

141. Hwang C. Overcoming docetaxel resistance in prostate cancer: a perspective review. *Ther Adv Med Oncol* 2012;**4**: 329-40.

142. Marin-Aguilera M, Codony-Servat J, Kalko SG, Fernandez PL, Bermudo R, Buxo E, Ribal MJ, Gascon P, Mellado B. Identification of docetaxel resistance genes in castration-resistant prostate cancer. *Mol Cancer Ther* 2012;**11**: 329-39.

143. Li GY, Wang W, Sun JY, Xin B, Zhang X, Wang T, Zhang QF, Yao LB, Han H, Fan DM, Yang AG, Jia LT, et al. Long non-coding RNAs AC026904.1 and UCA1: a "one-two punch" for TGF-beta-induced SNAI2 activation and epithelial-mesenchymal transition in breast cancer. *Theranostics* 2018;**8**: 2846-61.

144. Ran FA, Hsu PD, Wright J, Agarwala V, Scott DA, Zhang F. Genome engineering using the CRISPR-Cas9 system. *Nat Protoc* 2013;**8**: 2281-308.

145. Cao Z, Kyprianou N. Mechanisms navigating the TGF-beta pathway in prostate cancer. *Asian J Urol* 2015;**2**: 11-8.

146. Brunen D, Willems SM, Kellner U, Midgley R, Simon I, Bernards R. TGF-beta: an emerging player in drug resistance. *Cell Cycle* 2013;**12**: 2960-8.

147. Abida W, Cyrta J, Heller G, Prandi D, Armenia J, Coleman I, Cieslik M, Benelli M, Robinson D, Van Allen EM, Sboner A, Fedrizzi T, et al. Genomic correlates of clinical outcome in advanced prostate cancer. *Proc Natl Acad Sci U S A* 2019;**116**: 11428-36.

148. Shibue T, Weinberg RA. EMT, CSCs, and drug resistance: the mechanistic link and clinical implications.

Nat Rev Clin Oncol 2017;**14**: 611-29.

149. Formenti SC, Lee P, Adams S, Goldberg JD, Li X, Xie MW, Ratikan JA, Felix C, Hwang L, Faull KF, Sayre JW, Hurvitz S, et al. Focal Irradiation and Systemic TGFbeta Blockade in Metastatic Breast Cancer. *Clin Cancer Res* 2018;**24**: 2493-504.

150. Oishi Y, Manabe I, Tobe K, Tsushima K, Shindo T, Fujiu K, Nishimura G, Maemura K, Yamauchi T, Kubota N, Suzuki R, Kitamura T, et al. Kruppel-like transcription factor KLF5 is a key regulator of adipocyte differentiation. *Cell Metab* 2005;**1**: 27-39.

151. Body JJ, Casimiro S, Costa L. Targeting bone metastases in prostate cancer: improving clinical outcome. *Nat Rev Urol* 2015;**12**: 340-56.

152. James ND, Spears MR, Clarke NW, Dearnaley DP, De Bono JS, Gale J, Hetherington J, Hoskin PJ, Jones RJ, Laing R, Lester JF, McLaren D, et al. Survival with newly diagnosed metastatic prostate cancer in the "Docetaxel Era": data from 917 patients in the control arm of the STAMPEDE Trial (MRC PR08, CRUK/06/019). *Eur Urol* 2015;**67**: 1028-38.

153. Kirby M, Hirst C, Crawford ED. Characterising the castration-resistant prostate cancer population: a systematic review. *Int J Clin Pract* 2011;**65**: 1180-92.

154. Gandaglia G, Karakiewicz PI, Briganti A, Passoni NM, Schiffmann J, Trudeau V, Graefen M, Montorsi F, Sun M. Impact of the Site of Metastases on Survival in Patients with Metastatic Prostate Cancer. *Eur Urol* 2015;**68**: 325-34.

155. Bubendorf L, Schopfer A, Wagner U, Sauter G, Moch H, Willi N, Gasser TC, Mihatsch MJ. Metastatic patterns of prostate cancer: an autopsy study of 1,589 patients. *Hum Pathol* 2000;**31**: 578-83.

156. Himelstein AL, Foster JC, Khatcheressian JL, Roberts JD, Seisler DK, Novotny PJ, Qin R, Go RS, Grubbs SS, O'Connor T, Velasco MR, Jr., Weckstein D, et al. Effect of Longer-Interval vs Standard Dosing of Zoledronic Acid on Skeletal Events in Patients With Bone Metastases: A Randomized Clinical Trial. *JAMA* 2017;**317**: 48-58.

157. Smith MR, Saad F, Oudard S, Shore N, Fizazi K, Sieber P, Tombal B, Damiao R, Marx G, Miller K, Van Veldhuizen P, Morote J, et al. Denosumab and bone metastasis-free survival in men with nonmetastatic castration-resistant prostate cancer: exploratory analyses by baseline prostate-specific antigen doubling time. *J Clin Oncol* 2013;**31**: 3800-6.

158. Hegemann M, Bedke J, Stenzl A, Todenhofer T. Denosumab treatment in the management of patients with advanced prostate cancer: clinical evidence and experience. *Ther Adv Urol* 2017;**9**: 81-8.

159. Croucher PI, McDonald MM, Martin TJ. Bone metastasis: the importance of the neighbourhood. *Nat Rev Cancer* 2016;**16**: 373-86.

160. Martin TJ. Osteoblast-derived PTHrP is a physiological regulator of bone formation. *J Clin Invest* 2005;**115**: 2322-4.

161. Weilbaecher KN, Guise TA, McCauley LK. Cancer to bone: a fatal attraction. *Nat Rev Cancer* 2011;**11**: 411-25.

162. Guise TA, Chirgwin JM. Transforming growth factor-beta in osteolytic breast cancer bone metastases. *Clin Orthop Relat Res* 2003: S32-8.

163. Guise TA. Parathyroid hormone-related protein and bone metastases. *Cancer* 1997;**80**: 1572-80.

164. Duivenvoorden WC, Hirte HW, Singh G. Transforming growth factor beta1 acts as an inducer of matrix metalloproteinase expression and activity in human bone-metastasizing cancer cells. *Clin Exp Metastasis* 1999;**17**: 27-34.

165. Ye H, Cheng J, Tang Y, Liu Z, Xu C, Liu Y, Sun Y. Human bone marrow-derived mesenchymal stem cells produced TGFbeta contributes to progression and metastasis of prostate cancer. *Cancer Invest* 2012;**30**: 513-8.

166. Connolly EC, Freimuth J, Akhurst RJ. Complexities of TGF-beta targeted cancer therapy. *Int J Biol Sci*

2012;**8**: 964-78.

167. Herbertz S, Sawyer JS, Stauber AJ, Gueorguieva I, Driscoll KE, Estrem ST, Cleverly AL, Desaiah D, Guba SC, Benhadji KA, Slapak CA, Lahn MM. Clinical development of galunisertib (LY2157299 monohydrate), a small molecule inhibitor of transforming growth factor-beta signaling pathway. *Drug Des Devel Ther* 2015;**9**: 4479-99.

168. Roberts AB, Sporn MB. Transforming growth factors. *Cancer Surv* 1985;**4**: 683-705.

169. Roberts AB, Wakefield LM. The two faces of transforming growth factor beta in carcinogenesis. *Proc Natl Acad Sci U S A* 2003;**100**: 8621-3.

170. Pickup M, Novitskiy S, Moses HL. The roles of TGFbeta in the tumour microenvironment. *Nat Rev Cancer* 2013;**13**: 788-99.

171. Ikushima H, Miyazono K. TGFbeta signalling: a complex web in cancer progression. *Nat Rev Cancer* 2010;**10**: 415-24.

172. Akhurst RJ, Hata A. Targeting the TGFbeta signalling pathway in disease. *Nat Rev Drug Discov* 2012;**11**: 790-811.

173. Greenberg EF, Lavik AR, Distelhorst CW. Bcl-2 regulation of the inositol 1,4,5-trisphosphate receptor and calcium signaling in normal and malignant lymphocytes: potential new target for cancer treatment. *Biochim Biophys Acta* 2014;**1843**: 2205-10.

174. Lin Y, Fukuchi J, Hiipakka RA, Kokontis JM, Xiang J. Up-regulation of Bcl-2 is required for the progression of prostate cancer cells from an androgen-dependent to an androgen-independent growth stage. *Cell Res* 2007;**17**: 531-6.

175. Sartorius UA, Krammer PH. Upregulation of Bcl-2 is involved in the mediation of chemotherapy resistance in human small cell lung cancer cell lines. *Int J Cancer* 2002;**97**: 584-92.

176. Simonian PL, Grillot DAM, Nunez G. Bcl-2 and Bcl-XL can differentially block chemotherapy-induced cell death. *Blood* 1997;**90**: 1208-16.

177. Wei WJ, Sun ZK, Shen CT, Song HJ, Zhang XY, Qiu ZL, Luo QY. Obatoclax and LY3009120 Efficiently Overcome Vemurafenib Resistance in Differentiated Thyroid Cancer. *Theranostics* 2017;**7**: 987-1001.

178. Haldar S, Basu A, Croce CM. Bcl2 is the guardian of microtubule integrity. *Cancer Research* 1997;**57**: 229-33.

179. Haldar S, Jena N, Croce CM. Inactivation of Bcl-2 by Phosphorylation. *P Natl Acad Sci USA* 1995;**92**: 4507-11.

180. Haldar S, Chintapalli J, Croce CM. Taxol induces bcl-2 phosphorylation and death of prostate cancer cells. *Cancer Res* 1996;**56**: 1253-5.

181. Zhang B, Zhao R, He Y, Fu X, Fu L, Zhu Z, Fu L, Dong JT. MicroRNA 100 sensitizes luminal A breast cancer cells to paclitaxel treatment in part by targeting mTOR. *Oncotarget* 2016;**7**: 5702-14.

182. Heckman CA, Mehew JW, Ying GG, Introna M, Golay J, Boxer LM. A-Myb up-regulates Bcl-2 through a Cdx binding site in t(14;18) lymphoma cells. *J Biol Chem* 2000;**275**: 6499-508.

183. Dobin A, Davis CA, Schlesinger F, Drenkow J, Zaleski C, Jha S, Batut P, Chaisson M, Gingeras TR. STAR: ultrafast universal RNA-seq aligner. *Bioinformatics* 2013;**29**: 15-21.

184. Li H, Handsaker B, Wysoker A, Fennell T, Ruan J, Homer N, Marth G, Abecasis G, Durbin R, Genome Project Data Processing S. The Sequence Alignment/Map format and SAMtools. *Bioinformatics* 2009;**25**: 2078-9.

185. Barwick BG, Scharer CD, Bally APR, Boss JM. Plasma cell differentiation is coupled to division-dependent DNA hypomethylation and gene regulation. *Nat Immunol* 2016;**17**: 1216-25.

186. Robinson MD, McCarthy DJ, Smyth GK. edgeR: a Bioconductor package for differential expression analysis of digital gene expression data. *Bioinformatics* 2010;**26**: 139-40.

187. Langmead B, Salzberg SL. Fast gapped-read alignment with Bowtie 2. *Nat Methods* 2012;**9**: 357-9.

188. Zhang Y, Liu T, Meyer CA, Eeckhoute J, Johnson DS, Bernstein BE, Nusbaum C, Myers RM, Brown M, Li W, Liu XS. Model-based analysis of ChIP-Seq (MACS). *Genome Biol* 2008;**9**: R137.

189. Gillissen B, Wendt J, Richter A, Richter A, Muer A, Overkamp T, Gebhardt N, Preissner R, Belka C, Dorken B, Daniel PT. Endogenous Bak inhibitors Mcl-1 and Bcl-xL: differential impact on TRAIL resistance in Bax-deficient carcinoma. *J Cell Biol* 2010;**188**: 851-62.

190. Bailey TL, Johnson J, Grant CE, Noble WS. The MEME Suite. *Nucleic Acids Res* 2015;**43**: W39-49.

191. Khan A, Fornes O, Stigliani A, Gheorghe M, Castro-Mondragon JA, van der Lee R, Bessy A, Cheneby J, Kulkarni SR, Tan G, Baranasic D, Arenillas DJ, et al. JASPAR 2018: update of the open-access database of transcription factor binding profiles and its web framework. *Nucleic Acids Res* 2018;**46**: D1284.

192. Tsujimoto Y. Role of Bcl-2 family proteins in apoptosis: apoptosomes or mitochondria? *Genes Cells* 1998;**3**: 697-707.

193. Czabotar PE, Lessene G, Strasser A, Adams JM. Control of apoptosis by the BCL-2 protein family: implications for physiology and therapy. *Nat Rev Mol Cell Biol* 2014;**15**: 49-63.

194. Ishii K, Matsuoka I, Kajiwara S, Sasaki T, Miki M, Kato M, Kanda H, Arima K, Shiraishi T, Sugimura Y. Additive naftopidil treatment synergizes docetaxel-induced apoptosis in human prostate cancer cells. *J Cancer Res Clin Oncol* 2018;**144**: 89-98.

195. Kumar A, Coleman I, Morrissey C, Zhang X, True LD, Gulati R, Etzioni R, Bolouri H, Montgomery B, White T, Lucas JM, Brown LG, et al. Substantial interindividual and limited intraindividual genomic diversity among tumors from men with metastatic prostate cancer. *Nat Med* 2016;**22**: 369-78.

196. Bouwens L, De Blay E. Islet morphogenesis and stem cell markers in rat pancreas. *J Histochem Cytochem* 1996;**44**: 947-51.

197. Feuerhake F, Sigg W, Hofter EA, Dimpfl T, Welsch U. Immunohistochemical analysis of Bcl-2 and Bax expression in relation to cell turnover and epithelial differentiation markers in the non-lactating human mammary gland epithelium. *Cell Tissue Res* 2000;**299**: 47-58.

198. Zhou S, Schuetz JD, Bunting KD, Colapietro AM, Sampath J, Morris JJ, Lagutina I, Grosveld GC, Osawa M, Nakauchi H, Sorrentino BP. The ABC transporter Bcrp1/ABCG2 is expressed in a wide variety of stem cells and is a molecular determinant of the side-population phenotype. *Nature Medicine* 2001;**7**: 1028-34.

199. Potten CS, Loeffler M. Stem cells: attributes, cycles, spirals, pitfalls and uncertainties. Lessons for and from the crypt. *Development* 1990;**110**: 1001-20.

200. Zavadil J, Bottinger EP. TGF-beta and epithelial-to-mesenchymal transitions. *Oncogene* 2005;**24**: 5764-74.

201. Geng Y, Weinberg RA. Transforming growth factor beta effects on expression of G1 cyclins and cyclin-dependent protein kinases. *Proc Natl Acad Sci U S A* 1993;**90**: 10315-9.

202. Ewen ME, Sluss HK, Whitehouse LL, Livingston DM. Tgf-Beta Inhibition of Cdk4 Synthesis Is Linked to Cell-Cycle Arrest. *Cell* 1993;**74**: 1009-20.

203. Yamada D, Nishimatsu H, Kumano S, Hirano Y, Suzuki M, Fujimura T, Fukuhara H, Enomoto Y, Kume H, Homma Y. REDUCTION OF PROSTATE CANCER INCIDENCE BY NAFTOPIDIL, AN alpha 1 ADRENOCEPTOR ANTAGONIST AND INHIBITOR OF TRANSFORMING GROWTH FACTOR-beta SIGNALING. *J Urology* 2013;**189**: E711-E.

204. Tourinho-Barbosa R, Srougi V, Nunes-Silva I, Baghdadi M, Rembeyo G, Eiffel SS, Barret E, Rozet F, Galiano M, Cathelineau X, Sanchez-Salas R. Biochemical recurrence after radical prostatectomy: what does it mean? *Int Braz J Urol* 2018;**44**: 14-21.

205. Waning DL, Mohammad KS, Reiken S, Xie W, Andersson DC, John S, Chiechi A, Wright LE, Umanskaya A, Niewolna M, Trivedi T, Charkhzarrin S, et al. Excess TGF-beta mediates muscle weakness associated with bone

metastases in mice. *Nat Med* 2015;**21**: 1262-71.

206. Bhardwaj A, Srivastava SK, Singh S, Arora S, Tyagi N, Andrews J, McClellan S, Carter JE, Singh AP. CXCL12/CXCR4 signaling counteracts docetaxel-induced microtubule stabilization via p21-activated kinase 4-dependent activation of LIM domain kinase 1. *Oncotarget* 2014;**5**: 11490-500.

207. Domanska UM, Timmer-Bosscha H, Nagengast WB, Oude Munnink TH, Kruizinga RC, Ananias HJ, Kliphuis NM, Huls G, De Vries EG, de Jong IJ, Walenkamp AM. CXCR4 inhibition with AMD3100 sensitizes prostate cancer to docetaxel chemotherapy. *Neoplasia* 2012;**14**: 709-18.

208. Holohan C, Van Schaeybroeck S, Longley DB, Johnston PG. Cancer drug resistance: an evolving paradigm. *Nat Rev Cancer* 2013;**13**: 714-26.

209. Zheng B, Han M, Shu YN, Li YJ, Miao SB, Zhang XH, Shi HJ, Zhang T, Wen JK. HDAC2 phosphorylation-dependent Klf5 deacetylation and RARalpha acetylation induced by RAR agonist switch the transcription regulatory programs of p21 in VSMCs. *Cell Res* 2011;**21**: 1487-508.

210. Abraham M, Klein S, Bulvik B, Wald H, Weiss ID, Olam D, Weiss L, Beider K, Eizenberg O, Wald O, Galun E, Avigdor A, et al. The CXCR4 inhibitor BL-8040 induces the apoptosis of AML blasts by downregulating ERK, BCL-2, MCL-1 and cyclin-D1 via altered miR-15a/16-1 expression. *Leukemia* 2017;**31**: 2336-46.